JNC TN 4400 99-001

Feasibility study on plutonium burning in future Monju cores

December 1999

International Cooperation and Technology Development Center
Japan Nuclear Cycle Development Institute

JNC TN 4400 99-001

December 1999

Feasibility study on plutonium burning in future Monju cores

Udo Wehmann, Takeshi Kageyama

Abstract

These studies have been planned and performed as a contribution to the demonstration of the plutonium burning capabilities of fast reactors in future Monju cores. For an upgraded Monju core design with an increased average discharge burnup of 100 GWd/t_{HM}, burner cores with diluents and with diluting pins have been investigated, the main aim of which is to increase the average plutonium enrichment of the fuel and thus the plutonium burning rate. On the other side the consequences of the suppression of the radial and/or axial blanket have been investigated. The results of these studies had been documented separately in [1] to [5], while this reports gives the compilation of these studies and a judgement about the different burner concepts.

Among the burner concepts different types of diluents (containing sodium and steel or B_4C) and diluting pins (steel, moderator or B_4C) have been compared with each other. The diluent concept with B_4C-diluents has been found to be the preferable one, because it causes the smallest increase of the maximum linear rating and because it offers the largest design flexibility to adapt the core reactivity via a modification of the B_4C content.

For the case of the blanket suppression the replacement of the blanket zones by a steel reflector has been found to be the best solution, whereby the addition of some B_4C in the outer reflector regions may be necessary to increase the shielding efficiency. The main consequence of the suppression of both blankets is the increase of the maximum linear rating by up to 12 %. Whether this increase may lead to problems, will depend on the actual linear power level of the core and the maximum allowable value as defined by the non-melting criterion. For cores with partly reduced radial and/or axial blanket data are also provided.

Core Development Group, International Cooperation and Technology Development Center, JNC

Table of contents **page**

List of Tables ... iv
List of Figures ... v
1 Introduction ... 1
2 Basic data ... 2
3 Calculational methods ... 2
4 Results for the reference core ... 4
5 Results for the burner cores with diluting pins ... 5
5.1 General aspects ... 5
5.2 Parametric overview calculations ... 5
5.2.1 Neutron-physics aspects ... 5
5.2.2 Thermal-hydraulics aspects ... 6
5.3 Results for burner cores with steel pins only ... 8
5.4 Results for burner cores with $MgAl_2O_4$ and $^{11}B_4C$ pins ... 9
5.5 Results for burner cores with $^{nat}B_4C$ and $ZrH_{1.7}$ pins ... 11
5.6 Some further thermal-hydraulics considerations ... 12
5.7 Intermediate conclusions about the diluting pins concept ... 14
6 Results for the burner cores with diluents ... 15
6.1 Parametric studies ... 15
6.2 Results of more detailed investigations ... 17
6.2.1 Diluent cores with one fuel enrichment ... 17
6.2.2 Diluent cores with two fuel enrichments ... 18
6.2.3 Diluent cores with moderated diluents ... 18
6.2.4 Influence of small amounts of $^{nat}B_4C$ in steel diluents ... 19
6.2.5 Thermal-hydraulics considerations ... 20
6.3 Intermediate conclusions about burner cores with diluents ... 21
7 Results for the cores with reduced blankets ... 22
7.1 Cores with reduced radial blanket ... 22
7.1.1 Influence of the radial blanket reduction on the k_{eff} and burnup reactivity loss ... 22
7.1.2 Influence of the radial blanket reduction on the power distribution ... 23
7.1.3 Influence of the radial blanket reduction on the control rod worth ... 24
7.1.4 Influence of the radial blanket reduction on the boundary fluxes ... 25
7.1.5 Influence of the radial blanket reduction on the sodium void and Doppler effect ... 26
7.2 Cores with reduced axial blanket ... 26
7.2.1 Influence of the axial blanket reduction on the k_{eff} and burnup reactivity loss ... 26
7.2.2 Influence of the axial blanket reduction on the power distribution ... 27
7.2.3 Influence of the axial blanket reduction on the control rod worth ... 28
7.2.4 Influence of the axial blanket reduction on the boundary fluxes ... 28
7.2.5 Influence of the axial blanket reduction on the sodium void and Doppler effect ... 29

7.3 Cores with reduced radial and axial blanket 29
7.3.1 Influence of the radial and axial blanket reduction on the k_{eff} and burnup reactivity loss 30
7.3.2 Influence of the radial and axial blanket reduction on the power distribution 30
7.3.3 Influence of the radial and axial blanket reduction on the control rod worth 31
7.3.4 Influence of the radial and axial blanket reduction on the boundary fluxes 31
7.3.5 Influence of the radial and axial blanket reduction on the sodium void and Doppler effect 32
7.4 Thermal-hydraulics considerations 32
7.5 Intermediate conclusions about cores with reduced blankets 33
8 Final evaluation 35
8.1 Comparison of the main burner candidates 35
8.2 Conclusions 37
8.2.1 Conclusions about the diluting pins or diluents concepts 37
8.2.2 Conclusions about the blanket reduction 38
8.2.3 General conclusions 38
9 List of references 40

List of Tables

page

Table 1: Pu-balance of the upgraded Monju core 41
Table 2: Volume fractions and densities of the different materials 41
Table 3: Breeding ratios in the reference core and some burner cores 42
Table 4: Mass balances for the reference core 43
Table 5: Power balance of the reference core and some burner cores 44
Table 6: Linear power traverses and other data in cores with different numbers of diluting pins 45
Table 7: Thermal-hydraulics data of bundles with different numbers of steel pins 45
Table 8: Results of burner cores with diluting steel pins only 46
Table 9: Mass balances for the burner core with 43 steel pins (core no. 2a) 47
Table 10: Results for burner cores with diluting steel , $MgAl_2O_4$ and $^{11}B_4C$ pins 48
Table 11: Results for burner cores with diluting steel plus some $^{nat}B_4C$ and $ZrH_{1.7}$ pins 49
Table 12: Results for burner cores with diluting steel, $MgAl_2O_4$ and $^{11}B_4C$ pins plus $^{nat}B_4C$ and $ZrH_{1.7}$ pins 50
Table 13: Thermal-hydraulics data of cores without and with diluting steel pins 51
Table 14: Volume fractions and reactivity worths of diluent candidates 52
Table 15: Data of cores with different numbers of steel diluents 52
Table 16: Data of Monju plutonium burner cores with steel or B_4C diluents 53
Table 17: Results for steel and B_4C diluent burner cores with one or two Pu-enrichments 54
Table 18: Sodium void effect, Doppler coefficient and maximum linear power as a function of the $^{11}B_4C$ content in 27 steel diluents 55
Table 19: Sodium void effect, Doppler effect and maximum linear power as a function of the $^{11}B_4C$ content in 18 B_4C diluents 55
Table 20: Influence of diluents on neutron-physics and thermal-hydraulics data 55
Table 21: Mass balances for the burner core with 27 steel diluents 56
Table 22: Mass balances for the burner core with 18 B_4C diluents 57
Table 23: Results for burner cores with reduced or suppressed radial blanket 58
Table 24: Flux ratios at the radial outer boundary: Φ(case B2)/ Φ(ref. case) 59
Table 25: Results for burner cores with reduced or suppressed axial blanket 60
Table 26: Results for burner cores with reduced or suppressed radial and axial blanket 61
Table 27: Mass-balances of the core with reduced blankets (case D1.3) 62
Table 28: Mass-balances of the core without blankets (case D2.3) 63
Table 29: Consequences of the radial and axial blanket reduction on thermal-hydraulics data 64
Table 30: Comparison of some cores with reduced blankets and the reference core 64
Table 31: Comparison of the considered burner cores and the reference core 65

List of Figures **page**

Figure 1: Calculational scheme 66
Figure 2: RZ model for CITATION calculations 67
Figure 3: Axial structure of the subassemblies for the Pu-burner reference core 68
Figure 4 Maximum linear power per S/A of the reference core (core no. 1a) 69
Figure 5: Radial linear rating traverses in cores with different numbers of diluting steel pins 70
Figure 6: Coolant channel ΔT distribution in a reference core fuel S/A 71
Figure 7: Bundle designs with different numbers of diluting pins 72
Figure 8 Maximum linear power per S/A of the burner core with 43 steel pins (core no.2a) 73
Figure 9: Influence of steel, $MgAl_2O_4$ and $^{11}B_4C$ on the neutron spectrum 74
Figure 10: Na-void effect, Doppler effect and maximum linear rating of burner cores with different numbers of $ZrH_{1.7}$ and B_4C pins (relative to the reference core values) 75
Figure 11: Influence of $^{nat}B_4C$ and $ZrH_{1.7}$ on the neutron spectrum 76
Figure 12: Core cross-sections with different numbers of steel diluents 77
Figure 13: RZ-Model for 70 groups CITATION calculations with diluents 78
Figure 14: Radial linear power traverses for different steel diluent configurations 79
Figure 15: Core cross-sections with 18 B_4C diluents 80
Figure 16: Influence of diluents with steel, $^{nat}B_4C$ and $^{nat}B_4C+^{11}B_4C$ on the inner core spectrum 81
Figure 17: Cross-sections of the reference core and two burner cores 82
Figure 18: Maximum linear power per S/A of the burner core with 27 steel diluents 83
Figure 19: Maximum linear power per S/A of the burner core with 18 B_4C diluents (10 % B_4C) 84
Figure 20: Radial maximum linear power traverses per S/A for the reference case 1a and case B2 without radial blanket 85
Figure 21: Maximum linear power per S/A in the core without radial blanket (case B2) 86
Figure 22: Influence of the axial blanket suppression on the axial power distribution at BOL in pos. 10 87
Figure 23: Radial maximum linear power traverses per S/A for the reference case 1a and case D2.3 without radial blanket 88
Figure 24: Maximum linear power per S/A in the core without radial and axial blanket (case D2.3) 89

1 Introduction

The main goal of this study on plutonium burner cores in Monju was to find out, to which extent Monju could contribute to the demonstration of the fast reactor's flexibility to adapt their design to the requirements of the nuclear fuel cycle and to regulate the plutonium masses by either breeding plutonium or burning it effectively. It is well known, that this flexibility has become of increased interest due to the postponed fast breeder introduction and the consequent build-up of large plutonium stocks.

When applying the concept of Pu-burning to Monju, it is certainly clear, that Monju can not contribute quantitatively to the Pu-burning because of its limited power size. This is quickly obvious, when we look at the plutonium balance in Table 1, which is that of the upgraded Monju core. It is also the reference of the present study, and its balance looks as follows in terms of mass changes ΔM in kg per year or per $TW_e \cdot h$, also in comparison with a typical Light Water Reactor (LWR). Although the amount of about 100 kg burnt per year in the fissile zones of Monju is small compared with the 225 kg produced per year by a LWR of 1 GW_e, the core burning rate in terms of $kg/TW_e \cdot h$ is much larger than the corresponding LWR production value, and this indicates, that Monju could well contribute to a general demonstration of the burning capability of fast reactors.

In view of this goal, we had separated our work into two steps:

① To investigate possibilities to enhance the internal burning rate. Its further increase basically requires an increase of the plutonium enrichments, as we had discussed in [1], and for a core like Monju with its fixed outer boundary conditions an increase of the enrichments can mainly be reached by diluting the fuel. For this purpose two different design measures have been found attractive in our preliminary study [1] and have then been investigated in more detail:

- the diluting pin concept, in which a certain number of the 169 fuel pins of the standard fuel S/A is replaced by pins containing diluting material, and
- the diluent concept, in which some complete fuel S/As are replaced by diluents containing steel and/or B_4C.

② To suppress the radial and/or the axial blankets and to replace them by a reflector, which should have minimum negative consequences on the core properties and has also to fulfil the shielding requirements.

Our study had been started with the establishment of the reference core [1] including the definition of the basic data and the evaluation of the main operational data, which will serve as a basis for comparison with the different burner cores. After that, the results of the investigations of the burner variant with diluting pins have been documented in [2], and those with diluents are described in [3] and [4]. Finally, the study on cores without blankets is described in [5], whereby the radial and axial blankets have been suppressed one after the other in order to separate the effects of both blankets. In addition to the complete replacement of the blankets also a partial one has been looked at, which could be an intermediate step on the way to a complete replacement.

The present report gives a summary of the previous investigations, whereby this report shall be understandable for itself, so that only in detailed aspects reference will be made to the individual reports mentioned above.

In the following, the main basic data and boundary conditions for the core calculations will be given, followed by a description of the calculational methods. After that, the main data for the

reference core will be mentioned, and the results of the calculations for the cores with diluting pins, with diluents and without blankets will be described. Finally, a judgement about the different burner cores will be tried.

2 Basic data

The main basic data and boundary conditions for the reference core and the burner cores are the following:

- the plutonium composition

  Pu238/ 239/ 240/ 241/ 242/ Am241= 3.0/ 52.0/ 27.0/ 9.5/ 7.0/ 1.5,

  as it had been defined by Tokai for a LWR-plutonium with a discharge burnup of 45 GWd/t_{HM};
- the average discharge burnup of 100 GWd/t_{HM}, which is reached after 5 cycles with about 200 equivalent full-power days (efpd) in the reference core; when the linear power level is changed, for instance by introducing diluents or diluting pins, the cycle length will need an adaptation in order to keep the burnup constant;
- volume fractions, material densities and compositions, as collected in Table 2. Among others, it shows the fuel pellet density of 92 %, which leads to a (inside cladding) smeared fuel density of 87 %.

3 Calculational methods

The calculational scheme is shown in Figure 1. The cross-sections are based on the JENDL-3.2 library. This indicates one difference compared with the beginning of our study, for instance in [1], where we had used JENDL-2. The influence of this change had been documented separately in [6], where for most of the core parameters only small differences had been found. One exception concerned the Na void effect, which is smaller using JENDL-3.2 by 15 to 20 %. All data given in this report are however based on JENDL-3.2.

The calculational scheme in Figure 1 comprises furthermore the cell code SLAROM, which is used with its homogeneous presentation of the materials, except for the control rods and the backup rods. For the absorbers a heterogeneous model has been applied, in which the 19 absorber pins per S/A have been presented on 3 rings, containing the central one, the intermediate 6 pins and the outer 12 pins, respectively. SLAROM provides the 70 groups constants for RZ-CITATION, which calculates the fluxes for the cross-section collapsing process in JOINT to 7 groups. The seven groups scheme has the following lower group boundaries:

4, 6, 8, 10, 12, 15, 26 in the ABBN 26 groups scheme,

8, 13, 19, 25, 31, 40, 70 in the 70 groups scheme

1.35 MeV, 0.387 MeV, 86.5 KeV, 19.3 KeV, 4.307 KeV, 0.454 KeV, 10^{-5} eV, in energy.

The seven groups cross-sections are then used in the three-dimensional (tri-z)-code MOSES for calculating the power and burnup distribution, the absorber worth values and the mass-balances with the number densities of the burnt materials. These number densities are then recycled to SLAROM to calculate the cross-sections for the burnt materials including the perturbed states for the calculation of the sodium void effect (SVE) and the Doppler coefficient (DC) with RZ-CITATION. Both were calculated via direct k_{eff} calculations. The RZ-model is shown in Figure 2. The SVE was evaluated by reducing the sodium density in the inner and outer core to 20 % and dividing the resulting $\Delta\rho=(k_1-k_2)/(k_1 \cdot k_2)$ by 0.80. The density reduction to zero was not done in order to avoid a too large mistreatment of the leakage effects in the diffusion calculations.

The DC was calculated by increasing the fuel temperature of 1395 K in the inner core and of 1318 K in the outer core by 200 K and dividing the resulting $\Delta\rho$ by 200. Only the contributions of the inner and outer core were considered, so that the blankets were neglected hereby. In [3] we had shown, that both blankets have a Doppler coefficient of $-1.7 \cdot 10^{-6} \Delta\rho/K$, which is about 50 % of the core DC or 30 % of the core+blanket DC. Since the absolute temperature increase in the breeder zones in case of a core transient is, however, much smaller than in the fuel pins and since this increase in the radial blanket is additionally delayed because of the larger diameter of the breeder pins, that 30 % contribution is strongly reduced and will therefore be neglected in our discussion.

The calculation of the SVE and the DC has recently been improved by using the MOSES code in TRI-Z geometry with 20 energy groups instead of the RZ-CITATION in 70 groups, on which the results presented in this report are based upon.

Concerning the burnup calculations, it must be mentioned that they are being performed in a somewhat simplified manner by not representing each fuel S/A with its individual burnup, but by considering only the average burnup state of certain sub-zones of the two core zones. These sub-zones are numbered in Fig. 2. That means for instance, that instead of burning the fuel S/As individually during an equilibrium cycle from 0/1/2/3/4 to 1/2/3/4/5 all S/As of a group have the same burnup state and are burnt from 2/2/2/2/2 to 3/3/3/3/3. The whole effort for the calculations was thereby strongly reduced, since only 3 cycles instead of 9 cycles had to be considered. The following calculational steps were performed in this procedure:

	core batches	blanket rows	control rod insertion in cm
step 1 BOL	0/0/0/0/0 2/2/2/2/2	0/0/0 2/2/2	41.3 → 56.8 for BOL power distribution 41.3
step 2	2/2/2/2/2 2/2/2/2/2	2/2/2 3/3/3	41.3 (burnup only for the radial blanket) 41.3
step 3 BOEC EOEC	2/2/2/2/2 3/3/3/3/3	3/3/3 4/4/4	41.3 → 56.8 for BOEC power distribution 41.3 → 25.8 for EOEC power distribution

Step 2 was performed in order to have a burnup of 3 cycles for the radial blanket at the beginning of equilibrium cycle (BOEC), which should be typical for an equilibrium operation and should give a realistic value for the blanket power in the overall power balance. For the burnup calculation the control rod insertion was kept at 41.3 cm, whereas for the power distribution calculation the rods were moved down to 56.8 cm at BOEC and up to 25.8 cm at EOEC.

The consideration of the average zone burnup instead of the S/A-wise burnup has one important consequence on the maximum linear rating results of these calculations. In case of the S/A-wise burnup the fresh S/A have pronounced power peaks because they have to take over part of the power of the burnt S/A, whereas these peaks are levelled out in case of the average burnup, which results in a reduction of the maximum linear ratings. For the reference burner core a comparison of both methods had been performed in [1]. It revealed, that the averaging method leads to an underestimation of the maximum linear ratings between 10 and 15 % with the upper value of these burnup factors being reached in the positions with high flux and high linear power. The maximum linear rating values given later in this report are therefore increased by 15 %

The axial structure and mesh spacing of the different types of core S/A for MOSES is given in Figure 3.

4 Results for the reference core

The main data of the reference core are given together with those of the different burner cores, for instance in Table 8. The maximum linear ratings per S/A are also shown in Figure 4. Considering the burnup factor of 1.15, the maximum numbers in the inner/ outer zone have to be increased from

283/ 295 W/cm at BOEC and of 285/ 273 W/cm at EOEC to

325/ 339 W/cm at BOEC and 328/ 314 W/cm at EOEC.

Other data, worth to be mentioned, are:

- The worth of the control rods of 8.6 % $\Delta\rho$, which is quite consistent with the value of 9 % measured during the start-up experiments for the sum of the individual rods;
- The burnup reactivity loss of -2.75 % $\Delta\rho$ for a cycle of 195 efpd, which was used at this stage of the study for the steel pin burner cores.
- The sodium void effect of 1.5 % $\Delta\rho$ and the Doppler coefficient of $-3.4 \cdot 10^{-6} \Delta\rho/K$, both given for the fissile zones at EOEC;
- The breeding ratios are given in Table 3. The value of 1.09 at BOL is much smaller than the Monju first core value because of the increased enrichment, but the value increases to about 1.15 in the equilibrium cycle, mainly because the increasing blanket contributions.
- The mass balances per isotope are given in Table 4. They will be discussed later in context with the Pu-burning rates together with the breeder-less cores.
- The average discharge burnup can be deduced by using the zone-wise heavy metal inventories and power data (Table 5) together with the cycle length of 203 efpd:

zone		inner core	outer core	total core
HM-inventory	[t]	3478.6	2908.7	6387.3
BOEC power	[MW]	362.5	274.3	636.8
EOEC power	"	364.4	261.2	625.8
av. discharge b.u.	[GWd/t_{HM}]	106.0	93.4	100.3

We can see, that the average core discharge burnup meets very well the target value of 100 GWd/t_{HM}, whereby the inner core value is 6 % larger and the outer core value is smaller by about the same amount.

The maximum local burnup values can be deduced with the maximum linear ratings at BOEC and EOEC given above. The burnup factors have not to be considered here, because the larger ratings in cycles one and two of a fuel S/A are compensated by the smaller ones in cycles four and five, which means that the third cycle can be considered to be representative for the whole life of the S/A. Together with a heavy metal linear weight of 2.05 g/cm, we get maximum local burnups of 140.6 GWd/t_{HM} in both core zones. This indicates burnup form-factors of 1.33 in the inner core, 1.51 for the outer core and of 1.40 for the total core. As it has been discussed in [1], these numbers could be improved, when the residence time for the low rated S/As would be increased from five to six cycles. The average discharge burnup could then be increased by about 5 %, which could be used for a 5 % cycle length reduction with the benefit of a reduced reactivity loss.

5 Results for the burner cores with diluting pins

5.1 General aspects

As diluting materials steel, $MgAl_2O_4$ or $^{11}B_4C$ have been used, in some cases together with $^{nat}B_4C$ and $ZrH_{1.7}$ in order to improve some core characteristics. The data of these materials were the following:

material	effective density [g/cm³]
steel (SUS)	7.50
$MgAl_2O_4$	3.48
$^{11}B_4C$	2.24
$^{nat}B_4C$	2.24
$ZrH_{1.7}$	5.20

Basic idea of the diluting pin concept is to introduce these pins into the inner core fuel S/A in order to reduce their flux level to such an extend, that the higher outer core enrichment can also be used in these S/A. The combination of the high enrichment and the smaller number of fuel pins would also keep the reactivity of the fuel at the right level. By this means the goal of the burner cores of having an as high as possible average fuel enrichment could be achieved. The task of the core design is then to find that number of diluting pins, which flattens the radial power distribution as much as possible and results in similar maximum linear ratings for the inner core S/A with diluting pins and of the outer core S/A without diluting pins, and these values should exceed those of the reference core as little as possible.

In addition to the linear power, the important safety parameters (absorber worth, sodium void effect and Doppler effect) have also to be considered, and it has to be verified that the influence of the core changes on these parameters is acceptable.

5.2 Parametric overview calculations

5.2.1 Neutron-physics aspects

In a first step a parametric study was performed, in which we varied the number of steel pins, which replace the fuel pins in the 169 pin reference bundle, in order to see the influence of the number of steel pins on the power distribution. We started with a one-zone core without any steel pin and then replaced up to 71 of the fuel pins. Only the fresh state was considered in this study with the control rods inserted at the BOC height of 56.8 cm. The power distribution was calculated with MOSES and EVA. The results are collected in Table 6 and Figure 5, where they are compared with the data of the two-zone reference core.

The k_{eff}-values given in Tab. 6 show the expected trend of going down almost linearly with the number of steel pins or the plutonium mass (Pu). The gradient of $\Delta k/k = 0.67 \cdot \Delta Pu/Pu$ is somewhat larger than the usually observed value of 0.56. This is caused by the fact, that it is not the average Pu-content or Pu-mass of the total core, which is changed, but only that in the inner core with its higher importance, so that a smaller change is necessary for a certain change in k_{eff}. We also see, that the k_{eff} level of the two-zone reference core is reached with about 43 steel pins and the single enrichment of 33 %, which is the outer core value of the two-zone reference core.

When looking at the radial power distribution with different numbers of steel pins, we see that the starting case 169/0 without steel pins and one single enrichment has the expected radially rather steep power distribution and a maximum linear rating of 430 W/cm. The intro-

duction of the steel pins in the following cases then helps to flatten the radial flux and power distribution, but this flattening is not effective enough to reduce the maximum linear rating below the level of case 169/0, since due to reasons of normalisation the loss in fuel pins requires a global flux increase, which is stronger than the flux depression by the steel pins. Because of this normalisation together with the flattening effect of the steel pins, the power in the outer core S/A increases continuously with the number of steel pins, which is obvious in Fig. 5 as well as in the zone power data given in Table 6. The power flattening effect is also quantified with help of the radial form-factors given in the last column of Table 6. It is reduced continuously by the insertion of the steel pins from 1.566 without steel pins down to 1.229 in case of 71 steel pins. This value is close to those of the two-enrichment cases, but because of the presence of the steel pins the maximum linear rating is much higher.

These results seem to indicate, that steel as diluting material is not strong enough to reduce the flux level sufficiently in the area of the inner core S/A, so that they could be operated with the high outer core enrichment without having too high maximum linear ratings. One way out of this dilemma is to use a lower enrichment for the inner core S/A, which has been tried with case 2a, also included in Table 6 and Figure 5. It shows that the linear rating can be reduced strongly with help of the second enrichment, but it is still about 15 % larger than in the reference case. More details about this concept will be discussed in chap. 5.3.

5.2.2 Thermal-hydraulics aspects

The thermal-hydraulic boundary conditions for the choice of possible bundle designs with diluting pins is somewhat complex. In contrary to the burner cores with diluents, where a S/A-wise mass-flow redistribution occurs due to the different cooling requirements of the diluents and the fuel S/A, the mass-flows per S/A will not directly be influenced by the introduction of the diluting pins, which will have the same diameter as the fuel pins. But the insertion of the diluting pins into the fuel pin bundle will affect the power distribution within the bundle strongly, since the diluting pins are more or less powerless with a linear power of roughly 10 % of the fuel pin values, and consequently the temperature distribution within the bundle together with the average temperature rise (ΔT^{av}) and the maximum temperature rise (ΔT^{max}) will be strongly affected.

In order to get a feeling for these influences, we looked at a variety of bundle designs with varying numbers of diluting pins and calculated the channel-wise and average ΔT with help of the EXCEL formulas. Starting point was a typical inner core fuel S/A of the Monju first core, which we made 30° symmetric. The channel-wise ΔT-distribution is shown in Figure 6. The average S/A ΔT have been calculated by weighting the channel-wise ΔT with the multiplicity M, which is the number of channels in the S/A, and an additional factor of two for the edge and corner channels because their mass-flow is twice as large as that of the interior channels. Table 7 shows the main data of this reference S/A, which are:

maximum ΔT	= 196.3 K
average ΔT	= 174.1 K
temperature form-factor	= 1.128.

Mixing between the different sub-channels has not been taken into account here, so that the maximum ΔT may be somewhat too large. The above value for the reference core and the related temperature form-factor are, however, quite reasonable.

Into this bundle of 169 fuel pins we then inserted step by step steel pins and calculated the resulting temperature distribution with the final goal to find a steel pin distribution with a form-factor as close as possible to the reference bundle. When inserting the steel pins, the power of the remaining fuel pins was kept unchanged, which means that no adaptation of the power level has been performed to compensate for the loss in total power due to the presence of the steel pins. This adaptation will be considered later in this report (chap. 5.6), when we know how large this adaptation will have to be. For the steel pins themselves a power of 10 % of the fuel pin power was considered, so that for instance the bundle power of 2 fuel pins and one steel pin is not 66 % of the standard bundle but 70 %. More details about this procedure are given in [2].

The number of steel pins was varied between 30 and 72. For some of them the ΔT^{max} and the ΔT^{av} together with the radial temperature form-factors ($\Delta T^{max}/\Delta T^{av}$) are collected in Table 7. Some more details about these calculations are given in [2]. The bundle arrangements with 43, 57, 67 and 72 diluting pins are also shown in Figure 7.

Table 7 shows, that the ΔT^{max} go down continuously from 0 to 37 and 67 steel pins. In the cases with 37 and 43 steel pins many of the interior channels have got one steel pin (see Fig. 6), but there are still some channels with three fuel pins and therefore a relatively high ΔT^{max}. In case of 57 steel pins all interior channels have one steel pin, so that the edge channels are determining the ΔT^{max}. In case of 67 steel pins these edge channels also have got a steel pin each, so that the ΔT^{max} of 137.4 K is given by the hottest interior channel with one steel pin. A further reduction of the ΔT^{max} would require a rather large number of additional steel pins because of the flat channel-wise ΔT distribution, for instance 30 additional pins would be necessary to reduce the ΔT^{max} from 137.4 K to 126 K. The resulting number of steel pins would be too large and is not worth to be further considered.

In parallel with the ΔT^{max} the S/A average values ΔT^{av} are also reduced, but these reductions are stronger than those of the ΔT^{max}. In the case of 43 steel pins for instance 253 of all 336 coolant channels or 75 % have got a steel pin and therefore a reduction of their ΔT by 30 %, so that the average is reduced by 30x0.75 = 22 %. The hottest channel has then been moved from the centre to an outer position with its ΔT of 164.9 K being only 16 % smaller than the central one of 196.3 K. Consequently, the temperature form-factor is larger than that in case without steel pins.

The ideal condition to have just one steel pin in each channel cannot be reached perfectly due to simple geometrical reasons. But if we nevertheless consider that theoretical case (last column in Table 7), the temperature form-factor is larger than in the reference case, because in the edge and corner channels one out of two fuel pins is replaced and thus reducing the ΔT by 43 % instead of the 30 % for the ΔT^{max}. In reality the case with at least one steel pin per channel can only be achieved with some interior channels having two steel pins and one fuel pin and with some edge channels having two steel pins and consequently no fuel pin. This is the case with 67 steel pins, the temperature form-factor of which is similar to the cases with smaller numbers of steel pins.

In conclusion we can say, that from the thermal-hydraulic point of view the configurations with steel pin numbers between 37 and 67 are relatively similar with respect to the temperature form-factor, whereas larger numbers are not meaningful because of their too bad temperature

form-factors. Which number of steel pins finally can be feasible, will depend on the outcome of the detailed neutron-physics calculations to be presented below. Their important result will be, to which extent the maximum linear rating will increase, because this will compensate part of the above discussed unavoidable reduction of the ΔT^{av}. It will then have to be checked, whether the corrected ΔT^{av} fulfils the requirement to keep the average core ΔT constant and whether the related ΔT^{max} is compatible with the limit of the maximum temperature increase.

5.3 Results for burner cores with steel pins only

On the basis of the calculations described in chap. 5.2.1 a few cases with steel pins and one plutonium enrichment were extended to the burnup calculation in order to see how the power distribution develops during the burnup in these cores. They are collected in Table 8. In addition to the large linear rating values at BOL discussed in chap 5.2.1, we see that these values burn down strongly at BOEC and EOEC, but they are still much larger than the values of the reference core. Typical differences are +30 % at BOL, +16 % at BOEC and +20 % at EOEC. These in the inner core zone occurring peaks could be reduced somehow by using different insertions of the 6 inner 6 and the 12 outer control rods to flatten the power distribution. As a general rule we had shown in [2], that a 10 cm down-movement of the inner rods versus an up-movement of the outer rods would change the maximum linear ratings

at BOC: by -4 % in the inner core and ±0 % in the outer core, and

at EOC: by -4 % in the inner core and +2 % in the outer core.

If we would take into account a power flattening with the help of the control rod insertion effect, the above mentioned differences of 30 %/ 16 %/ 20 % could be somewhat reduced, but would still be too large, so that we have to conclude, that single enrichment cores with diluting steel pins are not feasible.

Consequently, some two-enrichment cases have been investigated, the results of which are also collected in Table 8. Starting from the enrichments of the reference case of 25.5/33.0 %, the insertion of the steel pins brings the two enrichments closer to each other, but in the outer core an increase is also necessary, so that the outer core value with 57 steel pins exceeds already our limit of 35 %. Taking that criterion strictly would limit the number of steel pins to only 30, but assuming some flexibility around the 35 % border, the cases with 43 and 57 are also included in the further discussion.

Concerning the maximum linear ratings we can state the following trend for the three cases with 30, 43 and 57 steel pins in comparison with the reference case, whereby for the inner core/ outer core values one average is given by making use of the control rod movement effect:

	refer. case	case 139/ 30	case 126/ 43	case112/ 57
BOL	328 (1.00)	355 (1.08)	370 (1.13)	388 (1.18)
BOEC	295 (1.00)	319 (1.08)	331 (1.12)	342 (1.16)
EOEC	277 (1.00)	296 (1.07)	306 (1.10)	315 (1.14)

We have to state the clear trend, that the maximum linear ratings are increasing continuously with increasing number of steel pins: 8 % with 30 pins, 12 % with 43 pins and about 16 % with 57 pins. In order to avoid an increase of the maximum linear rating by much more than 10 %, the case with 43 steel pins has been selected as just acceptable. Figure 8 shows the S/A-wise

maximum linear rating distribution for the three burnup states, and Table 9 gives the isotope-wise mass-balances.

With respect to the other core parameters, Table 8 shows that the insertion of the steel pins and the consequent increase of the fuel enrichments cause for the three fuel pin/ steel pin combinations:

	139/ 30	126/ 43	112/ 57
an increase of the burnup reactivity loss of	16 %	21 %	26 %
a decrease of the sodium void effect of	5 %	7 %	10 %
a decrease of the Doppler coefficient of	5 %	8 %	11 %

Concerning the increased burnup reactivity loss it will have to be checked, whether the related increased shutdown requirements can be fulfilled with the present design of the control rods or whether an increase of the ^{10}B-enrichment will be required. The control rod worths themselves are only slightly reduced by the introduction of the steel pins, as also indicated in Table 8. The changes of the sodium void effect and Doppler coefficient are also relatively small and should therefore be acceptable, especially since the reductions of the sodium void effect are compensating those of the Doppler coefficients in most of the transients of the core.

The main consequence of the steel pin introduction seems to be the increased maximum linear rating, so that other measures for a reduction of the linear rating have been investigated, which will be described below.

5.4 Results for burner cores with $MgAl_2O_4$ and $^{11}B_4C$ pins

In a first step it has been investigated whether the two alternative moderating materials $MgAl_2O_4$ and $^{11}B_4C$ would help to improve the situation with respect to the power distribution. Their main material parameter had been mentioned in chap.5.1 with the inside cladding smeared densities of 3.48 g/cm^3 and 2.24 g/cm^3, respectively. Table 10 shows the main data for the comparison of the two alternative diluting materials together with those of the steel pin case and the reference case.

First, we have the comparison for the case with one single enrichment and 57 diluting pins (cases 2d, 3a, 4a). We can see that the reactivity effects of the three diluting materials are relatively similar, since the k_{eff}-values for BOL don't change very much. Without any diluting pin the k_{eff} would be 1.228, so that the reactivity worth of the 57 pins are

-12.2 % $\Delta\rho$ for steel, -11.6 % $\Delta\rho$ for $MgAl_2O_4$ and -12.0 % $\Delta\rho$ for $^{11}B_4C$.

These values correspond more or less to the loss of fuel, since 57 out of 169 pins in 108 out of 198 fuel S/A mean a loss of 18.4 %, which in average should lead to a reactivity effect of about -9 %, which then is increased to about 12 %, since the loss is only occurring in the inner part of the core with high importance.

The maximum linear ratings are however changing somewhat, when steel is replaced by $MgAl_2O_4$ or $^{11}B_4C$. In the outer core zone they are remaining constant, but in the inner core they are increasing from steel to $MgAl_2O_4$ and $^{11}B_4C$. The reason for that is the spectrum softening effect of $MgAl_2O_4$ and $^{11}B_4C$, which is illustrated in Figure 9, showing the neutron spectra of the inner core zones of the reference case and the cases with 57 steel, $MgAl_2O_4$ and $^{11}B_4C$ pins. We can see, that the softening effect of steel is rather limited, but it is stronger with $MgAl_2O_4$ and

strongest in case of $^{11}B_4C$. This spectrum softening is causing an increase of the effective fission cross-section of ^{239}Pu in the inner zone relative to that of the outer zone, so that the cores have effectively no more a single enrichment, but a larger one in the inner zone.

Because of the high linear rating levels in the one-enrichment cores, all three diluting materials require the use of two enrichments. This has been realised for the last three cases in Table 10, for which the fuel enrichments have been adapted to get similar maximum linear ratings in both core zones. Because of the stronger moderating effects of $MgAl_2O_4$ and $^{11}B_4C$, discussed above, and the consequently larger plutonium fission cross-section in the inner core zone, the outer core values of $MgAl_2O_4$ and $^{11}B_4C$ have to be more increased than for the steel case. We can see in Table 10, that the maximum linear ratings for the three materials are now relatively similar with a slight increase from steel to $MgAl_2O_4$ and $^{11}B_4C$. After adapting the linear ratings of the inner and outer zone with help of the inner/outer control rod insertion, we get the following comparison for the maximum linear ratings in W/cm:

time	steel	$MgAl_2O_4$	$^{11}B_4C$
BOL	370	377	380
BOEC	331	337	340
EOEC	306	310	310

We can state small increases of 2 % and 3 % when going from steel to $MgAl_2O_4$ and $^{11}B_4C$. Concerning the other reactivity effects given in Table 10, we can note:

① The burnup reactivity losses are very similar because the average enrichments are similar.

② The absorber worth values are reduced when passing from steel to $MgAl_2O_4$ and $^{11}B_4C$, because the inner core neutron flux level is going down due to the higher ^{239}Pu fission cross-section. Typical inner core average flux values (in units of 10^{15} $cm^{-2}\cdot s^{-1}$) are:

3.30 for steel, 3.23 for $MgAl_2O_4$ and 3.09 for $^{11}B_4C$.

③ The sodium void effect is reduced in case of $MgAl_2O_4$ and $^{11}B_4C$ because of their stronger moderating efficiency, which reduces the spectrum hardening effect in case of voiding.

④ The Doppler effect is increasing for $MgAl_2O_4$ and $^{11}B_4C$ because of the spectrum softening, which is illustrated in Figure 9.

Taking all effects together, we see that the stronger moderating materials have some advantage with respect to the sodium void and Doppler effect, but they cause a further increase of the maximum linear rating compared with the steel pin case. $MgAl_2O_4$ seems to be preferable compared to $^{11}B_4C$, because it would avoid the stronger reduction of the control rod worth. With this material the Doppler coefficient would be similar to that of the reference case with the sodium void effect being reduced by 16 %. $MgAl_2O_4$ in contradiction to $^{11}B_4C$ also has the advantage to be a well established material (spinel), whereas $^{11}B_4C$ might be burdened by the high costs of the ^{10}B-enrichment process, of which ^{11}B is a by-product. But basically, the disadvantage of the steel pin concept of increasing the maximum linear rating by a little bit more than 10 % cannot be eliminated by the alternative materials $MgAl_2O_4$ or $^{11}B_4C$. Since the reason for that is, that all three materials are not strong enough to reduce the flux and consequently the power distribution sufficiently in the inner core zone, we tried to use $^{nat}B_4C$ as a stronger material.

5.5 Results for burner cores with $^{nat}B_4C$ and $ZrH_{1.7}$ pins

Since it is well known, that the introduction of B_4C with natural or higher ^{10}B-content has unfavourable consequences on the sodium void and Doppler effect of fast reactors, the combination of $^{nat}B_4C$ and $ZrH_{1.7}$ was considered with the hope, that the moderating effect of the $ZrH_{1.7}$ would compensate the negative consequences of the B_4C. Therefore a parametric study was performed, in which the number of $^{nat}B_4C$ and $ZrH_{1.7}$ pins was varied. The variation was performed for the case with 43 steel pins in the one-enrichment core with 36.1 % enrichment, and part of these 43 steel pins were then replaced by different numbers of $^{nat}B_4C$ and $ZrH_{1.7}$ pins.

The results of this study with respect to the sodium void effect, Doppler effect and the maximum linear rating are collected graphically in Figure 10, where these parameters are shown as a function of the number of $ZrH_{1.7}$ pins with the number of B_4C pins as a parameter. They are given for the EOEC situation as ratios to the corresponding value of the two-zone reference core, i.e. indicating the relative changes due to the introduction of B_4C or $ZrH_{1.7}$. It should be mentioned that all cases had been performed with the same single enrichment of 36.1 % without adaptation of the enrichment for the right EOL-k_{eff}, in order to see the influences of B_4C and $ZrH_{1.7}$ separately without overlapping influence of the enrichment. But the tendencies deduced from Figure 10 would not be changed by the missing enrichment adaptation. These tendencies are:

① The high maximum linear rating of the burner core without B_4C and $ZrH_{1.7}$ pins of 434 W/cm (not shown in Figure 10, but in Table 8, case 2g) or 1.31 compared with the reference case, can be reduced by inserting B_4C pins. In case of 9 B_4C pins for instance to 1.10.

② But the introduction of B_4C has the expected strong influence on the sodium void and Doppler effect: Depending on the number of B_4C pins the sodium void effect is increasing by about 20 % and the Doppler effect is reduced by about 40 %.

③ The deterioration of the sodium void and Doppler effects can be weakened by introducing some $ZrH_{1.7}$ pins. The upper part of Figure 10 shows that -quite roughly- the consequences of a certain number of B_4C pins can be compensated by about the same number of $ZrH_{1.7}$ pins, for instance by the combination of 6 B_4C and 6 $ZrH_{1.7}$ pins, which brings the Na void and the Doppler effect close to 1.00. The effects of B_4C and $ZrH_{1.7}$ on the neutron spectrum are illustrated in Figure 11. The spectrum hardening of the B_4C can be clearly seen and even more pronounced the softening due to the $ZrH_{1.7}$, which increases the flux level in the Doppler energy area around 100 eV considerably.

④ The lower part of Figure 10 shows, however, that the introduction of the $ZrH_{1.7}$ pins causes an increase of the maximum linear rating. This happens, because the moderating effect of the $ZrH_{1.7}$ leads to a further enhanced neutron flux softening and consequent increase of the ^{239}Pu-fission cross-section around the follower positions of the B-rods, where the linear rating maxima are already located without any $ZrH_{1.7}$. We had confirmed this effect by doing a calculation in which fuel S/A of the type with only 43 steel but no B_4C or $ZrH_{1.7}$ pins where placed just around the B-rod on position 71, and in this case the additional increase of the maximum linear rating was avoided. But such a concept with two types of fuel S/A and a special loading around the B-rods is too complicated and would have no chance for a realisation.

For a better and quantitative overview of these tendencies and results, the data of some of the considered cases are collected in Table 11. Starting from the reference case, first the two-zone case no. 2a with 43 steel pins is given together with the corresponding one-enrichment

case 2g, which shows again the rather high linear rating of 434 W/cm in the fresh state. Introducing 9 B_4C pins (case 5) reduces the linear rating to the level similar to the two-enrichment burner case 2a, but increases the sodium void effect and reduces the Doppler effect strongly. Adding 6 or 9 $ZrH_{1.7}$ pins then improves the safety parameters, but also increases the linear rating by 3 or 5 %, respectively. The following case no. 5l with 6 B_4C and 6 $ZrH_{1.7}$ pins finally shows an even further increased linear rating, because 6 B_4C pins are not effective enough to reduce the flux level in the inner core. Its sodium void effect is however similar to that of the reference core with the Doppler effect being 10 % smaller.

The main conclusion of this discussion is, that B_4C helps to reduce the maximum linear rating in a burner core with steel pins and a single enrichment to the level of a two-enrichment core with steel pins, but in order to compensate for the deterioration of the sodium void and Doppler effect, $ZrH_{1.7}$ has to be introduced too, and this causes a further increase of the linear rating. The use of one-enrichment cores with steel and some B_4C pins is therefore not possible.

On the basis of these conclusions, some calculations on cores with two enrichments have been performed. One relevant result is given in the last column of Table 11 for the combination of 6 $^{nat}B_4C$ and 6 $ZrH_{1.7}$ pins. We can note that its maximum linear ratings are reduced compared with the corresponding one-enrichment case 5l, but they are on a similar level as those of the two-zone steel pin core 2a. The Na void and Doppler effects of the one-zone and two-zone cores with $^{nat}B_4C$ and $ZrH_{1.7}$ pins are very similar to those of the reference case and also of the two-zone steel pin core. But their control rod worth is considerably smaller and they also require a much larger fuel enrichment. All together, we have to state, that there are only disadvantages for the cores with $^{nat}B_4C$ pins, so that their consideration for the burner cores does not make sense.

A few calculations were also performed on the combination of $MgAl_2O_4$ and $^{11}B_4C$ pins with $^{nat}B_4C$ and $ZrH_{1.7}$ pins. Some typical results for the two-enrichment cases with 6 $^{nat}B_4C$ and 6 $ZrH_{1.7}$ pins are shown in Table 12 (cases 5p, 6h and 7f) together with the reference case and the case 2a with 43 steel pins only. It can be noticed, that the data for the three diluting materials are very similar. They all have maximum linear ratings at a similarly high level with the tendency to increase from steel to $MgAl_2O_4$ and $^{11}B_4C$. Additionally, their sodium void and Doppler effects are very similar to those of the reference core and the steel pin core. The conclusion drawn above about the use of $^{nat}B_4C$ is, therefore, also valid in combination with $MgAl_2O_4$ and $^{11}B_4C$

5.6 Some further thermal-hydraulics considerations

In chapter 5.2.2 we had performed some thermal-hydraulic estimates to get an idea about the consequences of the replacement of fuel pins by diluting ones. We had seen, that depending on the number of diluting pins, the average temperature rise (ΔT^{av}) of the bundle and the maximum channel rise ΔT^{max} are both reduced with increasing number of diluting pins, but ΔT^{av} is stronger reduced than ΔT^{max}, so that the temperature form-factor $f_{rad} = \Delta T^{max}/\Delta T^{av}$ is increasing. It is clear that for a real thermal-hydraulic evaluation, the respective codes with sub-channel and whole-core cooling strategy analysis have to be applied, but for a further improvement of our understanding about possible thermal-hydraulic problems associated with the diluting pin concept, the estimates made in chap. 5.2.2 will be somewhat extended based on the neutron-physics results of the previous chapter.

The exercise will be performed for the reference two-zone core (no. 1a) and the burner cases with 43 and 57 steel pins (no. 2a and 2k in Table 8). The final choice of the material for the

diluting pins will not be relevant for these considerations. As a point of reference, some Monju design data will be taken from the core design report [7]. Since some data were not available, they were taken from a BRUST [8] calculation, the results of which agreed generally well with those of the design document. The main thermal-hydraulic data of the design case are

- the maximum pin power of 28.3 kW, which defines
- the maximum coolant mass-flow of 21.35 kg/s and
- the pressure drop (Δp) of 4.00 kg/cm^2 within the bundle, which -together with the 0.7 kg/cm^2 for the orificing and the 0.07 kg/cm^2 for the foot- leads to a total Δp of 4.77 kg/cm^2,
- the 196 and 201 K maximum coolant channel temperature increase in C1 and C2.

For the two-zones reference core and the two burner cores the thermal-hydraulic data are given in Table 13 for two versions, either without or with adaptation of the mass-flow distribution of the design case by a redistribution from the inner to the outer core. For their determination via extrapolation from the design case some basic rules were applied:

- proportionality of S/A power and S/A ΔT as well as of zone-wise power and zone-wise ΔT,
- constancy of the ratio of the maximum S/A mass-flow to the total mass-flow in the inner and the outer zone, which means no mass-flow redistribution between the cooling groups,
- quadratic increase of the Δp with the mass-flow.

The main results for the three cores are the following:

① Since the 2-zones reference core differs from the design case by a redistribution of the power from the inner to the outer core, also the coolant temperature rises increase in the outer core in case of no redistribution of the mass-flow. Consequently, the maximum fuel S/A ΔT occurs now in the outer zone and the maximum coolant channel ΔT increases strongly to 217 K. But that can be changed with help of a small coolant mass-flow redistribution from the inner to the outer zone. After this mass-flow adaptation the coolant temperature data of the two-zone reference core are rather similar to those of the design case.

② In case of the burner core with 43 steel pins the power is even more shifted from the inner core to the outer core. The integrated power of the two zones are now the same, but the maximum S/A power of 4.99 MW is much larger in the outer zone than in the inner zone with 3.76 MW. Without a mass-flow adaptation the resulting coolant temperatures are therefore much higher in the outer zone than in the inner zone. The maximum fuel S/A ΔT of 201 K has already reached the level of the hottest channel in the design case, so that the maximum channel ΔT reaches the unacceptable level of 237 K. In order to reduce this level, an increase of the mass-flow to the outer core S/A has been assumed to such an extend that the orificing in the hottest S/A of the outer core is reduced to a minimum of 0.25 kg/cm^2 , so that the mass-flow could be increased from 19.24 kg/s to 22.23 kg/s without an increase of the total pressure drop of 4.77 kg/cm^2. At the same time the inner core mass-flow is reduced. When doing that, the maximum S/A ΔT in C2 is reduced from 201 to 173 K and the maximum channel ΔT is reduced to 204 K, with the inner core maximum channel ΔT being increased to 203 K. These values are 7 K higher than those of the design case, so that the question raises, whether such an increase would be acceptable or not. In any case a real thermal-hydraulic analysis with sub-channel and core coolant strategy evaluation has to be performed. Possibly a somewhat larger mass-flow could be given to the cooling groups with large power, so that the maximum coolant channel ΔT's could be reduced. For instance in

order to reduce the maximum channel values to the level of the design case, a 3.5 % larger mass-flow would be necessary, which then would increase the pressure drop by 7 % beyond the present maximum of 4.77 kg/cm^2.

③ In the second burner case with 57 steel pins the effects of the power redistribution from the inner to the outer core and the consequent temperature increases in the outer core as discussed above are even more pronounced than in the core with 43 steel pins. Without mass-flow adaptation the maximum channel ΔT (ΔT^{max}) reaches 248 K in the outer zone. This can be reduced to 214 K by a mass-flow adaptation with respectation of the present Δp limit of 4.77·kg/cm^2, in which the inner core ΔT^{max} increases to 197 K. A further reduction of the outer core ΔT^{max} would require an increase of the Δp limit. In order to have both zone's ΔT^{max} at 205 K, a 4 % mass-flow increase for the outer core with the corresponding reduction for the inner core would be necessary. This, however, would cause the Δp to exceed the present limit by 8 %. Consequently, the concept with 57 steel pins would require either an increase of the ΔT^{max} to about 215 K or of the pressure drop by about 10 % (rounded up from 8 %).

As summary of these thermal-hydraulic discussions, we can state:

① The high burnup reference core seems to be compatible with the design case after some mass-flow redistribution from the inner to the outer core.

② The burner core with 43 steel pins per fuel S/A also requires a redistribution of the mass-flow from the inner to the outer core. By this means the maximum coolant channel ΔT's can be limited to a level, which is only 7 K higher than in the design case.

③ In case of 57 steel pins per fuel S/A the maximum channel ΔT's are almost 20 K larger than in the design case, if the pressure drop limit is kept at the present level of 4.77 kg/cm^2. If that limit would be increased by about 10 %, the maximum channel ΔT could be reduced to the level of the case with 43 steel pins.

We see, that in case that one or the other of the two burner concepts with diluting pins should be realised, two questions will require an answer:

a) Is an increase of the maximum coolant channel ΔT possible and if so, to what extent?

b) Is an increase of the pressure drop beyond 4.77 kg/cm^2 possible and if so, to what extent?

5.7 Intermediate conclusions about the diluting pins concept

With the two-zone reference core as a basis we have investigated several burner cores with different types of diluting pins. Since for the burner cores there is the incentive to have the average Pu-enrichment as high as possible, we tried to realise cores with only one enrichment. We started with steel as conventional material and studied the influence of the number of steel pins on the core behaviour. It became clear, that steel is not strong enough, in the sense of having not enough negative reactivity compared with the fuel, to reduce the flux and power level sufficiently in the inner core part, so that the use of a single enrichment is not possible. For the two-enrichment cores steel pin numbers in the range of 43 in the Monju bundle with 169 pins were found to be feasible. Larger numbers like 57 are not to be recommended in order to avoid a too strong increase of the maximum linear rating.

In a second step the alternative diluting materials $MgAl_2O_4$ and $^{11}B_4C$ have been studied in comparison with steel. We found, that these materials are similarly weak with respect to their negative reactivity worth, so that their use would also require two enrichment zones. The stronger

moderating effects of $MgAl_2O_4$ and $^{11}B_4C$ have some advantage with respect to the sodium void and Doppler effect, but they also cause a further increase of the maximum linear rating compared with the steel pin case. $MgAl_2O_4$ seems to be preferable compared to $^{11}B_4C$, because it would avoid the stronger reduction of the control rod worth. $MgAl_2O_4$ in contradiction to $^{11}B_4C$ also has the advantage to be a well established material (spinel), whereas $^{11}B_4C$, although ^{11}B being a by-product of the ^{10}B enrichment, might be burdened by the high costs for the enrichment process. With respect to a choice between steel and $MgAl_2O_4$ as diluting material, steel as the well established material is the preferred one, also in view of the smaller increase of the maximum linear rating. Additionally, the fabrication costs for solid steel pins should be much cheaper than those of cladding tubes and $MgAl_2O_4$ pellets or bars. But if later safety studies would reveal strong advantages of the smaller sodium void effect and larger Doppler coefficient, $MgAl_2O_4$ also could be realised.

We then tried to increase the negative reactivity of the diluting pins by adding some $^{nat}B_4C$. Since ^{10}B has the well known disadvantage to increase the positive Na-void effect and to reduce the Doppler effect, we tried to avoid these disadvantages by adding additionally some $ZrH_{1.7}$ pins. We did that successfully, but the moderating effect of the $ZrH_{1.7}$ leads to a strong increase of the linear power in the inner core zone, so that two enrichments are also necessary to reduce the linear power level to that of the two enrichment case with steel pins only. Consequently, there remains no advantage for the addition of $^{nat}B_4C$ and $ZrH_{1.7}$ compared the case with steel pins only, so that their use is not meaningful.

Based on the calculated power distributions with different numbers of diluting pins some thermal-hydraulic estimates have been performed in order to see, how the almost powerless diluting pins influence the temperature distribution within the fuel S/A and within the core. We have seen that 43 diluting pins seem to be compatible with the present design values, but numbers like 57 diluting pins would require an increase of the pressure drop beyond the present value of 4.77 kg/cm^2 and/or of the maximum coolant channel temperature rise. To confirm these results, some detailed calculations with thermal-hydraulic codes will be necessary.

Taking all points together, we came to the conclusion, that a bundle with 43 diluting steel pins would be the preferred candidate for the burner concept with diluting pins. It will be included in the final discussion and judgement in chap. 8.

6 Results for the burner cores with diluents

6.1 Parametric studies

In a first step of the investigation of diluent burner cores a parametric study was performed to get an idea about the necessary number and the positioning of possible diluents. At the beginning five different diluent candidates were envisaged, for which the volume fractions and the average reactivity worth per S/A were calculated, as given in Table 14.

On the basis of these reactivity values the follower type was eliminated from the further studies, since it would require the replacement of a too large number of fuel S/A and therefore would lead to a too strong increase of the maximum linear rating. Also the B_4C diluent type with 2 vol. % of B_4C was excluded from further work, because it is too similar to the steel type and did not promise a significant reduction of the required total number of diluents.

In the next step a systematic variation of the number and position of steel diluents was performed. Base-case for this study was the reference two-zone core with enrichments of 24.3 % and 33.0 %, defined as Pu/(Pu+U) with Pu and U in atom %, in the inner and outer zone, respectively. This core was then transformed into a one-zone core with 33.0 % in the inner and outer core S/As, in which successively up to 39 steel diluents were inserted. Figure 12 explains the different configurations. They are also listed in Table 15, where it is indicated, whether the diluents are equally distributed or gathered on a ring or in a central zone. For these configurations MOSES calculations were performed for the fresh state only with the control rods 56.8 cm inserted. The RZ-model used for the RZ-CITATION calculations is shown in Figure 13.

The main numerical results shown in Table 15 concern the k_{eff} values, the reactivity worth of all diluents and per diluent, the maximum linear ratings of the two core zones (even, if there is the same enrichment in both zones), and the radial form-factors expressed as maximum to average linear power in the fuel S/A only or as maximum to average in the fuel and diluent S/A.

The following comments can be made to these results:

- The reactivity worth per diluent is maximum at about 0.40 % $\Delta\rho$ for small numbers located near the core centre because of the high flux level in the inner core region. It goes down to values around 0.36 % $\Delta\rho$, which remain constant up to the larger number of 39 distributed diluents. If the diluents are concentrated in one zone around core centre as in case 18c, their reactivity worth is reduced to 0.31 % $\Delta\rho$.
- The high maximum linear rating of the one-zone core of 429 W/cm is step by step reduced by the introduction of the diluents and goes down to about 370 W/cm for 21 to 30 diluents. Compared with the reference core the increase of the linear rating is less than 10 %, although up to 15 % of the powerful inner core fuel S/A are replaced by diluents. This is explained by the rather flat power distribution, which is achieved by the insertion of the diluents. This is also reflected by the radial form-factors. They go continuously down, when they are restricted to the fuel S/A only, which indicates that the power distribution is getting flatter and flatter with help of the diluents. When the powerless diluents are also included in the definition, there is a minimum at 27 diluents, because beyond that number the loss in fuel S/A is stronger than the flattening of the power distribution. The effect of the power flattening is also illustrated in Figure 14, which shows the radial power traverses of some of the cases described in Table 15. We again can see, that the traverses for the cases with 18, 27 or 36 diluents are similarly flat as that of the two-zone reference core.

These results indicate, that there is an optimum number of diluents between 20 and 30, which caused us to concentrate the next step of the optimisation work on the steel diluents including burnt core states on that range of diluent numbers.

Concerning the B_4C diluents with either 5 % or 10 % B_4C volume fraction the search for an optimum configuration was limited to total numbers between 12 and 24, where after the first calculations the optimum was expected. It was found that for both volume fractions the number of 18 diluents offers the smallest linear power, however with slightly different positioning. These optimum configurations are shown in Figure 15.

6.2 Results of more detailed investigations

6.2.1 Diluent cores with one fuel enrichment

Based on the results of the previous chapter some configurations with steel and B_4C diluents were selected for more detailed calculations including the burnup history, absorber worth and the sodium void and Doppler coefficients. Besides the reference two-zone core, the burner cores with 21, 24, 27 and 30 steel diluents as well as with 18 B_4C diluents with 5 % and 10 % B_4C volume fraction were investigated. For the burner cores the outer core enrichment of the reference core of 33.0 % was kept unchanged, although an adaptation for the same EOL k_{eff} would be necessary. But at this stage this adaptation was not performed in order to have the clean influence of the number and type of diluents on the core characteristics without the influence of a changing enrichment. For the same reason, the cycle length was kept constant at 195 efpd for all cores. The necessary adaptation was performed in the next step of the study, see chap. 6.2.3.

The results of the power and burnup calculations for the reference core and the burner cores with steel and B_4C diluents are summarised in Table 16. They show the following trends:

- The EOEC k_{eff} values with the control rods inserted at 25.8 cm should be about 1.00 in order to have a reserve of about 1.5 % Δk for power control and uncertainties with the rods fully withdrawn. To reach that target, the enrichments need some adaptation, as is indicated in line 4 of Tab. 16. We can see, that the target enrichment of 35 % is reached with 27 steel diluents or 18 B_4C diluents with 10 % B_4C content.
- The burnup reactivity loss is increasing from 2.7 % $\Delta\rho$ in the reference core to values between 3.5 and 3.6 % $\Delta\rho$ in the burner cores because of their higher plutonium enrichment. For the cores with B_4C diluents it has to be mentioned, that in the burnup calculations the ^{10}B has not been burnt as it would be the case in reality. The reactivity worth of the 18 diluents with 5 % and 10 % B_4C is about 3.2 % $\Delta\rho$ and 4.7 % $\Delta\rho$, respectively, which would be reduced during 195 efpd by 14 % and 11 %, respectively. This would mean that a positive component +0.45 % $\Delta\rho$ and +0.52 % $\Delta\rho$, respectively, would have to be added to the negative burnup effects. The total effect of the cores with B_4C diluents would then be very similar to that of the reference core.
- The control rod worth of the reference case is reduced by about 5 % in the transition to the steel diluent burner cores. For the cores with B_4C diluents with 5 % and 10 % B_4C content, however, the reduction is further increased to 9 % and 14 %, respectively, because the ^{10}B of the diluents is causing a spectrum hardening. This reduction could have some consequences for the control rod design by requiring an increase of the ^{10}B-content.
- The maximum linear ratings of the steel diluent cores (given in line 7 of Tab. 16 for BOL, BOEC and EOEC) show a rather similar behaviour. At BOL they are 12-14 % larger than in the reference core. This increase decreases by a few % at BOEC and increases again at EOEC to the BOL level.

The two burner cases with B_4C diluents (as shown in Fig. 15) are also very similar with respect to the linear power data. For BOL and BOEC their maximum linear power is about 5 % larger than in the reference core, whereas at EOEC the difference increases to 11 %.

- In line 10 of Table 16 the average burnups for a cycle length of 195 efpd are also given. As mentioned already for the reference core in chap. 4, the cycle lengths need an adaptation to reach the target of 100 GWd/t_{HM}, which has been done in the next step of calculations.

- The sodium void effect (SVE) and Doppler coefficient (DC) have also been calculated. Typical values for the core with 27 steel diluents and 18 B_4C diluents in comparison with the reference core are:

		reference core	27 steel diluents	18 B_4C diluents
SVE	core	1.54	0.90	1.15
	core+dil.	1.54	1.30	1.37
DC	core	-3.36	-2.85	-2.08

We see, that the void effect of the fissile zones is strongly reduced in the diluent burner cores because of their larger plutonium content, but if the diluents are included into the voided zones, the reduction is limited to about 15 %. The higher enrichments are also causing a reduction of the Doppler coefficient, and in case of the B_4C diluents the presence of the ^{10}B leads to an additional spectrum hardening, so that the Doppler coefficient is reduced totally by about 40 %, compared with the 15 % reduction in case of the steel diluents.

6.2.2 Diluent cores with two fuel enrichments

Since the steel diluent burner cores had shown a similar effect as the burner cores with diluting steel pins, that the steel is not strong enough to reduce the flux and power distribution in a one-enrichment core sufficiently enough, some calculations were done with two enrichments in order to see, to what extent the second enrichment can help to flatten the power distribution and so to reduce the maximum linear rating. These tests were limited to the two cases with 27 steel diluents and 18 B_4C diluents with 10 % B_4C content. The results are collected in Table 17, whereby adaptations of the cycle length to achieve the target discharge burnup of 100 GWd/t_{HM} and of the Pu-enrichments to achieve a k_{eff} of about 1.00 at EOEC were performed. Therefore, the data for the diluent cores with one enrichment differ somewhat from the data given for these two cores in Table 16.

Comparing the two steel diluent cases 8f and 8k and the two B_4C diluent cases 9a and 9e in Tab. 17, we can see, that the second enrichment reduces the linear power of the steel diluent case by about 4 %. The improvement is, however, small for the B_4C diluent case, because the differences between the inner and outer core values in the one-enrichment case are already small. The other core parameters of the one- and two-enrichment cores show only small differences, except the control worth, which is reduced by 4 % due to the reduced importance of the inner core zone in case of two enrichments.

In conclusion of this part, we can say, that the second enrichment is beneficial for the steel diluent case, in a similar manner as it was stated in chap. 5.3 for the diluting steel pins case.

6.2.3 Diluent cores with moderated diluents

Since we had seen in chap. 6.2.1 and 6.2.2, that one main feature of the diluent burner cores is the reduced Doppler coefficient of the fuel zones, we investigated the possibility to improve the Doppler coefficient by introducing some additional moderating material into the diluents. $^{11}B_4C$ was used in this case.

Table 18 shows the consequences of the $^{11}B_4C$ introduction on the sodium void effect, the Doppler coefficient and the maximum linear rating in case of the steel diluents. Up to 20 absolute % of the 70 % steel volume fraction in the steel diluents were replaced by $^{11}B_4C$. We can see, that the introduction is quite beneficial for the Doppler coefficient and also for the sodium

void effect. This shows that the moderating effect of the $^{11}B_4C$ in the diluents is not limited to the diluents themselves, but is also influencing the fuel zones, so that the Doppler coefficient is made stronger negative and the positive reactivity effect of the spectrum hardening in case of voiding is reduced.

Concerning the maximum linear rating, however, there is an important disadvantage of the $^{11}B_4C$ introduction to be noticed, which is the strong further increase. This occurs at BOL, when the control rods are 60 % inserted, in fuel S/As next to diluents and to B-rods and at EOC, with the control rods only 28 cm inserted, also next to C-rods. In these fuel S/As the moderating effects of the follower and of the diluents overlap each other, so that in these regions with strongly softened spectrum the plutonium fission rate and therefore the power density is strongly increasing. If we would like to take benefit from the $^{11}B_4C$ on the sodium void effect and Doppler coefficient, about 10 % $^{11}B_4C$ would be necessary, and in this case the increase of the maximum linear rating would be 6 %. This, however, would not be acceptable, so that the concept of steel diluents with moderator has to be rejected.

For the B_4C diluents the case 9a in Table 17 with 10 % $^{nat}B_4C$ content was chosen. In a first step 48 absolute % of the 68 % steel were replaced by $^{11}B_4C$. Since the ^{10}B was gaining negative reactivity due to the spectrum softening, the k_{eff} decreased too much, so that the $^{nat}B_4C$ content was reduced from 10 % to 6 %. The results for these cases are collected in Table 19.

We can see, that the replacement of steel by $^{11}B_4C$ causes a decrease of the k_{eff} by about 2 %, because the negative worth of the diluents is increasing due to the spectrum softening effect of the $^{11}B_4C$. This also causes the sodium void effect to decrease and the Doppler coefficient to increase. When we then reduce the $^{nat}B_4C$ content from 10 % to 6 % in order to increase the k_{eff} to its original level, the void effect is only slightly, but the Doppler effect is strongly increased. It is then 26 % larger than in the case without $^{11}B_4C$, and the reduction compared with the value of the reference core ($-3.36 \cdot 10^{-6}$ $\Delta\rho$/K, Tab.17) is limited to 22 %. The effects of ^{10}B on one side and of ^{11}B on the other on the core spectrum are illustrated in Fig. 16. Starting from the reference case without any diluents, case 8k with steel diluents shows the softest spectrum, whereas case 9a with the 18 B_4C diluents has the hardest one. If we then insert the $^{11}B_4C$ into the diluents (case 9g), the spectrum is again softened, similar as in case of the steel diluents.

Finally, a comparison of the two moderating materials $^{11}B_4C$ and $MgAl_2O_4$ was performed. The main difference between the two materials is the smaller moderating efficiency of $MgAl_2O_4$, which causes a 6 % larger void effect and a 12 % smaller Doppler coefficient. It also makes the ^{10}B of the diluents less reactive, so that a larger amount of B_4C would be necessary to keep the reactivity constant. This increase then further deteriorates the void effect and Doppler constant, so that $^{11}B_4C$ would be the preferable material compared with $MgAl_2O_4$.

6.2.4 Influence of small amounts of $^{nat}B_4C$ in steel diluents

In order to check a possibility to increase the flexibility of the steel-diluents, we looked at the influence of a few percent of $^{nat}B_4C$ in the steel diluents on the core parameters. By this means, for instance, the fuel enrichments could be increased or the power distribution could be adjusted for a given number of diluents. For the case with 2 % $^{nat}B_4C$, the results are the following:

- The k_{eff} decreases by 1.5 % Δk, which means that the introduction of the $^{nat}B_4C$ would allow an enrichment increase of about 3 %, relative.
- With respect to the power distribution, the $^{nat}B_4C$ causes a flux depression in the inner core area, so that the power in the outer core S/A increases. The absolute level of the linear power is however not changed, since the power peaks are moved from the inner part of the zone with diluents to its outer part.
- The ^{10}B in the $^{nat}B_4C$ causes an increase of the sodium void effect by about 10% and decreases of the Doppler coefficient by about 15 % and of the control rod worth by 5 %.

These results show, that with the help of a few percent of $^{nat}B_4C$ some flexibility can be gained to adapt the reactivity worth of the steel-diluents for a given fuel enrichment. The level of the maximum linear rating is hardly influenced by the introduction of a few percent of $^{nat}B_4C$, but the safety parameters (void effect, Doppler coefficient, control rod worth) are worsened due to the presence of the ^{10}B.

6.2.5 Thermal-hydraulics considerations

The main consequence of the introduction of diluents into the core is the mass-flow redistribution from the diluent positions to the other fuel S/A positions. These positions, however, require an increased mass-flow in order to keep the maximum mid-clad temperature constant for the cases with increased linear rating. The increased mass-flows to the core positions will also cause a pressure drop increase.

In order to check the consequences of the mass-flow redistribution, some calculations with the code BRUST were performed, in which the number of diluents in the inner core zone was varied between 0 and 27. The related power data are somewhat different from those calculated by MOSES in our study, but the use of BRUST data has the advantage, that we get a consistent set of neutron-physics and thermal-hydraulics data. Since the diluents in BRUST are power-less, no difference between steel or B_4C diluents can be made. Therefore, the mass-flow redistribution to the core is slightly overestimated, because the diluents will also require some forced coolant flow. The results of this parametric study, collected in Table 20, indicate the following points:

- The power is shifted from the inner core to the outer core, whereas the maximum S/A-power increases in both zones by a similar amount according to the reduction of the number of S/A, for instance by 13 % in case of 27 diluents.
- The mass-flow per zone follows the redistribution of the power. But it should be mentioned, that the sum of the inner plus outer core mass-flow is slightly reduced, when the number of diluents is increasing, because the power of the radial blanket is increasing at the same time, so that some additional mass-flow is also given to the blanket. In case of 27 diluents for instance this increase is 2 %.
- The maximum mass-flows per S/A are increasing, for instance by about 12 % in case of 27 diluents, which causes an increase of the bundle pressure drop by twice that amount.
- The maximum channel ΔT is slightly increasing because of the small mass-flow redistribution to the radial blanket. The amount of 2 %, mentioned above, is the reason for the increase by 4 K in case of 27 diluents.

Both, the pressure drop and the maximum channel ΔT are increasing. Concerning the Δp, the increase should be acceptable in view of the design value of 4kg/cm^2. The value for the

case of 27 diluents is exceeding that value only slightly, whereby a detailed analysis including some mass-flow direction to the diluents will most probably reduce the fuel S/A pressure drop. The increase of the maximum channel ΔT of some K, however, will require careful consideration, if these concepts will be further pursued.

6.3 Intermediate conclusions about burner cores with diluents

Starting from the two-zone reference core, we have investigated several burner cores with steel diluents and with B_4C diluents with 5 and 10 volume % of B_4C with natural ^{10}B-content. Since a core with a single enrichment would offer the highest burning rate while respecting the upper limit of the enrichment of 35 %, we have increased mainly the inner core enrichment (25.5 % in the reference core) by introducing the diluents into the inner core zone only.

With respect to the steel diluents, we have seen that an optimum flat radial power distribution can be found for diluent numbers of up to 30. The radial form-factor is smaller than that of the two-zone reference core, so that the loss of about 15 % of the fuel S/A is partly compensated with the increase of the maximum linear rating being about 12 %. This increase can be further reduced by 3-4 %, when two enrichments are used instead of one enrichment.

The B_4C diluents have a stronger negative reactivity than the steel diluents, so that a smaller number is sufficient to reduce the flux and power level sufficiently in the inner core area. The optimisation of the positioning of the B_4C diluents has shown that an optimum radial power distribution can be realised for both investigated volume fractions with 18 S/A. Since the 35 % fuel enrichment target could be realised with 10 % volume fraction, this design is to be considered as the best candidate for this type of diluent. When making use of the control rod effect on the inner core and outer core peaks, the increase of the maximum linear ratings are 5 % at BOEC and 8 % at EOEC.

The use of moderating material inside the steel diluents would offer the improvement of the sodium void effect and Doppler constant, but it would also increase the maximum linear rating by about 6 %, which is not acceptable in view of the already increased linear rating level of the steel diluent burner cores. This concept of steel diluents with moderator can therefore not be recommended. For the $^{nat}B_4C$-diluents, however, it is interesting, since it reduces the sodium void effect by about 10 % and increases the Doppler effect by about 25 % with only a minor increase of the maximum linear rating of about 2 %. Since together with this increase the gap between the inner core and outer core linear rating level is enlarged, the implementation of a second Pu-enrichment would become more effective and could help to avoid that small increase completely.

From these discussions, we have to conclude, that the two concepts with

- 27 steel diluents and two fuel enrichments or
- 18 B_4C diluents and one fuel enrichment

would be the favourite ones. For these two concepts a core cross-section is shown in Figure 17, and the S/A-wise maximum linear ratings are given in Figures 18 and 19. Their mass-balances are shown in Tables 21 and 22. They will be used later (chap. 8) in the comparison of the burning capabilities of the different cores.

7 Results for the cores with reduced blankets

In order to separate the influences of the radial and axial blanket reduction or suppression from each other, the blankets were first reduced separately and then together.

Since it is to be expected, that the suppression of the radial and/or axial blanket will change the neutron leakage towards the tank internal structures, these changes need special attention. In order to get an impression about that, we have defined one zone at the radial boundary of our model (no. 22 in Fig. 2) and one zone at the lower boundary (no. 31 in Fig. 2), for which the neutron flux changes compared with the reference core are calculated. Since our core design methods are not adequate for these zones far away from the core, these data can only give a rough idea about the flux changes and the effectiveness of those design measures, which we propose to compensate for the consequences of the blanket suppression.

7.1 Cores with reduced radial blanket

The radial blanket has been reduced in a first step from three to one row (case B5 in Table 23) and then completely (case B2). Hereby the blanket S/As were basically replaced by S/As of the radial shield type, which contain 78 % steel (SUS316) and 22 % sodium (no. 6 in Tab. 2). Since the high steel content of 78 % can possibly not be realised, because at least in the first row with its relatively high gamma power a steel pin bundle may be required due to cooling reasons, the steel content was reduced to 50 % (case B3) in order to see the influence of the modified steel content. In addition to that, since the better reflection properties of steels with higher Nickel content are well known, the SUS-material with a Fe/Ni/Cr ratio of 65.5/13.5/17.0 was replaced by a PE16 type ratio of 35.5/43.5/17.0 with a larger Ni-content (case B4). Finally, two further variations were performed, which possibly could help to improve the sodium void effect by enhancing the neutron leakage from the core. In the first case (case B8) the UO_2 of the radial blanket S/A was simply replaced by a gas plenum leading to a rather transparent material, and in order to limit the radial neutron leakage to the tank internals, the third row of the former blanket was filled with a reflector material containing 58 % steel, 20 % $^{nat}B_4C$ and 22 % Na. The second variation consisted of a poisoned reflector directly adjacent to the core, in which either 10 % (case B6) or 20 % (case B7) of the 78 % steel were replaced by $^{nat}B_4C$.

The results for these cases are collected in Table 23 for their main core parameters.

7.1.1 Influence of the radial blanket reduction on k_{eff} and burnup reactivity loss

When the fresh blanket S/As are replaced by reflector material (cases B2 to B4), the k_{eff} increases because the UO_2 is acting as an absorber and because of the better reflecting properties of the steel. The outer core fuel enrichment has therefore been reduced from 33 % to 32 %, but despite of that the k_{eff} at BOL is still 7 ‰ larger with the standard SUS steel reflector in case B2. This difference is then almost used up during the burnup because of the larger burnup reactivity loss in the breeder-less core. For the same cycle length of 203 efpd the difference would be –2.86 %Δρ versus –3.34 %Δρ, i.e. a relative increase of 17 % because of the suppressed radial blanket contribution. But since the cycle length has been reduced to 190 efpd in order to keep the average core discharge burnup constant at about 100 GWd/t_{HM}, the increase of the burnup reactivity loss is limited to 9 %, relative.

When the standard steel reflector with 78 volume % SUS is replaced by a more transparent one like the SUS50 with 50 % steel, the k_{eff} is reduced by 0.4 %, and when the UO_2 is

replaced by gas-plenum the reduction reaches 3 %. This corresponds to case B8, which then required an increase of the enrichments to 26.0 % and 36.0 % in C1 and C2. On the other side the k_{eff} increases by about 0.3 %, when the SUS is replaced by the better reflecting PE-16 type material with higher Ni-content.

As it is to be expected, the poisoning of the reflector with B_4C (cases B6 and B7), causes a strong k_{eff}-reduction, which has to be compensated by an increase of the enrichments.

Finally, case B5 with the reduced blanket size also allows an enrichment reduction. The cycle length, however, has been set 4 % too short in this calculation, so that the reactivity loss for the correct cycle length of 198 efpd would be -2.89 %$\Delta\rho$ and so very close to that of the reference case.

7.1.2 Influence of the radial blanket reduction on the power distribution

The consequences of the radial blanket suppression on the power distribution are two-fold: on the integral level the total core power has to increase because of the missing blanket contribution, and secondly the changing absorption and reflection properties at the place of the blanket S/As have an influence on the local power distribution near the core/blanket interface.

In order to get a feeling for the integral effects, the following table shows (based on Table 5) the power balance for the reference case for the three time steps. Hereby, the power produced by non-fuel and non-breeder zones of about 4 MW_{th} is not shown in that table. The numbers are given in MW_{th} and in parenthesis in % of the total value.

zone	BOL	BOEC	EOEC
C1	394.6 (55.6)	362.5 (51.1)	364.6 (51.3)
C2	280.3 (39.5)	274.3 (38.7)	261.2 (36.8)
C1+C2	674.9 (95.1)	636.8 (89.8)	625.8 (88.1)
rad. blanket	22.4 (3.1)	47.5 (6.7)	54.4 (7.7)
ax. blanket	12.7 (1.8)	25.1 (3.5)	30.0 (4.2)
total	710.0 (100)	709.4 (100)	710.2 (100)

We can see, that the radial blanket power is increasing from 3.1 % in the fresh state to 6.7 % at BOEC and 7.7 % at EOEC, which means that the core has to take over these percentages in case of the suppression of the radial blanket. These increases are reflected in the data given in Table 23 for the C1+C2 power at BOEC and EOEC, which are 6 % and 7 %, respectively, in case B2 with the blanket replaced by the SUS-reflector. Case B5 with the reduced blanket of one row shows increases of 2.4 % at BOEC and of 2.8 % at EOEC.

Since the blanket suppression is also changing the radial power shape, these integral numbers are not directly reflected in the maximum linear ratings, also given in Table 23. Concerning the reference case and case B2 with the standard SUS-reflector S/A, we can see, that at BOL the maximum linear ratings of case B2 are even slightly smaller than those of the reference core. This is because of the good reflection and smaller absorption properties of the steel compared with the fresh blanket, which causes a flux and consequently a power increase in the outer most row of the core. Consequently, the S/A powers in the outer row of case B2 are in average 8 % larger than those of the reference case, which compensates the loss in the radial blanket power. Additionally, the radial form-factors within the S/As are 3 % smaller without blanket. These facts are illustrated in Fig. 20, where the radial traverses of the maximum linear

ratings per S/A are given for the three burnup states of the two cores. At BOL, we can see the slightly smaller level of the maximum linear rating in the inner core and the smaller gradient in the outer core, but at BOEC and EOEC the values of the reference case are clearly smaller because of the increasing radial blanket power, and the gradients in the two outer core S/A are similar in both cases. The maximum linear ratings per S/A of case B2 are given in Figure 21.

In order to have a quantitative judgement about the linear power increase due to the blanket suppression, an average value between the inner core and outer core values is made by assuming an adaptation of the fuel enrichments and a movement of the inner versus the outer control rods, as discussed in chap. 5.3. We then get the following maximum linear ratings for the two cores with three time steps:

	ref. core 1a	core B2	B2 / 1a
BOL	328	325	0.99
BOEC	295	302	1.02
EOEC	277	295	1.06

For the case with SUS reflector material the conclusion is consequently, that an increase of the maximum linear rating of 2 % at BOEC and of 6 % at EOEC has to be envisaged.

Concerning the other types of reflector material, the following differences compared with the SUS-reflector can be concluded from the numbers in Table 23:

- The more transparent SUS reflector with 50 % instead of 78 % steel content is very similar.
- The PE-16 type reflector (case B4) causes an increase of the outer core power level and a corresponding decrease in the inner core, but after the above mentioned adaptation, the maximum linear ratings are very similar to those of the SUS-78 case;
- When the rather transparent plenum material is located at the positions of the former blanket S/A (case B8), the favourable reflection effect of the steel is no more working, so that the maximum linear rating level is higher. At all time steps the increase compared with case B2 is close to 5 %.
- The consequences of the poisoned reflector (cases B6 and B7) are very similar to those of the transparent plenum material, since both cases cause an increase of the neutron leakage from the core, as it was also indicated by the necessary increase of the plutonium enrichment. The maximum linear ratings of case B6 with the smaller amount of B_4C mixed to the steel are rather similar to those of case B8, with an additional increase of about 5 % compared with case B2. Case B7 with its larger B_4C content shows a further increase of about 2 %.
- For the case with reduced radial blanket the integral core power increases by 2.5 % and so do the maximum linear ratings.

7.1.3 Influence of the radial blanket reduction on the control rod worth

The comparison of the values given for the different cores in Table 23 shows generally an increase of a few relative % compared with the reference core, which is caused by the higher flux level in the cores with reduced or suppressed radial blanket. These increases in absolute units are, however, smaller than those of the burnup reactivity losses per cycle, so that finally a small increase of the ^{10}B-enrichment will be required. Because of its small amount, this increase should, however, not raise special problems.

7.1.4 Influence of the radial blanket reduction on the boundary fluxes

The changes of the radial boundary fluxes have been checked by comparing the flux level in the zone no. 22 in Figure 2 at the radial reflector boundary of our model. In the axial direction the lower most zone no. 31 has been taken. In Table 23 the relative changes compared with the reference case are given for the three time steps BOL, BOEC and EOEC.

Looking first at case B2 with the standard SUS-reflector, we see that at BOL the fluxes are increasing strongly by 80 %, whereas at BOEC and EOEC the increases are somewhat smaller. This tendency is caused by the fact, that the fresh blanket is a rather good absorber, so that its replacement by steel causes a strong flux increase outside the blanket. The burnup of the blanket with the build-up of Pu-239 then causes an increase of the neutron leakage from the blanket, so that the flux increases in case of replacement by steel is smaller. These numbers indicate, that additional shielding measures, such as the implementation of some B_4C into one or two rows of the reflector, can be necessary, if the radial leakage has to be kept almost constant.

It has also to be mentioned, that these numbers can only give an indication about possible changes of the neutron leakage, since our calculational methods are not adequate to treat shielding problems. Additionally, the relative changes given in Table 23 are valid for the total neutron flux, whereas strong differences between the different energy groups do exist. This is illustrated in Tab. 24, where the relative differences between case B2 and the reference case at the position of the radial boundary zone no. 22 are given for the seven energy groups.

Table 24 shows for instance, that the average ratio of 1.81 at BOL for group 1-7 contains contributions between 0.32 in group 1 and 2.27 in group 3. The small numbers in group 1 are caused by the fission neutrons produced in the radial blanket itself, which is increasing during burnup due to the ^{239}Pu production and so reducing the ratio. Possibly, these high energy neutrons have to get a higher weighting in these considerations because of their larger probability to reach the tank internal structures, but this has to be answered by real shielding calculations.

Concerning the other cases, Table 23 shows, that in case of the reduced steel content (case B3), the flux ratio is strongly increasing, for instance from 1.81 to 2.39 at BOL, whereas the PE16-type with its better reflection properties reduces the ratio to 1.04. The case with plenum material (case B8) also shows a large ratio of 2.06 at BOL, although the two rows with plenum material are followed be one B_4C containing row. In this case another row with B_4C would be necessary. Cases B6 and B7, finally, show a small reduction compared with the standard reflector case B2 due to the first B_4C containing row.

Basically, the calculated flux changes in the radial direction should not be critical, since there is enough flexibility to reduce the flux level by improving the shielding efficiency of the reflector S/As.

The neutron fluxes at the lower level are hardly influenced by the design changes on the radial blanket positions, with the exception of case B8, where the transparent plenum area is also opening a downward leakage path.

Finally, it should be mentioned, that the reduction of the blanket from three rows to one row also causes a flux increase at the radial boundary, which is 45 % for the fresh blanket and about 20 % in the burnt state.

7.1.5 Influence of the radial blanket reduction on the sodium void and Doppler effect

Concerning the sodium void effect (SVE), we can state that the replacement of the radial blanket by steel with normal density has only a minor influence. However, when we reduce the content of the steel and make the reflector more transparent, the negative leakage component of the SVE is increasing and so reducing the positive SVE. In case of the plenum material (case B8), the reduction from 1.54 %Δρ to 1.19 %Δρ is quite significant. Since the poisoning of the reflector with B_4C has a similar effect on the leakage component of the SVE as the increased transparency, the consequences on the SVE are similar. Case B7 for instance has a similarly small SVE of 1.25 %Δρ. But the poisoned reflector has the disadvantage, that for a similar reduction of the SVE the increase of the maximum linear rating is larger.

The Doppler coefficient is slightly (almost 10 %) more negative, when we replace the blanket by steel reflectors. This is because the steel is causing a spectrum softening in the outer core zone. The poisoning of the reflector, however, causes a spectrum hardening, which, together with the necessary increase of the enrichment, causes a reduction of the Doppler effect.

Case B5 shows, that the reduction of the blanket from three rows to one row has only a negligible influence on the reactivity coefficients, whereby the core Doppler coefficient is becoming slightly more negative because of the small enrichment decrease.

7.2 Cores with reduced axial blanket

For the reduction of the axial blanket a similar procedure has been followed as for the radial blanket. In a first step the thickness was reduced from 30 cm (upper) plus 35 cm (lower) to 2_12 cm, and then it was completely removed and replaced by different materials, which filled up the 33.44 % UO_2 plus the 2.01 % gas within the fuel pins (see Tab. 2). Basically SUS316 was used as reflector material, but additionally some variations were performed:

- using PE16 with higher Ni-content instead of SUS;
- implementing a transparent plenum area by replacing the UO_2 by gas;
- using a poisoned SUS-reflector to study the influence of the poison on the sodium void effect.

The boundary fluxes were compared for the different cores at the lower boundary in zone number 31 in Figure 2, and if necessary, some additional shielding measures were taken to keep the fluxes similar to those of the reference case.

The results of the different cores with reduced or suppressed axial blanket are collected in Table 25 and will be discussed in the following.

7.2.1 Influence of the axial blanket reduction on the k_{eff} and burnup reactivity loss

When the fresh axial blanket is replaced by the steel reflector material the fuel enrichments can be kept unchanged, since similarly to the radial blanket suppression the k_{eff} at BOL is increasing because of the good reflecting characteristics of the steel and its smaller absorption cross-section. This difference decreases during the burnup due to the larger burnup reactivity loss in the cases without blanket, so that at EOEC the k_{eff} values are very similar. When the plenum with subsequent shielding zone, as in case C7.2, is introduced or the poisoned reflector as in case C4.2, the enrichments, however, need an increase to compensate for the larger leakage from the core.

The cycle length for the cores without axial blanket should be 195 efpd for an average discharge burnup of 100 GWd/t_{HM}, and with this reduced length the reactivity loss per cycle is -3.11 %Δρ. For the unchanged length of 203 efpd it would be -3.23 %Δρ or 13 % larger than in the reference core. This shows, that the axial blanket with its breeding of ^{239}Pu gives a non negligible contribution to the total burnup reactivity loss.

The cases with plenum and poisoned reflector with their increased enrichment necessarily have an increased burnup reactivity loss. On the other side case C1 with the reduced blanket thickness has only a slightly increased reactivity loss, since the thinner blanket is still effectively breeding.

7.2.2 Influence of the axial blanket reduction on the power distribution

The suppression of the axial blanket has similar consequences on the power distribution in the core as the radial blanket suppression, since both act on the integral power of the core and the local power distribution. The zone-wise power data in Table 25 show, that the integral core power is increasing by 4.0 % and 4.6 % at BOEC and EOEC, respectively, when the axial blanket is replaced by a steel reflector. In case of the plenum (case C6) the increase is slightly smaller, whereas in case of plenum plus following B_4C-shield (case C7.2) and of the poisoned reflector (case C4.2) the increases are larger. These somewhat unexpected, although small, tendencies were understood by looking at the power balances of the reactor. They show, that the radial blanket is the explanation, the total power of which changes from case to case, so that the core power is supported differently. The radial blanket gains power in case of the transparent axial reflector material because of the larger neutron leakage to its upper most and lower most regions (no. 17 and 18 in Fig. 2), whereas these zones are more shielded from the core and thus having a reduced power (15-20 %), when the former axial blanket area contains the stronger absorbing material.

In addition to the integral effect of the blanket suppression of about 4 %, the local power distribution is influenced somewhat differently by the different reflector materials. This can be seen in Figure 22, which shows the axial power distributions in the inner core position no. 10 at BOL for the reference case, case C2 with SUS-reflector, case C3 with PE16-reflector and case C4.2 with the poisoned SUS-reflector. We can see, that the reflectors with SUS and PE16 are very similar to each other and that both are increasing the power level at the upper and lower core boundary, so that the maximum linear ratings are almost the same, although the axial blanket power of ~1.5 % at BOL is lost. The axial power form-factors corresponding to the curves in Figure 22 are 1.249 (reference case), 1.232 (SUS) and 1.226 (PE16). When the axial reflector is poisoned as in case 4.2, the flux and power level at the upper and lower core boundaries are strongly reduced, causing the axial form-factor to increase to 1.30 and the maximum linear power by about 5 % compared with the reference case. During burnup all these form-factors are improving because of the stronger reduction of the plutonium concentration in the high flux region around and below core mid-plane, but the above mentioned differences between the axial form-factors remain.

Because the axial blanket contribution to the total power is increasing from ~1.5 % at BOL to ~ 4 % at BOEC and ~ 4.5 % at EOEC, the improvements of the axial form-factor can no more compensate the loss in blanket power, so that the maximum linear power levels are increasing in

the cores without axial blanket. This can be seen in Figure 22 with the axial linear rating traverses for the reference case and case C2 with the axial blanket replaced by the SUS-reflector. We see

- the similar values at BOL for both cores;
- the reduction of the linear power level from BOL to BOEC for both cores due to the flattening of the axial power distribution and the power build-up in the radial blanket, but also the somewhat stronger reduction in the reference core because of the increased axial blanket power;
- between BOEC and EOEC there are only smaller up and down changes in the inner core zone, mainly caused by the control rod withdrawal from 57 cm to 26 cm, whereas the outer zone values are systematically going down because of the fuel burnup and the rod movement.

This behaviour is very similar for the SUS- and PE16-cases and the plenum case C6 without additional B_4C-shielding zone. The comparison of cases C6 and case C7.2 with the additional poisoned reflector below and above the plenum zones near the core, however, show the sensitivity of the maximum linear power to the presence of the absorbing material. It disturbs the axial power distribution strongly in the upper and lower core areas so that the axial form-factors and consequently the maximum linear ratings are increasing by 3-4 %. The same is happening when the poisoned reflector is introduced (case 4.2).

When comparing the axial breeder-less cores with the reference core, we get the following relative changes:

	ref. case 1a	SUS (case C2.2)	PE16 (case C3)	plenum+B_4C (C7.2)	SUS+B_4C (C4.2)
BOL	1.00	0.99	1.00	1.04	1.06
BOEC	1.00	1.02	1.03	1.08	1.09
EOEC	1.00	1.05	1.04	1.09	1.10

We have to conclude, that the axial blanket replacement by the standard reflectors causes increases of the linear power of 2 % and 5 % at BOEC and EOEC. Using PE16 leads to a 1 % smaller increase, whereas the two alternative reflectors lead to 5-7 % larger increases.

Finally, the axial blanket reduction from 30+35 cm to 2x12 cm in case C1 causes an increase of the maximum linear rating of ~2 % in both burnup states, whereas in the fresh state the differences are negligible.

7.2.3 Influence of the axial blanket reduction on the control rod worth

The comparison of the values given in Table 25 for the worth of the 13 control rods shows a small increase of a few relative %, when the axial blanket is reduced in thickness or replaced by the standard reflectors. This is caused by the increase of the neutron flux in the core and a slight spectrum softening near the core/reflector interface. When B_4C, however, is introduced into the reflector directly adjacent to the core as in case C4.2 or below and above the plenum as in case 7.2, this has a strong hardening effect on the spectrum in the upper and lower core parts, so that the control rod worth drops significantly.

7.2.4 Influence of the axial blanket reduction on the boundary fluxes

The changes of the neutron leakage in the axial direction have been followed with the help of region no. 31 in Figure 2, which is located 30 cm below the lower axial blanket. The flux changes given in Table 25 show rather similar tendencies as they were discussed for the radial blanket suppression.

When the axial blanket is replaced by the standard SUS reflector (case C2), flux increases occur, which are largest at BOL because of the good absorbing qualities of the fresh UO_2. Case C2.2 shows that this increase can be avoided, when a 10 cm slice of B_4C containing material is introduced in the lower part of the former blanket zone. In case of the PE16-reflector (case C3) we again see the better reflecting properties because of the higher Nickel content, which reduces the flux increases compared with the SUS–reflector by about 20 %. When the transparent plenum is introduced in case C6, large increases have to be stated, which then can be reduced with the help of a B_4C containing slice as in case C4.2. As the values between 0.42 at BOL and 0.33 at EOEC show, the thickness of the slice could be smaller than the 23 cm in case C7.2. Similarly small values shows case C4.2 with the poisoned reflector, which means that its B_4C-content could be somewhat reduced. In general, these results show, that the axial blanket replacement will not raise basic problems for the shielding requirements, since the introduction of some B_4C can reduce the flux level.

Case C1 finally with the reduced blanket thickness shows flux increases of 20-30 % in the equilibrium cycle. Whether they are acceptable or not would be the outcome of detailed shielding calculations.

7.2.5 Influence of the axial blanket reduction on the sodium void and Doppler effect

With respect to the sodium void effect, Table 25 shows that the replacement of the axial blanket by a normal reflector material has only marginal consequences. The introduction of the plenum or the poisoned reflector, however, are increasing the axial leakage, so that the SVE is reduced. In case of the plenum case C6 the influence is still small (-10 %), but when the B_4C-containing slice is introduced additionally (Case C7.2) or in case of the poisoned reflector, the reductions of about 25 % are quite significant.

The Doppler coefficient shows a similar tendency as in case of the radial blanket suppression. It increases slightly for the different steel reflectors and also for the plenum case, because they all lead to an increase of the low energy fluxes as shown in Figure 3 for the radial blanket suppression. The cases C7.2 and C4.2 with their additional B_4C-containing reflector material then have smaller Doppler coefficients than the reference case because of the spectrum hardening of the B_4C and the higher plutonium enrichments.

As it is to be expected, the blanket reduction from 30+35 cm to 2x12 cm in case C1 has a negligible influence of the sodium void and Doppler effect.

7.3 Cores with reduced radial and axial blanket

Based on the results obtained by the calculations for the separate suppression of the radial and the axial blanket, only a few cases were run for the combined suppression of both blankets, with the results being collected in Table 26:

- In a first step the radial blanket was reduced to one row and the axial blanket to 2x12 cm with the rest of the former blankets being replaced by SUS-reflector materials (case D1.3).
- In the second case both blankets were completely replaced by SUS-reflector material. But in order to reduce the boundary fluxes, poisoned reflector material was introduced into the third row of the radial reflector and above and below the 25 cm of standard reflector replacing the upper and lower blanket (case D2.3).

- In the last case transparent materials were introduced into the first two rows of the former radial blanket and into the first 20 cm above and below the core. These zones were then followed by B_4C containing reflector materials to keep the boundary fluxes low (case D3.2).

The isotopic mass balances for the cases D1.3 with reduced blankets and D2.3 with the blankets replaced by a SUS-reflector are given in Tables 27 and 28. They will be discussed later in the summary (chap. 8) together with the breeding ratios, contained in Table 3.

7.3.1 Influence of the radial and axial blanket reduction on the k_{eff} and burnup reactivity loss

Since the calculations on the separate suppression of the radial and the axial blanket had shown, that the fuel enrichments can be either slightly reduced or kept unchanged, the enrichments of the reference case were overtaken in case D2.3 with the SUS-reflectors. We see, that the k_{eff} at BOL is almost 2 % larger in the breeder-less core and that it is reduced during the burnup because of the larger burnup reactivity loss. At EOEC it is still 0.8 % larger in case D2.3 than in the reference case, so that in principle a slight enrichment reduction could be performed. But that has not been done here. The reactivity loss in the shortened cycle of 180 efpd is -3.31 % $\Delta\rho$, which means an increase of 30 % compared with the reference case assuming the same cycle length. These 30 % are composed out of 17 % from the radial and of 13 % from the axial blanket suppression.

The implementation of the transparent reflector in case D3.2 again requires an increase of the fuel enrichments, so that the burnup reactivity loss is further increased to -3.52 % $\Delta\rho$, which is almost 40 % larger than in the cores with blankets for the same time interval.

7.3.2 Influence of the radial and axial blanket reduction on the power distribution

The power balance given in chap. 7.1.2 for the reference core shows, that the power of both blankets together increases from 4.9 % at BOL to 10.2 % at BOEC and 11.9 % at EOEC, which consequently have to be taken over by the core in case of the blanket suppressions. This is also confirmed by the BOEC and EOEC data for case D2.3 in Table 26, which are increasing by 10 % and 12 % compared with the reference case.

Concerning the maximum linear ratings, again local effects at the core/reflector-interface have to be taken into account, as it had been discussed separately for the cores without radial and without axial blanket. Especially the improvement of the axial and radial form-factors by the steel-reflector in comparison with the fresh blanket is rather effective, so that the maximum linear ratings for BOL are almost unchanged despite the loss of the fresh blanket power of 5 %. At BOEC and EOEC, however, the axial and radial form-factors in the reference core are improved because of the Pu build-up in the blankets and their larger power contribution, so that the advantage of the steel reflectors is getting smaller and the loss in blanket power is dominating. When we adapt the slightly different inner core and outer core linear ratings by assuming a relative movement of the inner and outer control rods, we get the following values in W/cm for case D2.3 without any blanket in comparison with the reference case:

	ref. core 1a	core D2.3	D2.3 / 1a
BOL	328	334	1.02
BOEC	295	320	1.08
EOEC	277	310	1.12

We have to state, that the level of the maximum linear rating is increasing by 8 % at BOEC and by 12 % at EOEC, whereas it is only 2 % larger for the completely fresh blankets at BOL. A graphical comparison of the two cases is given in Figure 23, which shows the radial traverses in the two cores at BOL, BOEC and EOEC. We see again the typical behaviour of the reference case with the strong reduction of the linear power level during the burnup due to the increased contributions of the blankets, whereas this reduction is much smaller in the case without blankets, where it is mainly caused by the flattening of the radial and axial power distributions during the burnup. Figure 24 finally shows the S/A-wise maximum linear rating values for case D2.3 at BOL, BOEC and EOEC. These data, in comparison with those of the reference case in Figure 4, show again the much smaller burnup dependence indicated above. Taking for example for the positions 3 in C1 and 140 in C2 the data for BOL→BOEC→EOEC, we see the following numbers, which make the different burnup behaviours quite obvious:

case	position 3 in C1	position 140 in C2
reference case	324.0→276.7→285.2	327.6→294.9→270.2
case D2.3	316.4→300.0→320.2	333.8→319.8→299.5

The disadvantage of the transparent reflector with respect to the maximum linear rating, which we had observed in cases of the individual suppressions of the radial and the axial blanket is again visible in the data given in Table 26. Because of the strongly reduced reflection of neutrons from the reflector back into the core, the flux and power level in the axially and radially outer most core regions is much lower than in case of the SUS-reflector in case D2.3, so that the power form-factor is worsened and the maximum linear ratings further increased. Already in the BOL case the values are 8 % larger than in the reference case, and this difference increases to 16 % at BOEC and 19 % at EOEC.

Finally, the reduction of, both, the radial and axial blanket size to one row radially and 2x12 cm axially has, as to be expected, only a small influence on the maximum linear ratings. At BOL the numbers are very similar, whereas at BOEC and EOEC increases of about 3 % can be noticed.

7.3.3 Influence of the radial and axial blanket reduction on the control rod worth

The worth of the 13 control rods is slightly increasing, when both blankets are replaced by a SUS-reflector. The increase by -0.16 %Δρ is, however, small compared with the increase of the burnup reactivity loss by -0.45 %Δρ, so that an increase of the ^{10}B-enrichment would be necessary, if the control rod worth has to be kept constant.

In case of the transparent reflectors in case D3.2 the increase of the control rod worth is even smaller, and for case D1.3 with the reduced blanket thickness' the worth is not changing, as it is to be expected.

7.3.4 Influence of the radial and axial blanket reduction on the boundary fluxes

Since the calculations on the individual suppressions of the radial and axial blankets had shown, that the boundary fluxes are strongly increasing in case that standard steel reflectors are replacing the blankets, we had implemented radially in the third row and axially in the upper most and lower most 10 cm of the former blanket a B_4C-containing reflector. The numbers in Table 26 show only small changes compared with the reference case, which indicates, that the additional

shielding measures seem to be adequate. In case D3.2 with the transparent plenum zones, however, the shielding efficiency of one row B_4C-containing reflector is not sufficient, so that additional measures would be necessary.

Case D1.3 with the reduced blankets shows again, that the fluxes are increasing when the blankets are simply replaced by steel reflectors. Whether these increases are acceptable or not, must be shown by accurate shielding calculations.

7.3.5 Influence of the radial and axial blanket reduction on the sodium void and Doppler effect

Since the individual replacements of the radial and the axial blanket by the standard reflector had very small consequences on the sodium void effect, this is also the case for the combined effect: The value of case D2.3 is (by accident absolutely) identical with that of the reference case. Also for the case of the transparent reflector (case D3.2) the effects of the two blanket suppressions are additive, but in this case it leads to a very pronounced reduction of the sodium void effect to 0.89 % $\Delta\rho$ instead of 1.54 %$\Delta\rho$ or a reduction by 42 %. This value has, however, to be considered with some caution, because the large leakage effects in this void effect may be overestimated by the diffusion theory, so that the reduction of the total effect may be also overestimated.

The Doppler coefficient of case D2.3 with standard reflector also shows the combined effects of the two separate blanket suppressions, which is now $-3.72 \cdot 10^{-6}\Delta\rho/K$ or 11 % more negative than the reference value of $-3.36 \cdot 10^{-6}\Delta\rho/K$. In case D3.2 with plenum, however, the increased enrichment causes a reduction of the Doppler coefficient by 9 % compared with the reference case.

In case D1.3 with the reduced blanket sizes no changes of the sodium void and Doppler effect are to be expected and do occur.

7.4 Thermal-hydraulics considerations

The reduction and suppression of the blankets was simulated with the code BRUST [8], whereby again, as in chap. 5.6 and 6.2.5, the thermal-hydraulic analysis is based on the neutron-physics data of BRUST itself.

With respect to the variation of the blanket thickness, Table 29 shows the changes of the main thermal-hydraulics parameters and the power per zone, whose changes are mainly responsible for the changes of the thermal-hydraulics parameters.

We see again the effect of the power redistribution, already discussed in the chapters above. In parallel with the increase of the total core power a redistribution of the total mass-flow does occur:

- when we reduce the axial blanket thickness, also the radial blanket power is reduced, so that some mass-flow can be redistributed from the radial blanket to the fuel S/As and
- when radial blanket S/As are replaced by reflector S/As with a strongly reduced mass-flow or even no forced flow in the third and possibly also the second row, the fuel S/As will automatically get a larger coolant flow.

This mass-flow redistribution between the core and the radial blanket is visible in Table 29, and the increasing core mass-flow then leads to an increase of the core pressure drop Δp. For its calculation the total length of the fuel pins has been kept constant in case of an axial blanket

length reduction, since we have assumed that the UO_2 is being replaced by some reflector material inside the fuel pin. In the last column of Table 20 finally the maximum nominal mid-clad temperature is given.

Concerning the S/A-Δp we can note, that the axial blanket suppression leads to an increase of about 6 % (no. 1 versus 3) or 5 % (no. 4 versus 6) because of the slightly increasing core mass-flow. In the cases 7-9, however, which have no radial blanket, no mass-flow redistribution can occur and the Δp consequently remain constant. The radial blanket suppression on the other hand is causing a much stronger Δp-increase, because the mass-flow redistributions are much larger. The effect is less pronounced in case of smaller axial blanket heights because, as mentioned above, this also reduces the radial blanket power and consequently the mass-flow redistribution effects in case of the radial blanket suppression. With 65 cm axial blanket height the Δp increases from 4.12 to 4.95 kg/cm^2 or 20 %, when the radial blanket is completely replaced, whereas without axial blanket it changes from 4.36 to 4.98 kg/cm^2 or 14 %.

The consequences of the blanket reduction on the mid-clad temperature are much smaller, since the increase of the core power is largely compensated by the increased mass-flow. This is not completely the case, when the axial blanket thickness is reduced, so that a small increase of the T_{clad} of 2-3 K occurs. The radial blanket suppression on the other hand causes a decrease of the T_{clad} of up to 6 K, because the mass-flow increase is overcompensating the power increase.

In conclusion of these considerations, the expected increase of the pressure drop of up to 20 % in case of the complete suppression of both blankets has to be kept in mind. If that increase would not be compatible with the constraints of the plant, one possibility would be to slightly reduce the fuel pin diameter. A reduction from 6.5 mm to 6.4 mm for instance would reduce the pressure drop by about 0.5 bar.

7.5 Intermediate conclusion about cores with reduced blankets

The suppression of the blankets has been investigated stepwise by suppressing the radial and the axial blanket separately and then together in order to separate the effects of both blankets from each other. As a standard case, the blanket zones were replaced by SUS-reflector zones, but some variations of the material were also performed to check the influence of some alternative materials on the main core properties. Additionally, intermediate steps were taken by reducing the radial blanket from three to one row and the axial blanket thickness from 30+35 cm to 2x12 cm, since these reductions also could possibly be realised in Monju. For a better overview the main data of the cores with no radial blanket, no axial blanket and no radial and axial blanket are collected in Table 30 and compared with those of the reference case and the case with reduced blankets. The following trends can be deduced from these results concerning the consequences of the blanket suppression:

① The cycle length has to be reduced by up to 10 % in order to keep the discharge burnup constant at 100 GWd/t_{HM}.

② The burnup reactivity losses in the shortened cycles increase, because the noticeable contribution of the blankets is lost.

③ The main consequence of the blanket suppression seems to be the increase of the maximum linear rating. While at BOL there is a negligible influence, the increases are:

	no radial blanket	no axial blanket	no rad. + ax. blanket
at BOEC	+ 3 %	+ 3 %	+ 8 %
at EOEC	+ 5 %	+ 5 %	+ 12 %

Whether the effect at BOEC or at EOEC is more important cannot be clearly said, because there are fuel S/As in the core, which have their maximum linear rating at the beginning of their first cycle as well as S/As with the maximum at the end of their first cycle because of the influence of the control rod movement. We have therefore to conclude that increases of up to 12 % have to be expected.

④ The control rod worth is slightly increasing. But this increase is smaller than that of the burnup reactivity loss, so that some increase of the ^{10}B-enrichment will be necessary, when the shut-down worth has to be kept constant.

⑤ The sodium void effect is almost unchanged, when the blankets are replaced by SUS-reflectors. This has been calculated for the EOEC situation with the burnt blankets, so that the effect may be different for states with smaller blanket burnup.

⑥ The Doppler coefficient is getting more negative because of the moderating effect of the steel reflectors. In case of replacement of both blankets the increase is about 10 %.

⑦ Not shown in Table 30, but discussed before, is the increase of the neutron leakage from the core/blanket-system to the tank internal structures, when the good absorber material UO_2, even when containing some plutonium in its burnt states, is replaced by steel. Detailed shielding calculations have to show, whether these increases of up to 65 % in the axial direction and up to 80 % in the radial direction are acceptable or require the implementation of some B_4C.

Taking these points together, we have to conclude that the main drawback of a complete blanket suppression would be the increase of the maximum linear rating by up to 12 %, with 7 % being caused by a radial blanket suppression and 5 % by the axial one. The second consequence of importance is the increase of the pressure drop by about 20 %, when both blankets are suppressed.

In addition to the standard SUS-reflector some alternative materials were also investigated to check their influence of the main core parameters and on the boundary flux level. The following results are worth to be summarized:

- The use of a steel with higher Nickel content like PE16 with 43.5 % instead of 13.5 % Nickel has a negligible influence on most of the investigated core parameters. Only the Doppler effect is slightly increasing by 1-2 % because of the better reflecting and moderating properties of Nickel. These properties on the other hand reduce strongly the boundary fluxes compared with the SUS-case, so that a PE16-type material could be an alternative in case that design measures other than implementing some B_4C would be necessary.
- The reduction of the steel volume fraction in the reflector S/As from 78 %, taken from the present shielding S/As of Monju, to 50 % causes an increase of the boundary fluxes by about 30 %, which shows the flux sensitivity to the steel content.
- Two other variations were performed by replacing the blankets by either a transparent plenum-type material or a reflector containing some B_4C. Both, the transparent and the poisoned reflector, increase the leakage from the core, and therefore their consequences on the sodium void effect and also their possible use as a design measure to increase the fuel enrichments and so the Pu-burning rate were of interest. Both effects occur, as could be seen in the cases

B8 and B6+7 in Table 23, cases C7.2 and C4.2 in Table 25 and in the (radially and axially) combined case D3.2 in Table 26. The enrichments have to be increased and the sodium void effect is reduced, especially in the combined case D3.2 the reduction is rather pronounced. The negative consequence of these two design measures is however the increased maximum linear rating, which about 8 % larger than in the case with standard SUS-reflector. These measures may therefore be interesting for general design purposes, where the core size could be adapted to the increased linear rating, but in Monju they are not applicable.

Finally, with respect to the cores with reduced radial and/or axial blanket size no special consequences had to be expected and have been found. For case D1.3 (Table 26) the cycle length has to reduced by 3 % to 196 efpd to keep the average burnup constant. The maximum linear rating increases by up to 3 %, and control rod worth, sodium void and Doppler effect are not influenced by the blanket reductions.

8 Final evaluation

8.1 Comparison of the main burner candidates

Within our feasibility study about the possibilities to demonstrate the Pu-burning potential of fast reactors, we have investigated different core concepts with respect to their applicability to Monju. These were:

- the concepts with diluting pins and with diluents, which could be applied to increase the average plutonium content and consequently the plutonium burning rate
- and cores with reduced or suppressed radial and axial blanket.

For each these core concepts several variants have been investigated to explore ways for a minimum deterioration of the main core parameters of Monju. For these variants a first judgement has already been performed in the respective intermediate summaries:

For the **diluting pin concept** it was shown in chap. 5.7, that steel is the preferable diluting material, and that 43 steel pins would be compatible with the thermal-hydraulic boundary conditions of the Monju plant. Alternative diluting materials such as $MgAl_2O_4$ or $^{11}B_4C$ would have no advantage compared with steel, and the use of $^{nat}B_4C$ has to be rejected because of the negative consequences of the ^{10}B on the sodium void effect and the Doppler constant. In order to limit the increase of the maximum linear rating, two plutonium enrichments should be used in steel diluent burner cores. The concept with 43 steel pins will therefore be used in the final comparison.

For the **diluent concept** (intermediate conclusions in chap. 6.3) the use of steel diluents or $^{nat}B_4C$ diluents has been found to be feasible. The additional insertion of moderating materials ($MgAl_2O_4$ or $^{11}B_4C$) has not been found advantageous for the steel diluents, but they could be used for the $^{nat}B_4C$ diluents to mitigate their influence on the sodium void and Doppler effect. For the steel diluents two Pu-enrichments should be used to limit the increase of the maximum linear rating, whereas $^{nat}B_4C$ diluent cores could be designed with a single enrichment. The concepts with 27 steel diluents and 18 $^{nat}B_4C$ diluents have been found to be most promising.

For the **cores with suppressed blankets**, the increase of the maximum linear rating by up to 12 % has been found to be the most important consequence. Standard steel reflectors, replacing the blankets, have been compared with alternative designs such as a PE16-type reflector, more transparent reflectors and poisoned reflectors. The two last ones are

advantageous for the sodium void effect, but they have to be ruled out for Monju, because they are causing an additional increase of the maximum linear rating. PE16 could be an alternative to the standard SUS-type reflector because of its better reflecting properties, which possibly would not require additional shielding measures as in case of SUS in order to keep the fluence on the tank internal structures unchanged. Since this questions requires accurate shielding calculations, we kept the SUS-reflector as a reference with some additional shielding measures by implementing some $^{nat}B_4C$ into the outer parts of the radial and axial reflector zones.

For a **core with reduced blankets** (1 row radially and 2x12 cm axially) no major changes compared with the reference core have been found.

A **general comparison** of the main data of some selected burner core candidates and a core with reduced blankets with those of the reference core is given in Table 31. The comparison shows the following points:

• The cycle length (line 2) has to be reduced from 203 efpd in the reference core according to the reduction of the heavy metal inventory (line 14) in order to keep the average discharge burnup (line 3) constant at 100 GWd/t_{HM}. The maximum burnups are around 140 GWd/t_{HM}. The reference core has the largest value, which indicates, that the burner cores have a better total form-factor.

• The increase of the maximum linear ratings (line 5) is the main consequence of the diluting pin or diluent insertion as well as of the blanket suppression. The increase is smallest for the B_4C diluent case with 5 %/ 8 % at BOEC/ EOEC, whereas it is 12 %/ 11 % for the steel pin case and 9 %/ 13 % for the steel diluent case. The blanket suppression causes increases of 8 %/ 12 %, whereas the reduced blanket case shows a small increase of 3 % only.

• The burnup reactivity losses (line 6) are increasing because of the higher fuel enrichments or because of the suppression of the blanket contribution. Since the control rod worth is reduced at the same time, an increase of the ^{10}B content of the control rods has to be envisaged to fulfil the shut-down requirements.

• The sodium void effect (lines 8+9) is reduced in the cores with steel pins and with diluents, even if voiding of the diluents is also considered. On the other side, the blanket reduction has negligible consequences for the void effect.

• The core Doppler coefficient (line 10) is reduced in the burner cores because of their higher Pu-enrichment, especially in the core with B_4C diluents because of the spectrum hardening effect of the ^{10}B. On the other hand the breeder-less core has a slightly stronger Doppler coefficient due to the spectrum softening effect of the steel reflectors.

• The Pu-burning rates in terms of kg/TW_e·h (line 13) are increasing by 25-35 % in the burner cores with diluting pins or diluents compared with the reference core, whereby the B_4C diluent core offers the largest increase because of its largest average enrichment. It allows burning rate of -71.6 kg per cycle or -141 kg per full-power year in the fissile zones. These correspond to -57.6 kg/TW_e·h. The breeder-less core shows also an increase of 10 % compared with the reference core because of its larger core power density.

• The breeding ratio (BR) is reflecting the changes of the Pu-burning rate. The reference core value of 1.147 (average during an equilibrium cycle, line 15) is reduced in the diluting pin and diluent cases because of their increasing enrichment, with the B_4C diluent case having the smallest BR of 1.00. The breeder-less core shows a somewhat surprising increase of its internal

BR of 0.63 compared with the reference core value 0.58. This can be understood when looking at a simplified expression for the BR with limitation to the captures in ^{238}U (C8) and the absorptions in ^{239}Pu (A9) and the indices C and B standing for core and blanket and Φ for the neutron flux:

$$BR=\Sigma_{C8,C}\cdot\Phi_C/(\Sigma_{A9,C}\cdot\Phi_C+\Sigma_{A9,B}\cdot\Phi_B)=\Sigma_{C8,C}/(\Sigma_{A9,C}+\Sigma_{A9,B}\cdot\Phi_B/\cdot\Phi_C)$$

Since the cross-sections are rather similar in the reference core and the breeder-less core because of their same enrichments, it is obvious that the above BR must be smaller than the $BR=\Sigma_{C8,C}/\Sigma_{A9,C}$ for the breeder-less core, which does not have the blanket contribution in the denominator.

• The thermal-hydraulic data (lines 16-18) indicate, that the burner cores with diluting pins or diluents should not raise problems with respect to the pressure drop, but they lead to a small increase of the maximum channel ΔT and consequently of the maximum mid-clad temperature by 4 K compared with the reference core or by 7 K compared with the design case. If one of these concepts will be considered in future, detailed thermal-hydraulic calculations will be necessary to provide accurate data, and it has to be checked whether a slight increase of the maximum mid-clad temperature can be possible. The breeder-less core, on the other hand, does not lead to problems with respect to the mid-clad temperature, but the blanket suppression causes the pressure drop to increase by about 20 % to 5 kg/cm^2. This increase has, however, also to be checked in more accurate calculations taking also into account the correct mass-flow association to the radial reflector. If it would turn out, that the resulting pressure drop is not compatible with the Monju plant, one possible design measure would be to reduce the fuel pin diameter slightly. A reduction from 6.5 to 6.4 mm, for instance would reduce the pressure drop by about 0.5·kg/cm^2.

8.2 Conclusions

8.2.1 Conclusion about the diluting pins or diluents concepts

When trying to judge about the burner concepts with diluting pins or diluents and to make a selection between the tree concepts, we have to consider the following main points:

• The B_4C diluent concept has a clear advantage of the smallest linear rating increase.

• The sodium void effect is reduced in all cases, but also the Doppler coefficients are less negative compared with the reference core. Since both reactivity effects are compensating each other in many core transients, their ratio is sometimes used as a rough criterion, which should be as small as possible. With the numbers in Table 31 and adding also the B_4C-diluent case with $^{11}B_4C$ moderator mentioned in chap. 6.2.3 (Tab. 19), we get the following values:

	reference core (core 1a)	43 steel pins (core 2a)	27 steel-diluents (core 8k)	18 $^{nat}B_4C$-diluents (case 9a)	18 $^{nat}B_4C$-diluents (with $^{11}B_4C$)
void/ Doppler	0.46	0.46	0.38	0.66	0.47

We can see, that the steel pin case is similar to the reference case, whereas the steel diluents case is even more favourable. The standard $^{nat}B_4C$ diluent case is worsened because of the strong reduction of the Doppler coefficient. The addition of some moderator might then be needed, the benefit of which is indicated in the last case. All three burner concepts would then reveal similar or smaller void/Doppler-ratios than the reference case, so that from the safety point of view no major cliff is to be expected, although real dynamic analysis' have to prove that.

• The control rod worth is reduced in the diluent cases, which will require an increase of the ^{10}B-enrichment, but it is not a decisive argument against this concept.

• The B_4C diluents allow the largest Pu-enrichment increase, so that in this case the Pu-burning rate is also the largest. In the fissile zones it is -57.6 kg/TW_e·h, corresponding to -71.6 kg/cycle or -141 kg per equivalent full-power year.

• With respect to the thermal-hydraulics, the three concepts show no difference.

Taking all arguments together, the most important point seems to be the difference in the maximum linear rating level, for which the B_4C diluents offer a clear advantage. This concept has another advantage in its flexibility to adapt its reactivity worth and efficiency by changing the B_4C content within the S/A without major consequences on the maximum linear rating or other core parameters and without changing the number of diluent S/As. The steel diluents or steel pins on the contrary would require a modification of their number, which would have a direct impact on the linear rating. The B_4C diluent concept is therefore the preferred one.

8.2.2 Conclusion about the blanket reduction

A reduction of the radial and axial blanket size without suppressing the blankets completely, will rise no problems. A core with for instance one row radial blanket and 2x12 cm axial blanket shows only minor differences compared with the reference core.

The main consequence of a complete suppression of both blankets is the increase of the maximum linear rating by 8 % at BOEC and 12 % at EOEC, which would mean, that values of about 370 W/cm would be reached at BOEC, including the burnup factor. Most probably, this level will not be a problem for the pin design, but one has to consider, that there will be other perturbations of the core lay-out, such as the presence of irradiation positions, which will cause a further increase of the linear ratings. Since the degree of these perturbations is not yet established and since the allowable maximum linear rating for a future fuel pin of Monju is (to the authors's knowledge) not yet defined, it cannot be said now, to what extent a blanket suppression will lead to problems with respect to the maximum linear ratings.

8.2.3 General conclusion

Different concepts have been investigated in this feasibility study, which would be suitable for Monju cores with enhanced plutonium burning. Among the concepts with diluting pins and diluents the choice of B_4C diluents has been found to be preferable compared with steel diluents or steel pins. Its application to future Monju cores has been found feasible, although some changes of some important core parameters have to be expected. Hereby, the increase of the maximum linear rating by 5 % at BOEC and 8 % at EOEC may be the most important one.

A similar conclusion can be drawn for the case of a suppression of both blankets. With the restriction, that the related maximum linear rating increase of 8 % at BOEC and of 12 % at EOEC can be shown to be feasible, no basic problem should be linked with this design measure.

As had been discussed in the introduction, this feasibility study had the main aim to show, that Monju could be able to demonstrate the plutonium burning capability of fast reactors. Therefore, the core concepts with diluting pins or diluents were investigated separately from the blanket suppression, and the plutonium burning rates were given only for the core regions. In this manner for instance the increase of the burning rate per cycle of the reference core of -58 kg to -72 kg in the core with 18 $^{nat}B_4C$ diluents are given in Table 31. These –72 kg per cycle correspond to burning rate of –140 kg per equivalent full-power year. If we would add the plutonium production per cycle of the blankets of +70 kg in the reference case and of +61 kg in

the burner core, we would even get a positive value of +12 kg for the reference core and only a small negative value of -11 kg for the burner core.

In case that an overall negative plutonium balance of Monju would be requested, the combination of the blanket suppression and the diluent introduction would have to be done. In a similar manner as for both design measures separately, their combination would not lead to major design problems, except that the feasibility of the further increased maximum linear rating has to be proven. On the other hand, there are also design measures to reduce the maximum linear rating. One way would be a core height increase with a simultaneous axial blanket height reduction. An increase of the core height for instance by 10 cm from 93 cm to 103 cm would reduce the maximum linear rating by about 9 %, whereby the core height increase by 10.7 % is slightly reduced due to the worsening of the axial power form-factor. The core height increase would have acceptable consequences for the other core parameters, whereby the increase of the positive sodium void effect by about 10 % would perhaps be the most disadvantages one.

Another design measure would be an increase of the number of fuel pins per S/A from 169 to 217 pins and the use of a fuel pin diameter of 5.7 mm outer diameter very similar to that of JOYO with 5.5 mm, which has been operated very successfully. Such a transition would reduce the maximum linear rating by 22 % according to the larger pin number, and as it was additionally shown in [9], such a transition would have negligible consequences on other core parameters. The reason for that is, that the volume fractions of fuel, sodium and steel are very similar in case of a bundle of 169 pins with 6.5 mm diameter and of 217 pins with 5.7 mm diameter, so that all integral core parameters, including the plutonium enrichments, are also very similar. Such a core with reduced maximum linear rating would additionally offer a lot of operational flexibility for Monju as the future irradiation facility, into which many irradiation and test subassemblies could be inserted without approaching the limit of the allowable maximum linear rating.

The short discussion of these two design measures to reduce the maximum linear rating shall indicate, that even a diluent burner core without blankets with its strong overall negative plutonium balance is not completely unrealistic.

In general, the results of this study shall provide some quantitative information for future considerations and discussions about possible core modifications of Monju, when a reduction of its plutonium production may be required.

9 List of references

[1] Conceptual design studies on plutonium burning in Monju
U. Wehmann, PNC Report ZN-2410 97-010, July 1997

[2] Investigation of plutonium burner cores with diluting pins for future Monju cores
U. Wehmann, T. Kageyama, JNC Internal Technical Note, 16. 10. 1998

[3] Investigation of plutonium burner cores with diluents for future Monju cores
U. Wehmann, T. Kageyama, PNC Internal Technical Note, 15. 05. 1998

[4] Supplementary investigations of Pu-burner cores with diluents for future Monju cores
U. Wehmann, T. Kageyama, JNC Internal Technical Note, 25. 11. 1998

[5] Investigations of Pu-burner cores for Monju without blankets
U. Wehmann, T. Kageyama, JNC Internal Technical Note, 29. 07. 1999

[6] Comparison of core data calculated with JENDL-2 and JENDL-3.2
U. Wehmann, T. Kageyama, PNC Internal Technical Note, 21. 11. 1997

[7] MHI Core Design Report, D16/975C/0000M/20/Z0, 30.06. 1987

[8] Short description of the code BRUST, its capabilities and some calculational results
U. Wehmann, PNC Internal Technical Note, 07. 11. 1995

[9] JOYO type fuel pins as a back-up solution for future Monju cores
U. Wehmann, PNC Internal Technical Note, 14. 09. 1995

zone	ΔM in kg/year	ΔM in kg/TW_e·h
core	-104.2	- 42.3
radial blanket	+ 82.3	+33.6
axial blanket	+ 44.0	+17.9
total reactor	+ 22.1	+ 9.0
LWR (1 GW_e)	+ 225	+ 25.7

Table 1: Pu-balance of the upgraded Monju core

no.	name	MOX	UO_2	gas	Na	SUS316[1)]	PNC1520[2)]	B_4C
1	inner core	33.45 11.00x0.92	-	2.01 -	39.87 0.8382	-	24.67 8.04	-
2	outer core	33.45 11.04x0.92	-	2.01 -	39.87 0.8382	-	24.67 8.04	-
3	radial blanket	-	44.78 10.96 x0.93	1.74 -	33.70 0.8404	-	19.78 8.04	-
4	upper blanket	-	33.44 10.96x0.93	2.01 -	38.65 0.8404	-	25.90 8.04	-
5	lower blanket	-	33.46 10.96x0.93	2.01 -	39.86 0.8404	-	24.67 8.04	-
6	radial shield	-	-	-	22.00 0.8569	78.00 7.98	-	-
7	upper shield (core)	-	-	36.99 -	37.67 0.8569	-	26.91 8.04	-
8	lower shield (core)	-	-	-	39.13 0.8569	-	60.87 8.04	-
9	upper shield (blanket)	-	-	43.61 -	34.62 0.8569	-	21.77 8.04	-
10	lower shield (blanket)	-	-	-	42.65 0.8569	-	57.35 8.04	-
11	follower	-	-	-	91.20 0.8569	8.80 7.98	-	-
12	control rod (α=39 %)	-	-	2.27 -	48.52[3)] 0.8569	30.02[3)] 7.98	-	19.19 2.459x0.95
13	back-up rod (α=90 %)	-	-	2.62 -	48.53[3)] 0.8569	22.85[3)] 7.98	-	26.00 2.382x0.95

[1)]: Cr : Mn : Fe : Ni : Mo = 17.0 : 1.5 : 65.5 : 13.5 : 2.5; [2)]: Cr : Mn : Fe : Ni : Mo = 14.5 : 1.7 : 60.8 : 20.5 : 2.5
[3)]: values estimated from geometrical data of pins and tubes

Table 2: Volume fractions and densities of the different materials (first line: volume fractions; second line: densities in g/cm^3)

reference core (core 1a)

	BOL	BOEC	EOEC
C1	0.367	0.363	0.381
C2	0.197	0.209	0.208
C1+C2	0.564	0.572	0.588
radial blanket	0.337	0.375	0.365
axial blanket	0.189	0.199	0.194
total reactor	1.089	1.146	1.148

core with 43 steel pins (core 2a)

	BOL	BOEC	EOEC
C1	0.266	o.265	0.285
C2	0.199	0.214	0.213
C1+C2	0.465	0.479	0.498
radial blanket	0.360	0.409	0.397
axial blanket	0.183	0.194	0.194
total reactor	1.007	1.081	1.090

core with 27 steel diluents (core 8k)

	BOL	BOEC	EOEC
C1	0.250	0.251	0.272
C2	0.209	0.222	0.220
C1+C2	0.459	0.473	0.492
radial blanket	0.376	0.419	0.407
axial blanket	0.157	0.166	0.165
total reactor	0.993	1.058	1.063

core with 18 $^{nat}B_4C$ diluents (core 9a)

	BOL	BOEC	EOEC
C1	0.234	0.237	0.255
C2	0.194	0.210	0.211
C1+C2	0.428	0.447	0.466
radial blanket	0.352	0.399	0.394
axial blanket	0.139	0.149	0.149
total reactor	0.920	0.996	1.009

core with reduced blankets (core D1.3)

	BOL	BOEC	EOEC
C1	0.365	0.373	0.393
C2	0.202	0.217	0.217
C1+C2	0.567	0.590	0.610
radial blanket	0.160	0.172	0.166
axial blanket	0.103	0.109	0.107
total reactor	0.831	0.870	0.883

core without blankets (core D2.3)

	BOL	BOEC	EOEC
C1	0.360	0.387	0.418
C2	0.208	0.229	0.232
C1+C2	0.568	0.616	0.650
radial blanket	-	-	-
axial blanket	-	-	-
total reactor	0.568	0.616	0.650

Table 3 : Breeding ratios of the reference core and some burner cores

isotope	inner core	outer core	total core	axial blanket	radial blanket
Pu-238	27.155	29.407	56.562	0.0	0.0
Pu-239	470.682	509.729	980.411	0.0	0.0
Pu-240	244.392	264.666	509.058	0.0	0.0
Pu-241	85.990	93.123	179.113	0.0	0.0
Pu-242	63.361	68.617	131.978	0.0	0.0
Pu-tot	891.579	965.544	1857.122	0.0	0.0
Am-241	13.577	14.704	28.281	0.0	0.0
U-235	5.147	3.857	9.004	8.953	25.603
U-238	2568.330	1924.639	4492.969	4467.565	12775.753
HM	3478.633	2908.743	6387.376	4476.518	12801.356

Isotopic weights in kg at beginning of life

isotope	inner core	outer core	total core	axial blanket	radial blanket
Pu-238	21.701	25.280	46.981	0.0	0.0
Pu-239	432.768	464.936	897.704	49.301	134.791
Pu-240	242.048	261.974	504.022	0.973	2.848
Pu-241	70.506	79.821	150.327	0.018	0.053
Pu-242	61.991	67.560	129.551	0.0	0.001
Pu-tot	829.013	899.571	1728.585	50.292	137.693
Am-241	14.424	16.892	31.316	0.000	0.001
U-235	3.876	3.209	7.084	8.066	23.066
U-238	2469.544	1875.481	4345.024	4412.708	12624.200
HM	3316.856	2795.153	6112.009	4471.067	12784.960

Isotopic weights in kg at beginning of equilibrium cycle (BOEC)

isotope	inner core	outer core	total core	axial blanket	radial blanket
Pu-238	19.396	23.361	42.757	0.0	0.0
Pu-239	416.264	444.095	860.359	72.565	178.520
Pu-240	240.368	260.114	500.482	2.136	4.846
Pu-241	64.799	74.281	139.081	0.056	0.115
Pu-242	61.084	66.870	127.954	0.001	0.001
Pu-tot	801.911	868.721	1670.632	74.758	183.483
Am-241	14.514	17.567	32.081	0.001	0.003
U-235	3.361	2.913	6.274	7.646	22.243
U-238	2420.984	1850.044	4271.028	4384.088	12570.848
HM	3240.770	2739.245	5980.016	4466.494	12776.577

Isotopic weights in kg at end of equilibrium cycle (EOEC)

isotope	inner core	outer core	total core	axial blanket	radial blanket
Pu-238	-2.305	-1.919	-4.224	0.0	0.0
Pu-239	-16.504	-20.841	-37.345	23.264	43.730
Pu-240	-1.680	-1.860	-3.540	1.163	1.998
Pu-241	-5.706	-5.540	-11.246	0.039	0.061
Pu-242	-0.907	-0.690	-1.597	0.001	0.001
Pu-tot	-27.103	-30.850	-57.953	24.467	45.790
Am-241	0.090	0.675	0.765	0.001	0.002
U-235	-0.515	-0.295	-0.810	-0.420	-0.823
U-238	-48.559	-25.437	-73.996	-28.620	-53.352
HM	-76.086	-55.907	-131.993	-4.573	-8.383

Changes of the isotopic weights in kg (EOEC - BOEC)

Table 4 : Mass balances for the reference core (ΔT_{cycle}=203 efpd)

reference core (core 1a)

	BOL	BOEC	EOEC
C1	394.6	362.5	364.6
C2	280.3	274.3	261.2
C1+C2	674.9	636.8	625.8
radial blanket	22.4	47.5	54.4
axial blanket	12.7	25.1	30.0
total reactor	710	709.4	710.2

core with 43 steel pins (core 2a)

	BOL	BOEC	EOEC
C1	348.8	310.8	315.8
C2	323.6	317.5	300.4
C1+C2	672.4	628.3	616.2
radial blanket	24.9	56.7	64.3
axial blanket	12.4	24.1	29.3
total reactor	709.7	709.1	709.8

core with 27 steel diluents (core 8k)

	BOL	BOEC	EOEC
C1	343.6	312.2	318.2
C2	328.0	320.1	303.7
C1+C2	671.6	632.3	621.9
radial blanket	25.7	55.4	62.5
axial blanket	10.6	19.6	23.5
total reactor	707.9	707.3	707.9

core with 18 $^{nat}B_4C$ diluents (core 9a)

	BOL	BOEC	EOEC
C1	370.3	336.0	338.9
C2	304.0	302.3	289.3
C1+C2	674.3	638.3	628.2
radial blanket	23,7	52.0	59.5
axial blanket	10.0	17.0	20.1
total reactor	708.0	707.3	707.8

core with reduced blankets (core D1.3)

	BOL	BOEC	EOEC
C1	394.7	372.9	377.3
C2	286.7	283.8	271.8
C1+C2	681.4	656.7	649.1
radial blanket	17.5*	32.2*	37.3*
axial blanket	9.8*	19.3*	22.6*
total reactor	708.7	708.2	709.0

core without blankets (core D2.3)

	BOL	BOEC	EOEC
C1	398.3	395.7	407.6
C2	303.3	304.8	293.8
C1+C2	701.6	700.5	701.4
radial blanket	5.4*	6.0*	6.0*
axial blanket	3.0*	3.2*	3.2*
total reactor	710.0	709.7	710.6

* : including the power in the reflector zones, which replace the blankets

Table 5 : Power balance of the reference core and some burner cores (in MW_{th})

	one fuel enrichment					two enrichments	
no. of fuel/SS pins	169/0	139/30	126/43	112/57	98/71	169/0	126/43
PU/HM [%],C1/C2	33.0/ 33.0					25.5/33.0	32.0/36.1
k_{eff}	1.1673	1.0866	1.0512	1.0134	0.9780	1.0471	1.0603
S/A position: 3	427.9	430.6	424.7	412.1	392.7	322.1	361.5
11	429.7	434.9	433.8	428.0	415.8	327.5	375.2
25	420.2	430.9	431.3	428.4	419.7	326.4	376.2
(inner core) 44	401.8	421.4	425.8	426.4	425.9	322.0	375.0
70	365.4	393.5	403.8	412.8	425.3	307.9	365.8
102	324.7	365.8	384.8	405.5	425.0	293.1	360.7
(outer core) 140	270.7	317.2	340.5	367.5	395.2	330.5	369.0
183	209.9	256.1	280.8	310.6	343.1	273.8	313.6
(blanket) 232	54.3	69.1	77.5	87.8	99.5	75.9	83.7
288	22.0	28.0	31.4	35.6	40.4	30.7	33.7
zone power: C1	467.0	413.4	384.6	349.6	310.7	393.0	348.8
[MW] C2	216.0	263.6	289.2	320.3	354.6	281.6	323.6
f_{rad}	1.566	1.443	1.380	1.299	1.229	1.209	1.200

Table 6: Linear power traverses and other data in cores with different numbers of diluting pins (BOL, control rods 56.8 cm inserted)

	number of steel pins						
	0	37	43	57	67	72	1 per ch.
ΔT^{max} [K]	196.3	171.4	164.9	151.6	137.4	137.4	137.4
	(1.00)	(0.87)	(0.84)	(0.77)	(0.70)	(0.70)	(0.70)
ΔT^{av} [K]	174.1	141.0	136.4	122.3	112.8	108.6	118.5
	(1.00)	(0.81)	(0.78)	(0.70)	(0.65)	(0.62)	(0.68)
$f_{rad} = \Delta T^{max}/\Delta T^{av}$	1.128	1.216	1.209	1.239	1.218	1.265	1.159

Table 7: Thermal-hydraulics data of bundles with different numbers of steel pins

	(1a)	(2l)	(2b)	(2g)	(2h)	(2d)	(2f)	(2e)	(2a)	(2k)
core type	refer.	burner cores with								
	core*		one enrichment					two enrichments		
number of MOX / steel pins	169 / --	169 / --	139 / 30	126 / 43	112 / 57	112 / 57	98 / 71	139/ 30	126/ 43	112/ 57
Pu / HM in at %, C1 / C2	25.5/33.0	33.0/ 33.0				36.1/36.1	33.0/33.0	30.0/ 35.0	32.0/ 36.1	35.0/38.0
k_{eff} (BOL , CR=56.8 cm)	1.05231	1.16733	1.08659	1.05115	1.01343	1.06833	0.97803	1.05885	1.06028	1.07*
k_{eff} (EOEC, CR=25.8 cm)	0.99790	-	-	0.98230	0.94859	0.99505	-	0.99853	0.99567	1.00*
max. BOL, C1/C2 [W/cm]	328/328	430/271	435/317	434/341	428/367	431/368	426/395	365/353	376/369	387/388*
linear BOEC, " "	283/295	-	-	346/313	348/328	353/333	-	306/319	317/331	333/342*
power EOEC, " "	285/273	-	-	342/287	341/299	348/305	-	307/291	316/302	322/311*
$\Delta\rho$ burnup per 195 efpd in %	-2.75	-	-	-3.55	-3.59	-3.62	-	-3.19	-3.34	-3.6*
$\Delta\rho$ control rods in %	-8.57	-	-	-	-	-8.60	-	-8.53	-8.44	-8.3*
Na void effect in % $\Delta\rho$	1.54	-	-	-	-	1.37	-	1.47	1.43	1.4*
Doppler coeff. in 10^{-6} $\Delta\rho$/K	-3.36	-	-	-	-	-3.00	-	-3.18	-3.10	-3.0*

*** : reference core calculated with ΔT_{cycle}=203 efpd**

Table 8: Results for burner cores with diluting steel pins only (ΔT_{cycle}= 195 efpd)

isotope	inner core	outer core	total core	ax. blanket	rad. blanket
Pu-238	25.470	32.203	57.673	-	-
Pu-239	441.478	558.194	999.672	-	-
Pu-240	229.229	289.831	519.061	-	-
Pu-241	80.655	101.978	182.632	-	-
Pu-242	59.430	75.141	134.571	-	-
Pu-tot	836.262	1057.348	1893.610	-	-
Am-241	12.735	16.102	28.837	-	-
U-235	3.505	3.679	7.183	8.953	25.603
U-238	1748.751	1835.673	3584.425	4467.565	12775.753
HM	2601.252	2912.802	5514.054	4476.518	12801.356

Isotopic weights in kg at beginning of life

isotope	inner core	outer core	total core	ax. blanket	rad. blanket
Pu-238	20.563	27.627	48.190	-	-
Pu-239	390.707	502.869	893.576	47.708	140.618
Pu-240	227.478	286.089	513.567	0.905	3.059
Pu-241	66.848	87.328	154.177	0.016	0.059
Pu-242	58.298	73.891	132.190	0.000	0.001
Pu-tot	763.895	977.805	1741.699	48.630	143.737
Am-241	13.514	18.305	31.819	0.000	0.001
U-235	2.670	3.058	5.728	8.093	22.947
U-238	1683.443	1788.395	3471.839	4414.716	12616.780
HM	2463.523	2787.563	5251.086	4471.439	12783.464

Isotopic weights in kg at beginning of equilibrium cycle (BOEC)

isotope	inner core	outer core	total core	ax. blanket	rad. blanket
Pu-238	18.481	25.484	43.965	-	-
Pu-239	369.247	477.053	846.300	70.315	185.927
Pu-240	225.879	283.580	509.459	1.989	5.344
Pu-241	61.721	81.175	142.896	0.050	0.134
Pu-242	57.547	73.084	130.631	0.001	0.002
Pu-tot	732.875	940.376	1673.250	72.355	191.406
Am-241	13.616	18.953	32.569	0.001	0.003
U-235	2.330	2.772	5.102	7.684	22.090
U-238	1651.389	1763.713	3415.102	4387.138	12560.258
HM	2400.210	2725.814	5126.025	4467.178	12773.758

Isotopic weights in kg at end of equilibrium cycle (EOEC)

isotope	inner core	outer core	total core	ax. blanket	rad. blanket
Pu-238	-2.083	-2.142	-4.225	-	-
Pu-239	-21.460	-25.817	-47.277	22.606	45.309
Pu-240	-1.599	-2.509	-4.108	1.084	2.285
Pu-241	-5.128	-6.153	-11.280	0.034	0.074
Pu-242	-0.751	-0.808	-1.559	0.001	0.001
Pu-tot	-31.020	-37.429	-68.449	23.725	47.669
Am-241	0.102	0.648	0.750	0.001	0.002
U-235	-0.340	-0.285	-0.626	-0.409	-0.857
U-238	-32.054	-24.682	-56.737	-27.578	-56.521
HM	-63.312	-61.749	-125.061	-4.261	-9.707

Changes of the isotopic weights in kg (EOEC - BOEC)

Table 9: Mass balances for the burner core with 43 steel pins (core 2a, ΔT_{cycle}=195 efpd)

	(1a)	(2d)	(3a)	(4a)	(2a)	(3d)	(4d)
core type	ref. core*	burner cores with 1 enrichment			burner cores with 2 enrichments		
diluting pin type	none	steel	$MgAl_2O_4$	$^{11}B_4C$	steel	$MgAl_2O_4$	$^{11}B_4C$
no. of MOX / diluting pins	169 / --	112 / 57	112 / 57	112 / 57	126 / 43	126 /43	126 / 43
Pu / HM in at %, C1 / C2	25.5 / 33.0	36.1 / 36.1	36.1 / 36.1	36.1 / 36.1	32.0 / 36.1	31.5 / 36.7	31.5 /37.5
k_{eff} (BOL , CR=56.8 cm)	1.05231	1.06833	1.07457	1.06995	1.06028	1.06207	1.06402
k_{eff} (EOEC, CR=25.8 cm)	0.99790	0.99505	0.99939	0.99201	0.99567	0.99874	0.99862
max. BOL, C1/C2 [W/cm]	328/328	431/368	452/368	469/365	376/369	375/377	376/380
linear BOEC, " "	283/295	353/333	365/336	381/336	317/331	320/337	327/340
power EOEC, " "	285/273	348/305	362/307	371/306	316/302	318/306	320/308
$\Delta\rho$ burnup per 195 efpd in %	-2.75	-3.62	-3.64	-3.70	-3.34	-3.29	-3.29
$\Delta\rho$ control rods in $\%\Delta\rho$	-8.57	-8.60	-	-	-8.44	-8.36	-7.90
Na void effect in % $\Delta\rho$	1.54	1.37	-	-	1.43	1.29	1.18
Doppler coeff. in 10^{-6} $\Delta\rho/K$	-3.36	-3.00	-	-	-3.10	-3.42	-4.06

* : reference core calculated with ΔT_{cycle}=203 efpd

Table 10: Results for burner cores with diluting steel, $MgAl_2O_4$ and $^{11}B_4C$ pins (ΔT_{cycle}=195 efpd)

		(2a)	(2g)	(5)	(5b)	(5h)	(5l)	(5p)
core type	refer. core*	burner cores with one or two enrichments						
no. of MOX/SS/ $^{nat}B_4C$/ZrH pins	169/--/--/--	126/43/--/--	126/43/--/--	126/34/9/--	126/28/9/6	126/25/9/9	126/31/6/6	126/31/6/6
Pu / HM in at %, C1 / C2	25.5 / 33.0	32.0 / 36.1	33.0 / 33.0	36.1 / 36.1	36.1 / 36.1	36.1 / 36.1	37.5 / 37.5	36.0/ 39.0
k_{eff} (BOL , CR=56.8 cm)	1.05231	1.06028	1.05115	1.05113	1.03721	1.03198	1.07861	1.07391
k_{eff} (EOEC, CR=25.8 cm)	0.99790	0.99567	0.98230	0.97810	0.96542	0.95494	0.99828	0.99749
max. BOL, C1/C2 [W/cm]	328/328	376/369	434/341	377/352	387/348	394/346	403/344	377/363
linear BOEC, " "	283/295	317/331	346/313	324/319	339/318	346/317	348/318	333/330
power EOEC, " "	285/273	316/302	342/287	307/292	316/291	321/289	325/292	312/301
$\Delta\rho$ burnup per 195 efpd in %	-2.75	-3.34	-3.55	-3.53	-3.59	-3.62	-3.58	-3.45
$\Delta\rho$ control rods in %$\Delta\rho$	-8.56	-8.44	-	-7.34	-6.72	-6.47	-6.85	-6.56
Na void effect in % $\Delta\rho$	1.54	1.43	-	1.94	1.71	1.63	1.54	1.51
Doppler coefficient in 10^{-6} $\Delta\rho$/K	-3.36	-3.10	-	-1.99	-2.91	-3.33	-3.04	-3.04

* : reference core calculated with ΔT_{cycle}=203 efpd

Table 11: Results for burner cores with diluting steel pins plus some $^{nat}B_4C$ and $ZrH_{1.7}$ pins (ΔT_{cycle}=195 efpd)

	(1a)	(2a)	(5p)	(6h)	(7f)
core type	ref. core*	burner cores			
diluting pin type	none	steel	steel	$MgAl_2O_4$	$^{11}B_4C$
no. of MOX / dil/ $^{nat}B_4C$/ ZrH pins	169/--/--/--	126/43/--/--	126/31/6/6	126/31/6/6	126/31/6/6
Pu / HM in at %, C1 / C2	25.5 / 33.0	32.0 / 36.1	36.0 / 39.0	36.0 / 39.0	36.0 / 39.0
k_{eff} (BOL , CR=56.8 cm)	1.05231	1.06028	1.07391	1.07585	1.07205
k_{eff} (EOEC, CR=25.8 cm)	0.99790	0.99567	0.99749	0.99895	0.99441
max. BOL, C1/C2 [W/cm]	328/328	376/369	377/ 363	381/ 364	387/ 363
linear BOEC, " "	283/295	317/331	333/ 330	337/ 331	342/ 331
power EOEC, " "	285/273	316/ 302	312/301	315/ 302	319/ 302
$\Delta\rho$ burnup per 195 efpd in %	-2.75	-3.34	-3.45	-3.46	-3.47
$\Delta\rho$ control rods in $\%\Delta\rho$	-8.57	-8.44	-6.56	-6.58	-6.42
Na void effect in % $\Delta\rho$	1.54	1.43	1.51	1.45	1.40
Doppler coefficient in 10^{-6} $\Delta\rho$/K	-3.36	-3.10	-3.04	-3.13	-3.41

* : reference core calculated with ΔT_{cycle}=203 efpd

Table 12: Results for burner cores with diluting steel, $MgAl_2O_4$ and $^{11}B_4C$ plus $^{nat}B_4C$ and $ZrH_{1.7}$ pins (ΔT_{cycle}=195 efpd)

parameter		design case	high burnup cores					
			2-zones reference core		43 steel pins		57 steel pins	
max. linear power [W/cm]	C1/C2	357/ 350	323/ 344		365/ 380		383/ 393	
max. pin power [KW]	C1/C2**	28.3/ 26.2	26.6/ 27.1		29.1/ 30.0		31.1/ 31.1	
max. S/A power [MW]	C1/C2**	4.73/ 4.14	4.46/ 4.45		3.76/ 4.99		3.48/ 5.21	
power per zone [MW]	C1/C2**	387/ 282*	377/ 285		327/ 327		301/ 344	
with or without mass-flow adaptation		no	no	yes	no	yes	no	yes
max. S/A mass-flow [kg/s]	C1/C2	21.35/ 19.24	→	19.81/ 20.47	→	18.42/ 22.33	→	18.13/ 22.33
mass-flow per zone [kg/s]	C1/C2	2000/ 1538	→	1856/ 1636	→	1725/ 1785	→	1698/ 1785
total mass-flow [kg/s]	C1+C2	3538	→	3492	→	3520	→	3483
pressure drop, [kg/cm^2]	C1	4.00/0.70/4.77	→	3.44/1.26/4.77	→	2.98/1.86/4.77	→	2.88/1.82/4.77
(bundle/ orifice/ total)	C2	3.33/1.40/4.77	→	3.77/0.96/4.77	→	4.48/0.25/4.77	→	4.48/0.25/4.77
average ΔT [K]	C1/C2	154/ 144*	150/ 146	162/ 137	136/ 167	158/ 144	126/ 176	148/ 152
average ΔT [K]	C1+C2	150	148	150	149	150	148	150
maximum fuel S/A ΔT [K]	C1/C2	174/ 167*	164/ 180	177/ 169	145/ 201	168/ 173	135/ 210	159/ 181
S/A temperature form-factor	C1/C2	1.128/ 1.18	1.128/ 1.18	1.128/ 1.18	1.209/ 1.18	1.209/ 1.18	1.239/ 1.18	1.239/ 1.18
max. coolant channel ΔT [K]	C1/C2	196/ 197	185/ 212	200/ 199	175/ 237	203/ 204	167/ 248	197/ 214

* : BRUST data ** : including axial blankets → : design data overtaken

Table 13: Thermal-hydraulics data of cores without and with diluting steel pins

diluent type	volume % sodium	steel	B_4C	reactivity [% Δρ]
follower	91.2	8.8	-	-0.30
steel	22.0	78.0	-	-0.35
2 % B_4C	22.0	76.0	2.0	-0.40
5 % B_4C	22.0	73.0	5.0	-0.48
10 % B_4C	22.0	68.0	10.0	-0.56

Table 14: Volume fractions and reactivity worths of diluent candidates

no.	number of diluents	k_{eff}	% Δρ total/ per diluent	max. linear power [W/cm] inner/outer core	radial form-factor fuel only	fuel+diluents
1	0 (2 zones)	1.03005	-	309/343	1.259	1.259
2	0 (1 zone)	1.16856	-	429/244	1.575	1.575
3	3	1.15219	1.21/ 0.405	401/286	1.446	1.472
4	6d[1)]	1.13771	2.32/ 0.387	391/300	1.384	1.435
5	6r[2)]	1.13726	2.36/ 0.393	390/299	1.381	1.431
6	12d	1.11062	4.46/ 0.372	377/320	1.285	1.384
7	12r	1.11325	4.25/ 0.354	378/322	1.289	1.387
8	18d	1.08598	6.51/ 0.362	377/339	1.236	1.384
9	18c[3)]	1.09799	5.50/ 0.306	383/339	1.256	1.406
10	21	1.07268	7.65/ 0.364	373/333	1.199	1.369
11	24	1.06112	8.66/ 0.361	373/330	1.175	1.369
12	27	1.05040	9.27/ 0.357	371/334	1.144	1.362
13	30	1.03786	10.78/ 0.359	373/344	1.126	1.369
14	33	1.02691	11.80/ 0.358	383/359	1.131	1.406
15	36	1.01446	13.00/ 0.361	390/369	1.127	1.431
16	39	1.00307	14.12/ 0.362	390/368	1.101	1.431

d[1)] =distributed r[2)] = ring c[3)] = centered

Table 15: Data of cores with different numbers of steel diluents (case 1 with Pu-contents 24.3/ 33.0 %, all others with 33.0 % only)

no.	parameter	reference core*	steel 21	steel 24	diluents 27	diluents 30	B_4C 18 (5 %)	diluents 18 (10 %)
1	Pu/ HM [%] , C1/ C2	25.5/ 33.0	33.0/ 33.0	33.0/ 33.0	33.0/ 33.0	33.0/ 33.0	33.0/ 33.0	33.0/ 33.0
2	k_{eff}: BOL (CR=56.8 cm)	1.05231	1.07267	1.06112	1.05040	1.03786	1.06007	1.04320
	BOEC (CR=56.8 cm)	0.98969	0.99792	0.98688	0.97681	0.96550	0.98752	0.97281
	BOEC (CR=41.3 cm)	1.00866	1.01901	1.00793	0.99742	0.98551	1.00745	0.99105
	EOEC (CR=41.3 cm)	0.98038	0.98416	0.97334	0.96315	0.95178	0.97349	0.95806
	EOEC (CR=25.8 cm)	0.99790	1.00219	0.99131	0.98072	0.96882	0.99070	0.97392
3	k_{eff}: BOEC (CR=out)	1.04911	1.06136	1.05026	1.03900	1.02621	1.04728	1.02753
	BOEC (CR= in)	0.96254	0.97731	0.96638	0.95677	0.94622	0.96800	0.95497
4	Pu/HM for k_{eff}=1.0 at EOEC*	25.5/ 33.0	33.0	34.0	35.0	35.5	34.0	35.0
5	$\Delta\rho$ per 195 efpd [%]	-2.75	-3.48	-3.53	-3.57	-3.60	-3.46	-3.47
6	$\Delta\rho$ of control rods [%]	-8.57	-8.10	-8.26	-8.27	-8.24	-7.82	-7.39
7	max. BOL [W/cm]	328 (± 0)	368 (+12 %)	373 (+14 %)	371 (+13 %)	373 (+14 %)	349 (6 %)	348 (6 %)
	linear BOEC "	295 (± 0)	326 (+11 %)	326 (+11 %)	322 (+9 %)	328 (+11 %)	311 (5 %)	311 (5 %)
	power* EOEC "	277 (± 0)	311 (+12 %)	316 (+14 %)	318 (+15 %)	318 (+15 %)	307 (11 %)	307 (11 %)
8	f_{rad} BOL/BOEC/EOEC	1.26/1.20/1.11	1.20/1.14/1.12	1.20/1.13/1.12	1.18/1.10/1.11	1.16/1.11/1.10	1.16/1.11/1.11	1.16/1.11/1.11
9	core power: BOEC	632.8	633.8	630.7	627.7	623.7	634.2	632.0
	[MW] EOEC	622.6	622.7	619.2	615.5	611.0	623.3	620.5
10	burnup: average	95.9 (± 0%)	107.1 +11.7%)	108.3(+13.4%)	109.7(+14.4%)	110.8(+15.5%)	105.4 (+9.9%)	105.0 (+9.5%)
	[GWd/t_{HM}] max. local	138.0	149.1	149.8	149.8	151.2	145.1	145.1

* : reference core calculated with ΔT_{cycle}=203 efpd, but burnup in line 10 given for 195 efpd

Table 16: Data of Monju plutonium burner cores with steel or B_4C diluents (ΔT_{cycle}=195 efpd)

	(1a)	(8f)	(8k)	(9a)	(9e)
core type	ref.core	27 steel diluents		18 B_4C diluents	
vol % of Na/ SS/ $^{nat}B_4C$	-	22/ 78/--	22/ 78/--	22/ 68/ 10	22/ 68/ 10
Pu / HM in at %, C1 / C2	25.5 /33.0	33.5 / 33.5	32.5 / 35.0	35.0/ 35.0	34.0/ 35.0
k_{eff} (BOL , CR=56.8 cm)	1.05231	1.05981	1.06067	1.07405	1.06310
k_{eff} (EOEC, CR=25.8 cm)	0.99790	1.00118	1.00377	1.00714	0.99865
max. BOL, C1/C2 [W/cm]	328/ 328	373/ 344	356/ 358	347/ 334	343/ 340
linear BOEC, " "	283/ 295	330/ 312	316/ 322	316/ 310	312/ 314
power EOEC, " "	285/ 273	327/ 306	312/ 315	305/ 295	300/ 298
cycle length [efpd]	203	175	175	185	185
$\Delta\rho$ burnup in %	-2.86	-3.15	-3.06	-3.23	-3.18
$\Delta\rho$ control rods in %	-8.57	-8.30	-8.00	-7.06	-7.04
Na void effect [% $\Delta\rho$] core	1.54	0.92	0.92	1.15	1.15
Na void effect [% $\Delta\rho$] core + dil.	1.54	1.15	1.14	1.37	1.37
Doppler coefficient [10^{-6} $\Delta\rho$/K]	-3.36	-3.03	-2.97	-2.08	-2.12

Table 17: Results for steel and B_4C diluent burner cores with one or two Pu-enrichments

case			sodium void effect [% Δρ]		core Doppler	max. lin. power
			core only	core + diluents	coeff. [10^{-6}Δρ/K]	C1/ C2 [W/cm]
reference case			1.54	1.54	- 3.36	328/ 328
Na	SS	$^{11}B_4C$				
22	78	0	0.92	1.15	- 2.97	373/ 344
22	73	5	0.88	1.10	- 3.14	385/ 343
22	68	10	0.85	1.07	- 3.34	397/ 342
22	58	20	0.79	1.00	- 3.54	421/ 346

Table 18: Sodium void effect, Doppler coefficient and maximum linear power as a function of the $^{11}B_4C$ content in 27 steel diluents

volume % of				k_{eff}	sodium void effect [% Δρ]		Doppler coeff.	max. lin. power
Na	SS	$^{nat}B_4C$	$^{11}B_4C$	BOEC	core only	core+diluents	[10^{-6}Δρ/K]	[W/cm]
22	68	10	0	1.0071	1.15	1.37	-2.08	347/ 334
22	20	10	48	0.9877	0.99	1.19	-2.39	350/ 338
22	24	6	48	1.0015	1.04	1.24	-2.63	353/ 330

Table 19: Sodium void effect, Doppler coefficient and maximum linear power as a function of the $^{11}B_4C$ content in 18 B_4C diluents

parameter	number of diluents			
	0	12	18	27
zone power [MW] C1/ C2	378/ 285	356/ 303	344/ 312	324/ 327
max. S/A power [kW] C1/ C2	4.47/ 4.17	4.73/ 4.42	4.86/ 4.56	5.08/ 4.78
zone mass-flow [kg/s] C1/ C2	1952/ 1587	1837/ 1672	1775/ 1718	1676/ 1791
max. S/A mass-flow [kg/s] C1/C2	20.3/ 19.6	21.3/ 20.6	21.8/ 21.2	22.6/ 22.0
Δp(bundle) [kg/cm^2]	3.37	3.67	3.94	4.10
max. channel ΔT [K]	201	203	204	205

Table 20: Influence of diluents on neutron-physics and thermal-hydraulics data (BRUST data)

isotope	inner core	outer core	total core	axial blanket	radial blanket
Pu-238	26.026	31.171	57.197	-	-
Pu-239	451.114	540.306	991.420	-	-
Pu-240	234.232	280.543	514.776	-	-
Pu-241	82.415	98.710	181.125	-	-
Pu-242	60.727	72.733	133.460	-	-
Pu-tot	854.514	1023.464	1877.978	-	-
Am-241	13.013	15.586	28.599	-	-
U-235	3.499	3.745	7.244	7.732	25.603
U-238	1746.202	1868.512	3614.714	3858.352	12775.753
HM	2617.228	2911.306	5528.534	3866.084	12801.356

Isotopic weights in kg at beginning of life

isotope	inner core	outer core	total core	axial blanket	radial blanket
Pu-238	21.616	27.031	48.647	-	-
Pu-239	403.174	491.714	894.888	36.647	130.716
Pu-240	232.245	277.184	509.429	0.659	2.643
Pu-241	69.805	85.513	155.318	0.012	0.048
Pu-242	59.705	71.616	131.321	0.000	0.000
Pu-tot	786.545	953.058	1739.603	37.318	133.407
Am-241	13.879	17.461	31.341	0.000	0.001
U-235	2.771	3.153	5.924	7.057	23.135
U-238	1691.000	1823.723	3514.723	3817.958	12628.979
HM	2494.196	2797.394	5291.590	3862.333	12785.522

Isotopic weights in kg at beginning of equilibrium cycle (BOEC)

isotope	inner core	outer core	total core	axial blanket	radial blanket
Pu-238	19.692	25.094	44.786	-	-
Pu-239	382.382	469.043	851.425	54.084	172.737
Pu-240	230.663	275.007	505.670	1.445	4.607
Pu-241	64.901	79.912	144.813	0.038	0.108
Pu-242	59.043	70.909	129.952	0.001	0.001
Pu-tot	756.682	919.965	1676.646	55.568	177.453
Am-241	14.055	18.038	32.093	0.001	0.002
U-235	2.464	2.880	5.344	6.735	22.341
U-238	1663.678	1800.541	3464.220	3796.967	12577.162
HM	2436.879	2741.424	5178.303	3859.271	12776.959

Isotopic weights in kg at end of equilibrium cycle (EOEC)

isotope	inner core	outer core	total core	axial blanket	radial blanket
Pu-238	-1.924	-1.937	-3.861	-	-
Pu-239	-20.792	-22.671	-43.463	17.437	42.021
Pu-240	-1.582	-2.177	-3.759	0.786	1.964
Pu-241	-4.904	-5.600	-10.505	0.026	0.060
Pu-242	-0.662	-0.707	-1.369	0.000	0.001
Pu-tot	-29.863	-33.093	-62.956	18.250	44.046
Am-241	0.176	0.577	0.752	0.001	0.002
U-235	-0.308	-0.272	-0.580	-0.322	-0.794
U-238	-27.321	-23.181	-50.503	-20.990	-51.817
HM	-57.317	-55.970	-113.287	-3.062	-8.564

Changes of the isotopic weights in kg (EOEC - BOEC)

Table 21: Mass balances for the burner core with 27 steel diluents (core 8k, ΔT_{cycle}=175 efpd)

isotope	inner core	outer core	total core	axial blanket	radial blanket
Pu-238	31.171	31.171	62.343	-	-
Pu-239	540.306	540.306	1080.612	-	-
Pu-240	280.543	280.543	561.087	-	-
Pu-241	98.710	98.710	197.419	-	-
Pu-242	72.733	72.733	145.467	-	-
Pu-tot	1023.464	1023.464	2046.928	-	-
Am-241	15.586	15.586	31.171	-	-
U-235	3.745	3.745	7.489	7.732	25.603
U-238	1868.512	1868.512	3737.023	3858.352	12775.753
HM	2911.306	2911.306	5822.611	3866.084	12801.356

Isotopic weights in kg at beginning of life

isotope	inner core	outer core	total core	axial blanket	radial blanket
Pu-238	26.152	27.057	53.209	-	-
Pu-239	480.652	492.103	972.754	32.849	130.023
Pu-240	275.911	277.033	552.944	0.441	2.613
Pu-241	83.266	85.324	168.590	0.005	0.047
Pu-242	71.321	71.605	142.925	0.000	0.000
Pu-tot	937.301	953.122	1890.423	33.296	132.683
Am-241	17.152	17.740	34.892	0.000	0.001
U-235	3.025	3.160	6.185	7.146	23.149
U-238	1813.714	1824.332	3638.045	3822.265	12629.734
HM	2771.192	2798.354	5569.546	3862.707	12785.568

Isotopic weights in kg at beginning of equilibrium cycle (BOEC)

isotope	inner core	outer core	total core	axial blanket	radial blanket
Pu-238	23.942	25.107	49.049	-	-
Pu-239	454.593	469.281	923.874	48.896	172.212
Pu-240	273.074	274.764	547.838	0.990	4.579
Pu-241	77.120	79.598	156.719	0.017	0.106
Pu-242	70.455	70.882	141.338	0.000	0.001
Pu-tot	899.184	919.633	1818.817	49.903	176.898
Am-241	17.574	18.409	35.983	0.000	0.003
U-235	2.716	2.887	5.603	6.859	22.352
U-238	1786.485	1801.150	3587.635	3803.308	12577.916
HM	2705.959	2742.080	5448.039	3860.071	12777.170

Isotopic weights in kg at end of equilibrium cycle (EOEC)

isotope	inner core	outer core	total core	axial blanket	radial blanket
Pu-238	-2.210	-1.950	-4.160	-	-
Pu-239	-26.059	-22.821	-48.880	16.047	42.189
Pu-240	-2.837	-2.269	-5.106	0.549	1.965
Pu-241	-6.146	-5.725	-11.871	0.012	0.060
Pu-242	-0.865	-0.723	-1.588	0.000	0.001
Pu-tot	-38.117	-33.489	-71.606	16.607	44.215
Am-241	0.422	0.669	1.091	0.000	0.002
U-235	-0.310	-0.273	-0.582	-0.287	-0.797
U-238	-27.229	-23.181	-50.410	-18.956	-51.817
HM	-65.233	-56.274	-121.508	-2.636	-8.398

Changes of the isotopic weights in kg (EOEC - BOEC)

Table 22: Mass balances for the burner core with 18 B_4C diluents (core 9a, ΔT_{cycle}=186 efpd)

	1a	B5	B2	B3	B4	B8	B6	B7
core type	reference core	1 row blanket rest SUS78[1)]	no radial blanket SUS78[1)]	SUS50[1)]	PE16-78[1)]	Plen.+ B_4C[4)]	SUS78+B_4C[2)]	SUS78+B_4C[3)]
Pu / HM in at %, C1 / C2	25.5 / 33.0	25.5/ 32.0	→	→	→	26.0/ 36.0	26.0/ 35.0	26.3/ 36.3
cycle length in efpd	203	190	190	→	→	→	→	→
k_{eff} (BOL , CR=56.8 cm)	1.05231	1.04908	1.05984	1.05593	1.06243	1.05923	1.06382	1.06651
k_{eff} (EOEC, CR=25.8 cm)	0.99790	0.99786	0.99930	0.99583	1.00165	0.99663	0.99984	1.00107
max. BOL, C1/C2 [W/cm]	328.0/ 327.7	336.3/ 321.8	322.9/ 326.3	327.5/ 323.7	319.5/ 327.2	342.0/ 343.7	337.3/ 345.1	345.5/ 350.9
linear BOEC, " "	282.6/ 294.9	297.2/ 296.8	301.6/ 303.8	304.4/ 301.8	299.2/ 304.3	314.2/ 320.2	312.4/ 321.2	317.4/ 326.7
power EOEC, " "	285.3/ 272.7	300.3/ 276.0	310.7/ 283.7	313.3/ 282.1	308.5/ 284.0	322.3/ 299.7	321.5/ 299.9	326.2/ 305.5
zone power BOEC: C1/ C2	362.5/ 274.3	377.5/ 274.7	384.7/ 289.5	386.5/ 287.2	382.8/ 291.9	393.8/ 283.6	394.0/ 284.1	397.8/ 281.5
[MW_{th}] BOEC/EOEC: C1+C2	636.8/ 625.8	652.2/ 643.4	674.2/ 669.4	673.7/ 668.7	674.7/ 670.0	677.4/ 672.7	678.1/ 673.8	679.3/675.2
reactivity loss per cycle in % Δρ	-2.86	-2.78	-3.13	-3.12	-3.11	-3.23	-3.25	-3.30
$\Phi_{rad.\ boundary}$ rel. BOL/BOEC/EOEC	1.00/1.00/1.00	1.45/1.22/1.17	1.81/1.40/1.30	2.39/1.84/1.72	1.04/0.80/0.74	2.06/1.61/1.51	1.38/1.07/1.01	1.12/0.88/0.82
$\Phi_{ax.\ boundary}$ rel. BOL/BOEC/EOEC	1.00/1.00/1.00	1.03/1.04/1.03	1.05/1.08/1.09	1.08/1.11/1.12	1.02/1.06/1.07	1.20/1.21/1.21	1.01/1.04/1.04	0.99/1.01/1.02
control rod worth in % Δρ, BOEC	-8.57	-8.72	-8.73	-8.81	-8.68	-8.88	-8.78	-8.80
Na void effect in % Δρ, core, EOEC	1.54	1.55	1.59	1.52	1.59	1.19	1.39	1.25
Doppler coeff. in 10^{-6} Δρ/K, EOEC	-3.36	-3.45	-3.63	-3.66	-3.66	-3.24	-3.17	-3.06

[1)]: 78 and 50 mean 78 % and 50 % vol. % SUS or PE16; [2)]: SUS :B_4C :Na = 68 :10 :22 in 1st row; [3)]: SUS :B_4C :Na = 58 :20 :22 in 1st row; [4)]: B_4C[3)] in 3rd row

Table 23: Results for burner cores with reduced or suppressed radial blanket

	group number and lower energy boundary in eV							
	1 1.35+6*)	2 0.387+6	3 86.5+3	4 19.3+3	5 4.31+3	6 454	7 10^{-5}	1-7 10^{-5}
BOL	0.32	1.43	2.27	1.97	1.81	1.66	1.52	1.81
BOEC	0.15	0.86	1.62	1.51	1.41	1.32	1.25	1.40
EOEC	0.13	0.76	1.48	1.41	1.32	1.25	1.19	1.30
$\Phi_{ref.\ case}$ [10^{12} $cm^{-2}s^{-1}$]	0.012	0.63	2.95	4.40	2.20	3.60	4.31	18.1

*) means $1.35 \cdot 10^{+6}$

Table 24: Flux ratios at the radial outer boundary: Φ(case B2) / Φ(ref. case)

	1a	C1	C2	C2.2	C3	C6	C7.2	C4.2
core type	reference core	2x12 cm bl. rest SUS60[1]	no axial blanket					
			SUS60[1]	25 cm SUS60[1] +10 cm B_4C[2]	PE16-60[1]	Plenum	12 cm Plenum +23 cm B_4C[3]	35 cm SUS with B_4C[2]
Pu / HM in at %, C1 / C2	25.5/ 33.0	25.5/ 33.0	→	→	→	→	27.0/ 34.5	27.0/ 34.5
cycle length in efpd	203	200	200	195	200	200	195	200
k_{eff} (BOL , CR=56.8 cm)	1.05231	1.05448	1.06207	1.05968	1.06360	1.05359	1.06934	1.06385
k_{eff} (EOEC, CR=25.8 cm)	0.99790	0.99855	0.99808	0.99830	0.99954	0.99030	1.00300	0.99446
max. BOL, C1/C2 [W/cm]	328.0/ 327.7	329.4/ 327.2	331.4/ 324.4	330.6/ 326.5	330.3/ 323.1	334.1/ 330.4	344.9/ 341.0	347.9/ 345.8
linear BOEC, " "	282.6/ 294.9	290.3/ 298.9	294.0/ 302.9	294.6/ 305.0	293.2/ 302.1	295.6/ 306.8	303.0/ 320.4	304.7/ 325.0
power EOEC, " "	285.3/ 272.2	292.0/ 277.1	297.3/ 283.2	299.6/ 285.5	296.8/ 282.6	298.9/ 286.1	312.1/ 298.4	314.5/ 301.8
zone power BOEC: C1/ C2	362.5/ 274.3	370.9/ 276.9	378.9/ 282.9	379.4/ 284.1	379.5/ 282.9	375.7/ 283.7	379.5/ 286.4	379.0/ 287.3
[MW_{th}] BOEC/EOEC: C1+C2	636.8/ 625.8	647.8/ 637.7	661.8/ 654.3	663.5/ 656.3	662.4/ 655.0	659.4/651.1	665.9/ 659.3	666.3/659.5
reactivity loss per cycle in % $\Delta\rho$	-2.86	-2.91	-3.18	-3.11	-3.17	-3.19	-3.29	-3.43
$\Phi_{rad.\ boundary}$ rel. BOL/BOEC/EOEC	1.00/1.00/1.00	1.00/0.94/0.95	0.99/0.95/0.98	1.00/0.96/0.97	0.99/0.95/0.97	1.03/0.99/1.01	1.38/1.07/1.01	1.01/0.97/0.99
$\Phi_{ax.\ boundary}$ rel. BOL/BOEC/EOEC	1.00/1.00/1.00	1.39/1.27/1.21	1.65/1.37/1.27	0.99/0.82/0.76	1.37/1.14/1.05	2.80/2.34/2.18	0.42/0.36/0.33	0.43/0.36/0.34
control rod worth in % $\Delta\rho$, BOEC	-8.57	-8.65	-8.77	-8.73	-8.79	-8.66	-8.28	-8.11
Na void effect in % $\Delta\rho$, EOEC	1.54	1.55	1.56	1.52	1.57	1.42	1.16	1.13
Doppler coeff. in 10^{-6} $\Delta\rho$/K, EOEC	-3.36	-3.40	-3.59	-3.54	-3.68	-3.54	-3.00	-2.96

[1]: 60.13 % SUS or PE16 and 39.87 % Na; [2]: SUS : B_4C : Na = 42.13 : 18.0 : 39.87 ; [3]: SUS : B_4C : Na = 24.67 : 35.46 : 39.87 ;

Table 25: Results for burner cores with reduced or suppressed axial blanket

	1a	D1.3	D2.3	D3.2
core type	reference core	1 row radial blanket + 2 rows SUS78[1] 2x12 cm ax.bl.+SUS60[1]	2 rows SUS78[1] + 1 row (SUS78[1]+B_4C[2]) 25 cm SUS60+10 cm B_4C[2]	2 rows plenum + 1 row (SUS78[1]+B_4C[3]) 20 cm plenum +15 cm B_4C[3]
Pu / HM in at %, C1 / C2	25.5/ 33.0	25.5/ 33.0	25.5/ 33.0	26.8/ 37.0
cycle length in efpd	203	196	180	180
k_{eff} (BOL , CR=56.8 cm)	1.05231	1.05805	1.07101	1.06688
k_{eff} (EOEC, CR=25.8 cm)	0.99790	1.00305	1.00559	0.99795
max. BOL, C1/C2 [W/cm]	328.0/ 327.7	325.3/ 329.3	321.4/ 333.9	352.7/ 357.6
linear BOEC, " "	282.6/ 294.9	291.0/ 303.1	306.8/ 319.8	327.8/ 343.4
power EOEC, " "	285.3/ 272.7	294.8/ 282.1	320.2/ 302.3	343.4/ 324.7
zone power BOEC: C1/ C2	362.5/ 274.3	372.9/ 283.8	395.7/ 304.8	403.9/ 297.8
[MW_{th}] BOEC/EOEC: C1+C2	636.8/ 625.8	656.7/ 649.1	700.3/ 701.4	701.7/ 702.6
reactivity loss per cycle in % $\Delta\rho$	-2.86	-2.88	-3.31	-3.52
$\Phi_{rad.\ boundary}$ rel. BOL/BOEC/EOEC	1.00/ 1.00/ 1.00	1.48/ 1.25/ 1.20	1.20/ 0.94/ 0.89	2.17/ 1.73/ 1.64
$\Phi_{ax.\ boundary}$ rel. BOL/BOEC/EOEC	1.00/ 1.00/ 1.00	1.41/ 1.29/ 1.24	1.02/ 0.87/ 0.82	1.25/ 1.08/ 1.01
control rod worth in % $\Delta\rho$, BOEC	-8.57	-8.56	-8.73	-8.63
Na void effect in % $\Delta\rho$, EOEC	1.54	1.59	1.54	0.89
Doppler coeff. in 10^{-6} $\Delta\rho$/K, EOEC	-3.36	-3.36	-3.72	-3.06

[1]: 78 and 60 mean 78 % and 60 % volume % SUS or PE16; [2]: SUS : B_4C : Na = 42.13 : 18.0 : 39.87; [3]: SUS : B_4C : Na = 58 : 20 : 22

Table 26: Results for burner cores with reduced or suppressed radial and axial blanket

isotope	inner core	outer core	total core	axial blanket	radial blanket
Pu-238	27.155	29.407	56.562	0.0	0.0
Pu-239	470.682	509.729	980.411	0.0	0.0
Pu-240	244.392	264.666	509.058	0.0	0.0
Pu-241	85.990	93.123	179.113	0.0	0.0
Pu-242	63.361	68.617	131.978	0.0	0.0
Pu-tot	891.579	965.544	1857.122	0.0	0.0
Am-241	13.577	14.704	28.281	0.0	0.0
U-235	5.147	3.857	9.004	3.264	5.860
U-238	2568.330	1924.639	4492.969	1628.942	2928.496
HM	3478.633	2908.743	6387.376	1632.206	2934.365

Isotopic weights in kg at beginning of life

isotope	inner core	outer core	total core	axial blanket	radial blanket
Pu-238	21.852	25.321	47.173	0.0	0.0
Pu-239	433.821	465.209	899.030	25.591	39.720
Pu-240	242.245	262.151	504.396	0.750	0.969
Pu-241	70.951	80.092	151.043	0.028	0.027
Pu-242	62.055	67.589	129.644	0.000	0.000
Pu-tot	830.924	900.369	1731.286	26.370	40.716
Am-241	14.393	16.762	31.155	0.000	0.000
U-235	3.908	3.212	7.120	2.782	5.077
U-238	2472.521	1875.921	4348.442	1599.035	2882.386
HM	3321.746	2796.258	6118.003	1628.188	2928.180

Isotopic weights in kg at beginning of equilibrium cycle (BOEC)

isotope	inner core	outer core	total core	axial blanket	radial blanket
Pu-238	19.554	23.402	42.957	0.0	0.0
Pu-239	417.361	444.295	861.656	37.054	58.192
Pu-240	240.631	260.349	500.980	1.604	2.121
Pu-241	65.280	74.616	139.895	0.086	0.086
Pu-242	61.169	66.910	128.078	0.002	0.001
Pu-tot	803.994	869.571	1673.566	38.746	68.400
Am-241	14.453	17.380	31.833	0.002	0.002
U-235	3.393	2.916	6.309	2.564	4.708
U-238	2424.385	1850.484	4274.869	1583.555	2858.080
HM	3246.225	2740.352	5986.576	1624.867	2923.190

Isotopic weights in kg at end of equilibrium cycle (EOEC)

isotope	inner core	outer core	total core	axial blanket	radial blanket
Pu-238	-2.298	-1.919	-4.217	0.0	0.0
Pu-239	-16.460	-20.914	-37.374	11.463	18.472
Pu-240	-1.614	-1.802	-3.416	0.853	1.153
Pu-241	-5.671	-5.476	-11.148	0.057	0.059
Pu-242	-0.886	-0.680	-1.566	0.001	0.001
Pu-tot	-26.930	-30.791	-57.721	12.376	19.684
Am-241	0.060	0.619	0.678	0.001	0.001
U-235	-0.515	-0.297	-0.811	-0.218	-0.369
U-238	-48.136	-25.437	-73.573	-15.480	-24.306
HM	-75.521	-55.906	-131.427	-3.321	-4.990

Changes of the isotopic weights in kg (EOEC - BOEC)

Table 27: Mass balances of the core with reduced blankets (core D1.3, ΔT_{cycle}=196 efpd)

isotope	inner core	outer core	total core	axial blanket	radial blanket
Pu-238	27.155	29.407	56.562	-	-
Pu-239	470.682	509.729	980.411	-	-
Pu-240	244.392	264.666	509.058	-	-
Pu-241	85.990	93.123	179.113	-	-
Pu-242	63.361	68.617	131.978	-	-
Pu-tot	891.579	965.544	1857.122	-	-
Am-241	13.577	14.704	28.281	-	-
U-235	5.147	3.857	9.004	-	-
U-238	2568.330	1924.639	4492.969	-	-
HM	3478.633	2908.743	6387.376	-	-

Isotopic weights in kg at beginning of life

isotope	inner core	outer core	total core	axial blanket	radial blanket
Pu-238	22.151	25.423	47.575	-	-
Pu-239	435.797	465.748	901.545	-	-
Pu-240	242.615	262.490	505.105	-	-
Pu-241	71.873	80.748	152.622	-	-
Pu-242	62.182	67.659	129.841	-	-
Pu-tot	834.619	902.068	1736.687	-	-
Am-241	14.291	16.479	30.770	-	-
U-235	3.973	3.225	7.199	-	-
U-238	2478.517	1877.426	4355.943	-	-
HM	3331.400	2799.198	6130.598	-	-

Isotopic weights in kg at beginning of equilibrium cycle (BOEC)

isotope	inner core	outer core	total core	axial blanket	radial blanket
Pu-238	19.896	23.528	43.423	-	-
Pu-239	419.585	444.830	864.415	-	-
Pu-240	241.170	260.881	502.051	-	-
Pu-241	66.340	75.492	141.833	-	-
Pu-242	61.355	67.020	128.375	-	-
Pu-tot	808.346	871.750	1680.097	-	-
Am-241	14.295	16.988	31.283	-	-
U-235	3.464	2.931	6.395	-	-
U-238	2431.934	1852.514	4284.448	-	-
HM	3258.039	2744.183	6002.222	-	-

Isotopic weights in kg at end of equilibrium cycle (EOEC)

isotope	inner core	outer core	total core	axial blanket	radial blanket
Pu-238	-2.256	-1.895	-4.151	-	-
Pu-239	-16.212	-20.918	-37.130	-	-
Pu-240	-1.445	-1.609	-3.054	-	-
Pu-241	-5.533	-5.256	-10.789	-	-
Pu-242	-0.827	-0.639	-1.466	-	-
Pu-tot	-26.273	-30.317	-56.590	-	-
Am-241	0.004	0.509	0.513	-	-
U-235	-0.509	-0.295	-0.803	-	-
U-238	-46.583	-24.912	-71.496	-	-
HM	-73.361	-55.016	-128.376	-	-

Changes of the isotopic weights in kg (EOEC - BOEC)

Table 28: Mass balances of the core without blankets (core D2.3, ΔT_{cycle}=180 efpd)

no	rad. bl.	ax. bl.	EOEC zone power [MW_{th}]			mass-flow [kg/s]			$\Delta p_{S/A}$	max. T_{clad}
	rows	height	core	ax. bl.	rad. bl.	core	rad. bl.	max. S/A	[kg/cm^2]	[°C]
1	3	65	638	25	51	3543	425	20.3	4.12	612.7
2	3	24	650	19	45	3585	383	20.6	4.21	613.4
3	3	0	676	(1)*	37	3651	317	21.0	4.36	615.1
4	1	65	648	26	40	3623	345	20.7	4.26	611.3
5	1	24	659	20	35	3659	309	20.9	4.34	612.0
6	1	0	684	(1)*	29	3715	253	21.3	4.47	613.5
7	0	65	682	28	(4)*	3938	30	22.5	4.95	606.1
8	0	24	690	20	(4)*	3942	26	22.5	4.97	606.9
9	0	0	710	(1)*	(3)*	3946	22	22.5	4.98	609.6

(1)* means 1% power is produced in Na+steel of former blanket zone

Table 29: Consequences of the radial and axial blanket reduction on thermal-hydraulics data

	1a	B2	C2.2	D2.3	D1.3
	ref. case	no radial bl.	no axial bl.	no blanket	reduced bl.
radial blanket size	3 rows bl.	SUS-refl.	3 rows bl.	SUS-refl.	1 row bl.
axial blanket size	30 + 35 cm	30 + 35 cm	SUS-refl.	SUS-refl.	2 x 12 cm
Pu/HM C1/C2 [at %]	25.5/ 33.0	25.5/ 32.0	25.5/ 33.0	25.5/ 33.0	25.5/ 33.0
cycle length [efpd]	203	190	195	180	196
burnup react. loss [% $\Delta\rho$]	-2.86	-3.13	-3.11	-3.31	-2.88
max. BOL [W/cm]	328	326	328	334	328
linear BOEC "	295	304	305	320	297
power EOEC "	277	292	291	310	285
control rod worth [% $\Delta\rho$]	-8.57	-8.73	-8.73	-8.73	-8.56
Na-void effect [% $\Delta\rho$]	1.54	1.59	1.52	1.54	1.59
Doppler coeff. [10^{-6} $\Delta\rho$/K]	-3.36	-3.63	-3.54	-3.72	-3.36

Table 30: Comparison of some cores with reduced blankets and the reference core

			(1a)	(2a)	(8k)	(9a)	(D2.3)	(D1.3)
no.	parameter	unit	reference case	43 steel pins	27 steel diluents	18 $^{nat}B_4C$ diluents	no blankets	reduced blankets
1	Pu/HM: C1/C2	at %	25.5/33.0	32.0/36.1	32.5/35.0	35.0/35.0	25.5/33.0	25.5/33.0
	average	"	28.9	34.1	33.8	35.0	28.9	28.9
2	cycle length	efpd	203	177	175	185	180	196
3	average burnup	GWd/t_{HM}	100.3	99.7	99.3	100.6	98.8	100.2
4	maximum burnup	"	142.6	137.5	135.9	137.6	138.2	141.8
5	max. BOL	W/cm	328	370	358	334	334	329
	linear BOEC	"	295	331	322	310	320	303
	power* EOEC	"	277	307	314	299	310	286
6	burnup react. loss	% Δρ	-2.86	-3.03	-3.06	-3.23	-3.31	-2.88
7	control rod worth	"	-8.57	-8.61	-8.00	-7.06	-8.73	-8.56
8	$\Delta\rho_{void}$ core	% Δρ	1.54	1.43	0.92	1.15	1.54	1.59
9	" core+diluents	"	1.54	1.43	1.14	1.37	1.54	1.59
10	Doppler coefficient	$10^{-6}\Delta\rho/K$	-3.36	-3.10	-2.97	-2.08	-3.72	-3.36
11	fresh Pu-inventory	kg	1857	1894	1894	2047	1857	1857
12	ΔPu, core only	kg/cycle	-57.95	-62.13	-62.96	-71.61	-56.59	-57.72
13	ΔPu, "	kg/TW_eh	-42.48	-52.24	-53.53	-57.60	-46.78	-43.82
14	fresh HM-inventory	kg	6387	5514	5528	5822	6387	6387
15	breeding ratio: core	-	0.580	0.488	0.483	0.456	0.633	0.600
	(equ. cycle) total	-	1.147	1.085	1.061	1.002	0.633	0.877
16	S/A pressure drop	kg/cm^2	4.77	4.77	4.77	4.77	4.98	4.77
17	max. channel ΔT	K	200	204	204	204	192	198
18	max. $T_{mid\text{-}clad}$	°C	613	619	618	618	610	612

* without the burnup factor of 1.15

Table 31: Comparison of the considered burner cores and the reference core

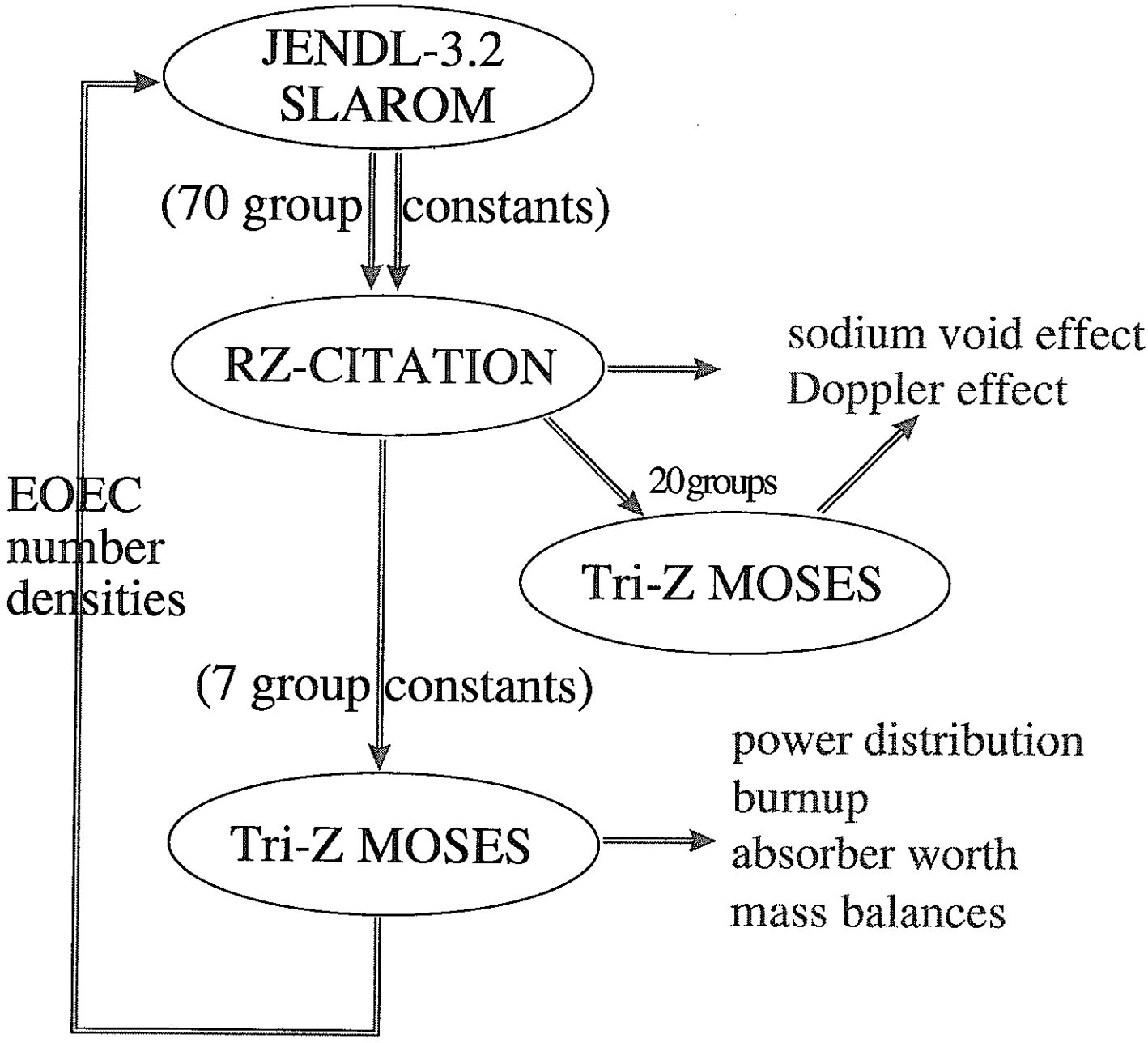

Figure 1: Calculational Scheme

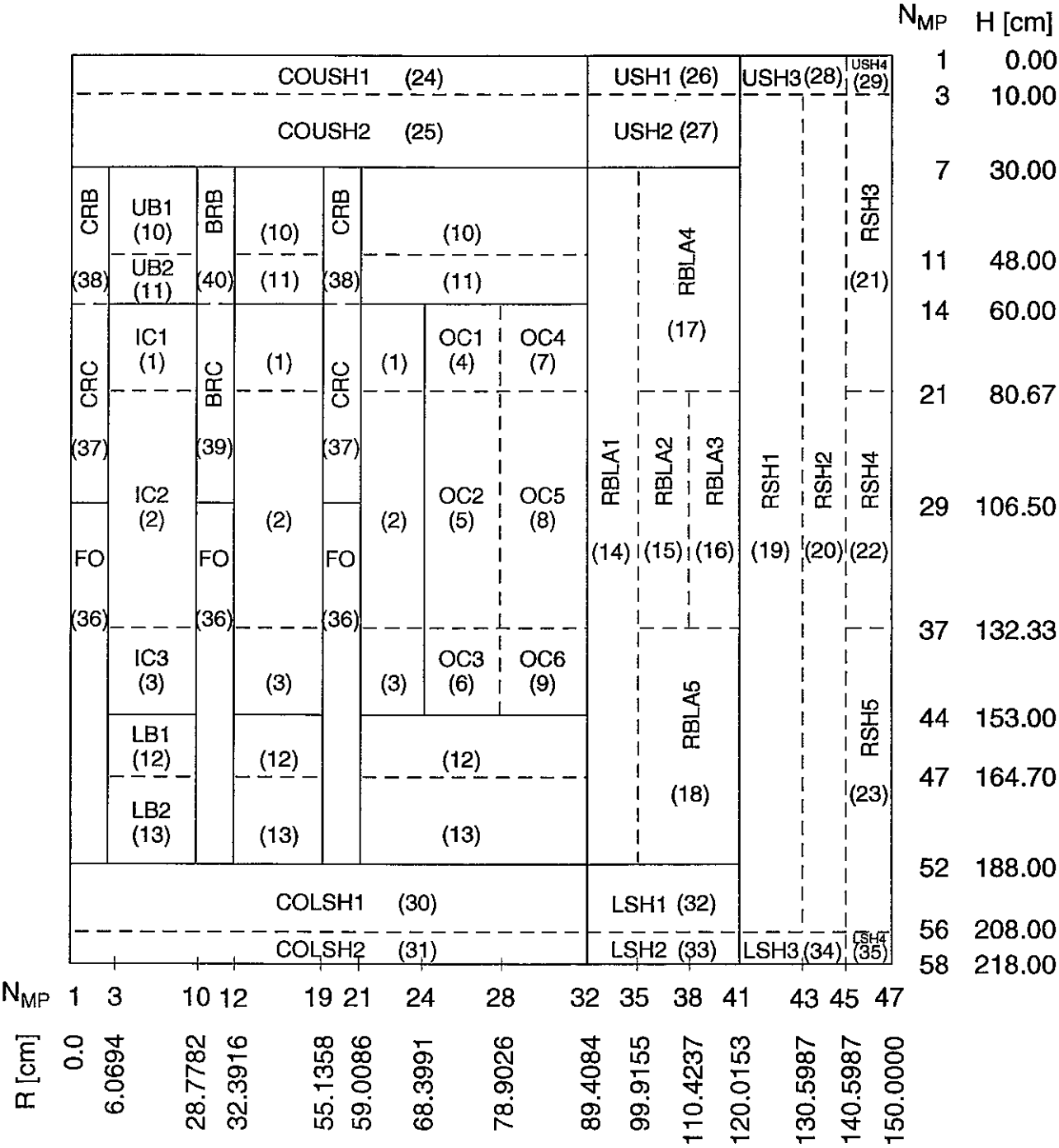

Figure 2: RZ-Model for CITATION calculations

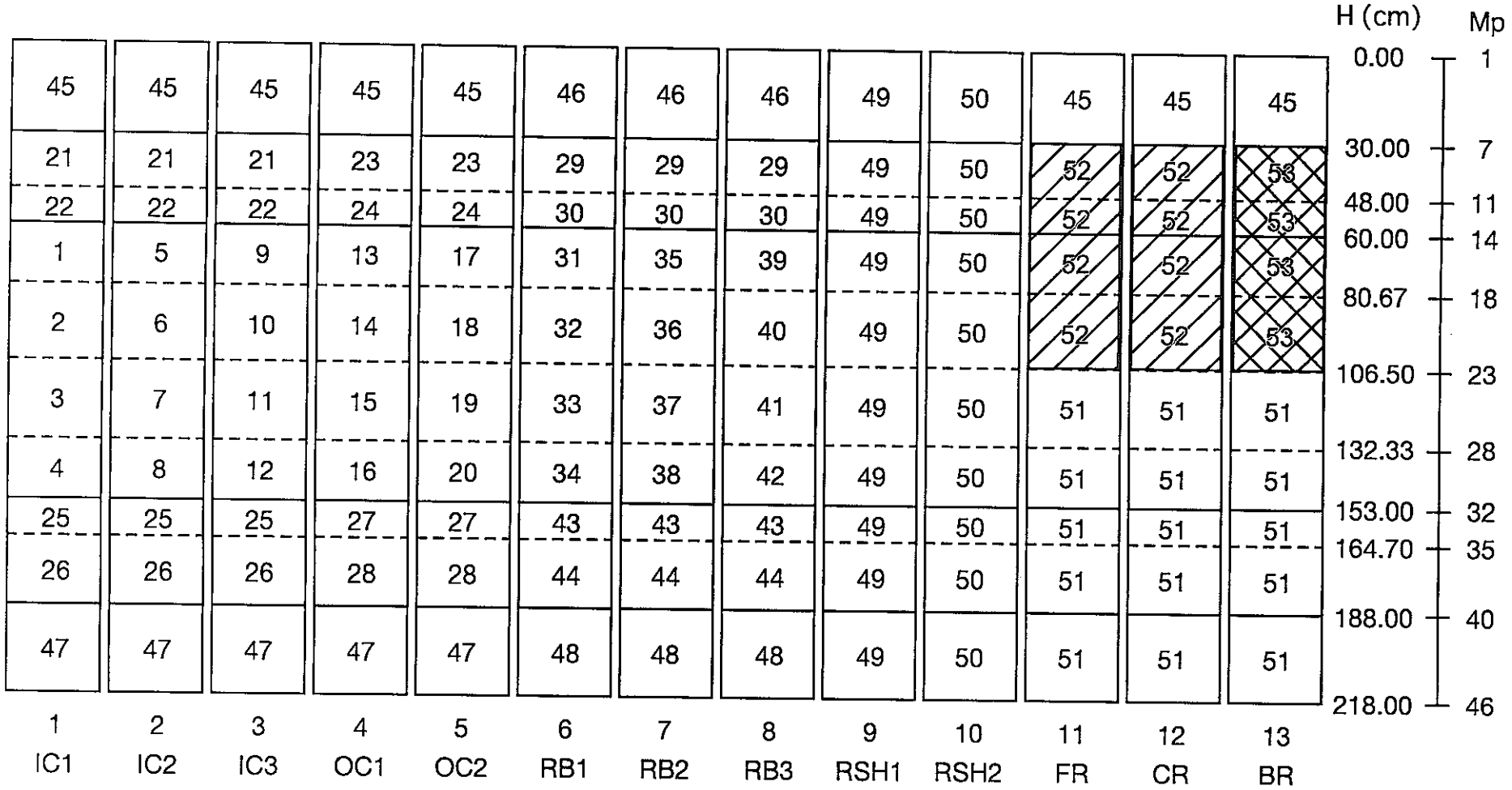

Figure 3: Axial structure of the subassemblies for the Pu-burner reference core

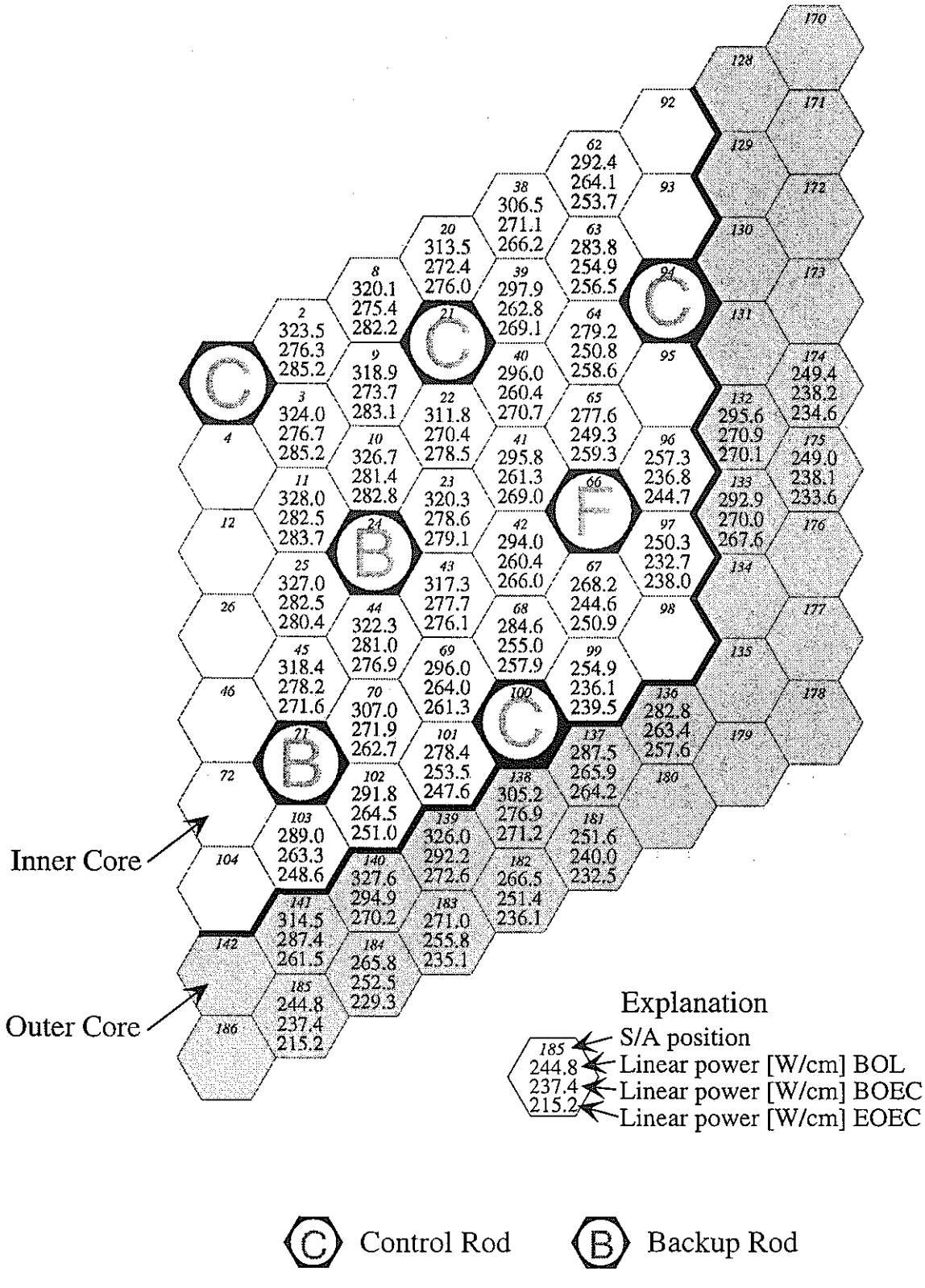

Figure 4 : Max. linear power per S/A of the reference core (core 1a)

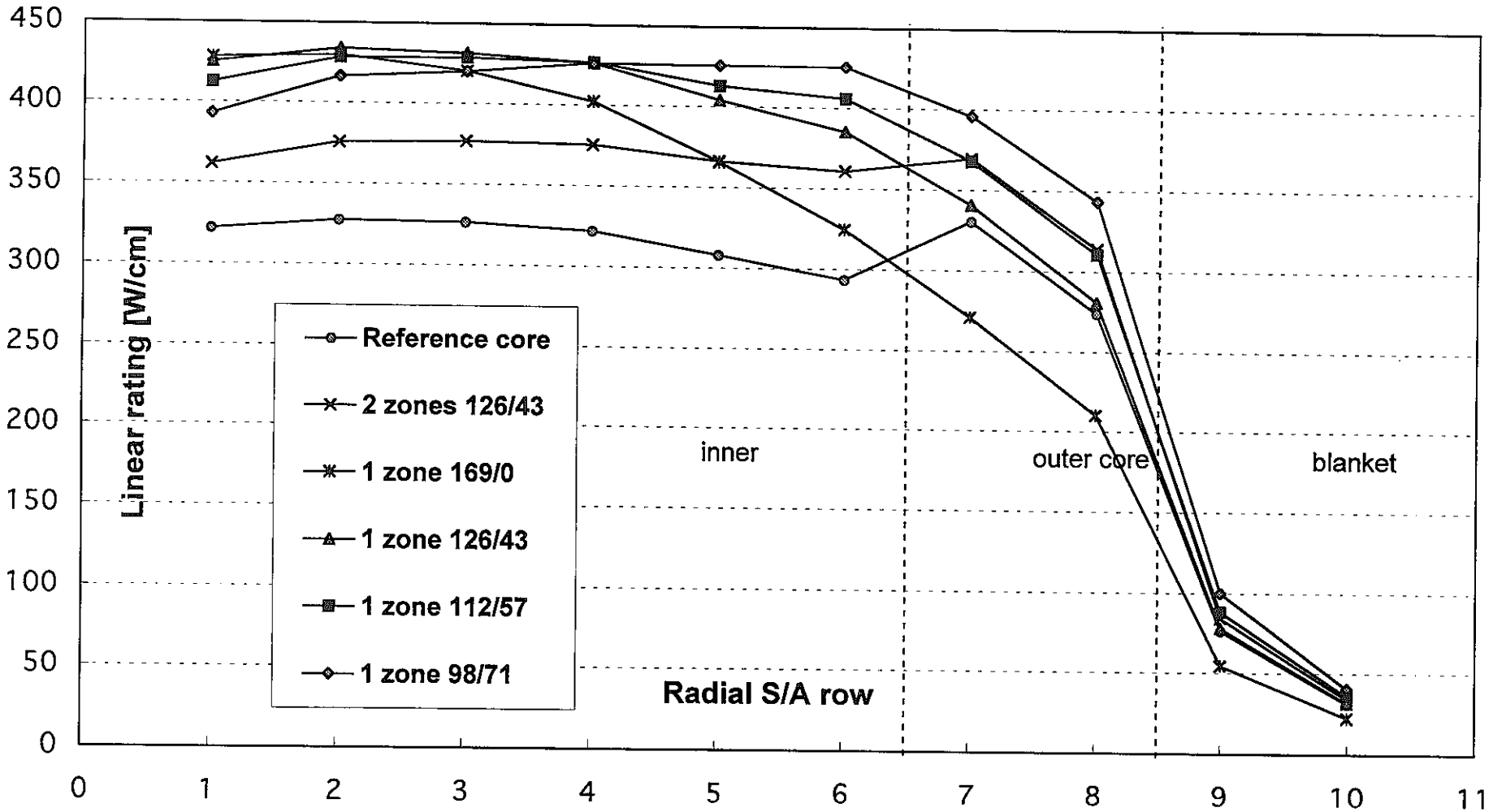

Figure 5: Radial linear rating traverses in cores with different numbers of diluting steel pins (at begin of life)

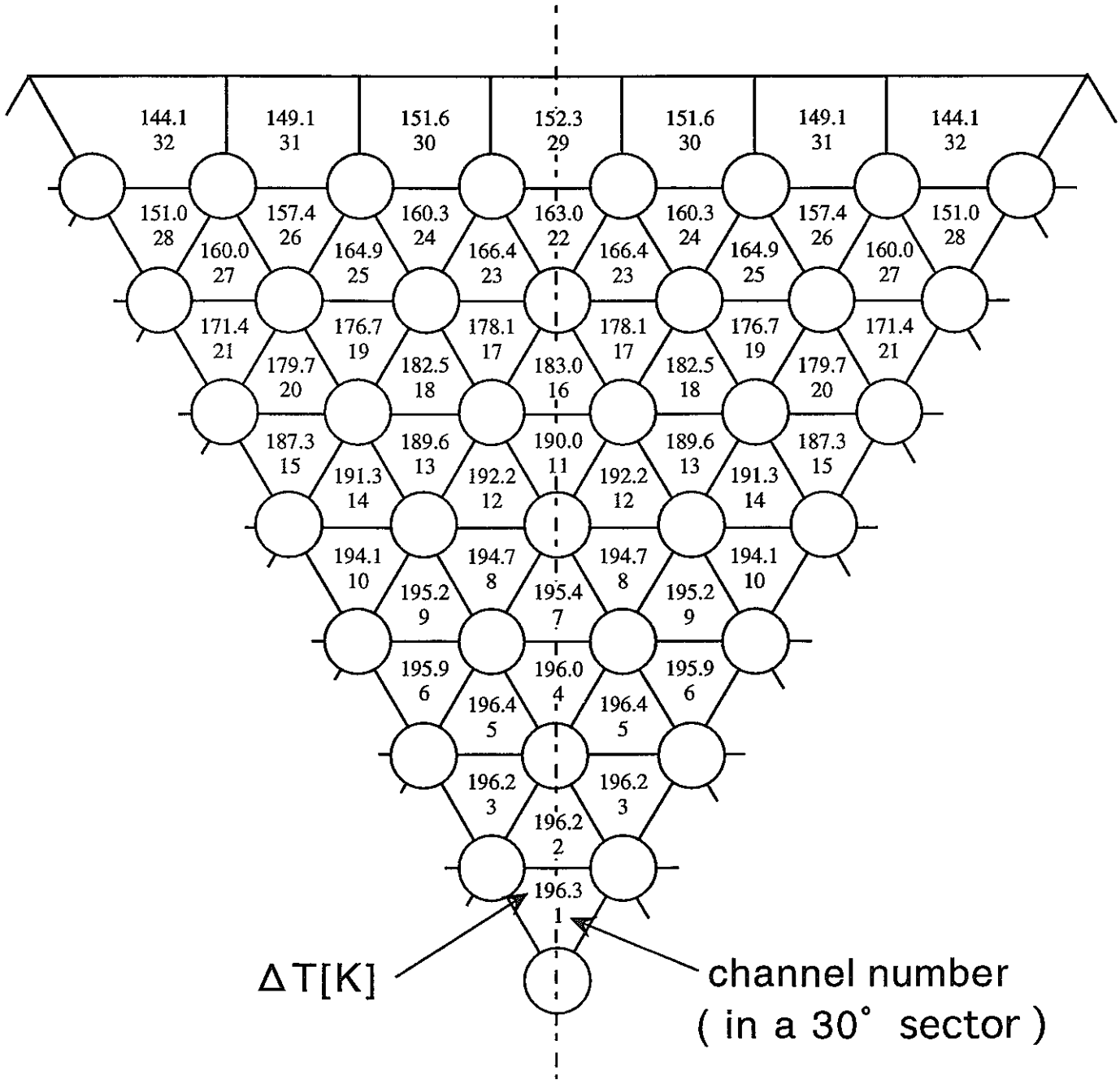

Figure 6 : Coolant channel ΔT distribution
in a reference core fuel S/A

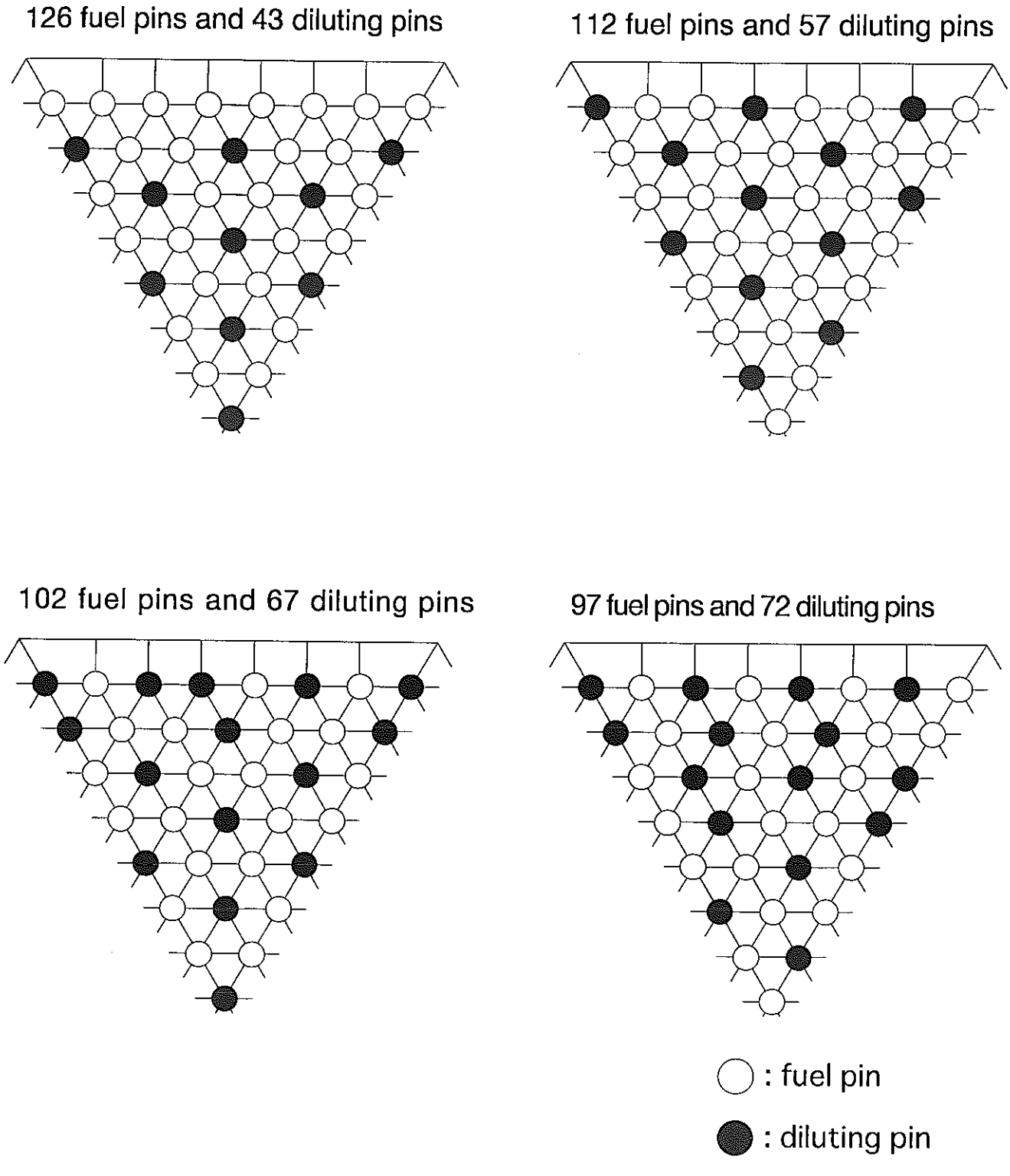

Figure 7 : Bundle designs with different numbers of diluting pins

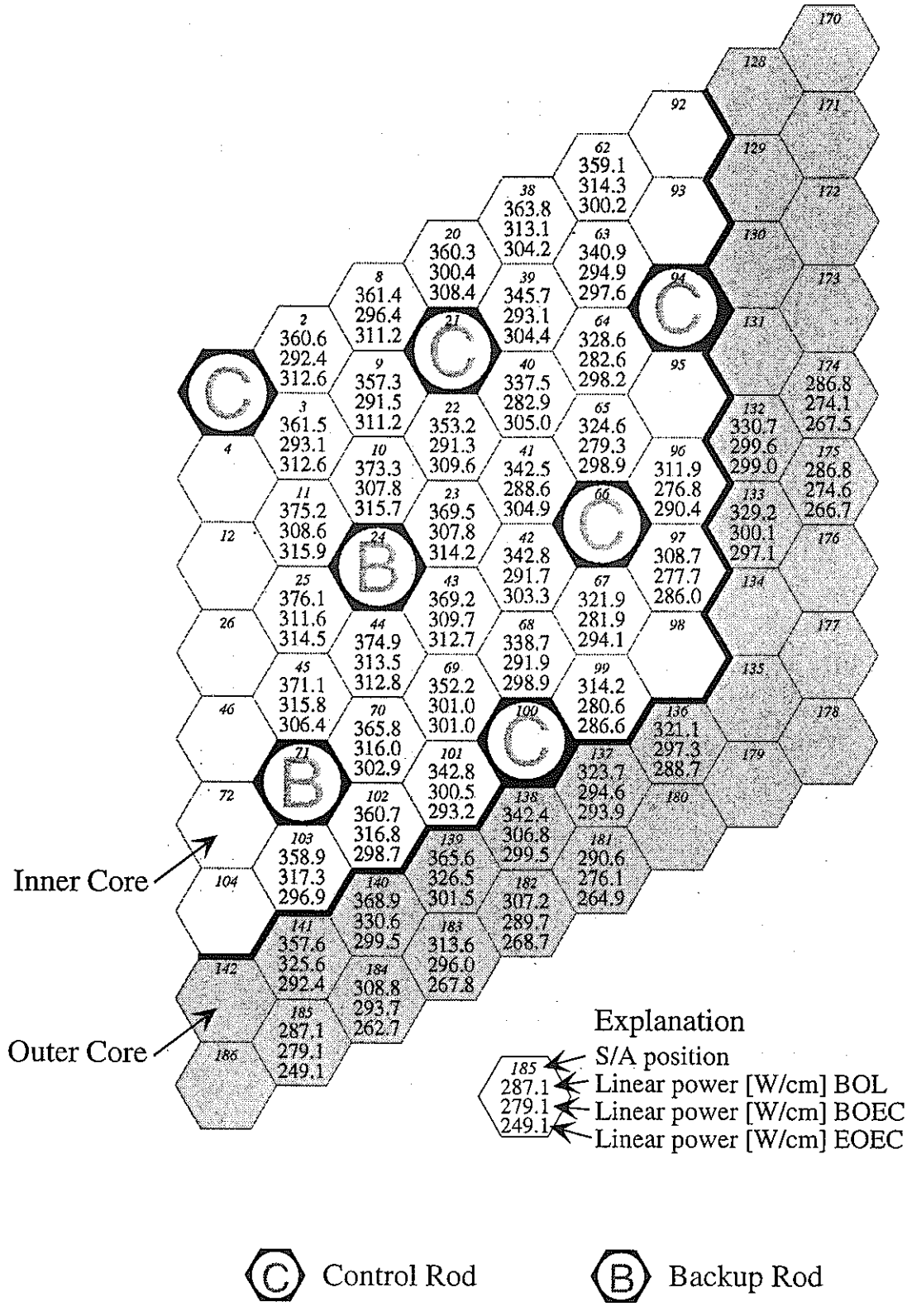

Figure 8 : Max. linear power per S/A of the burner core with 43 steel pins (core 2a)

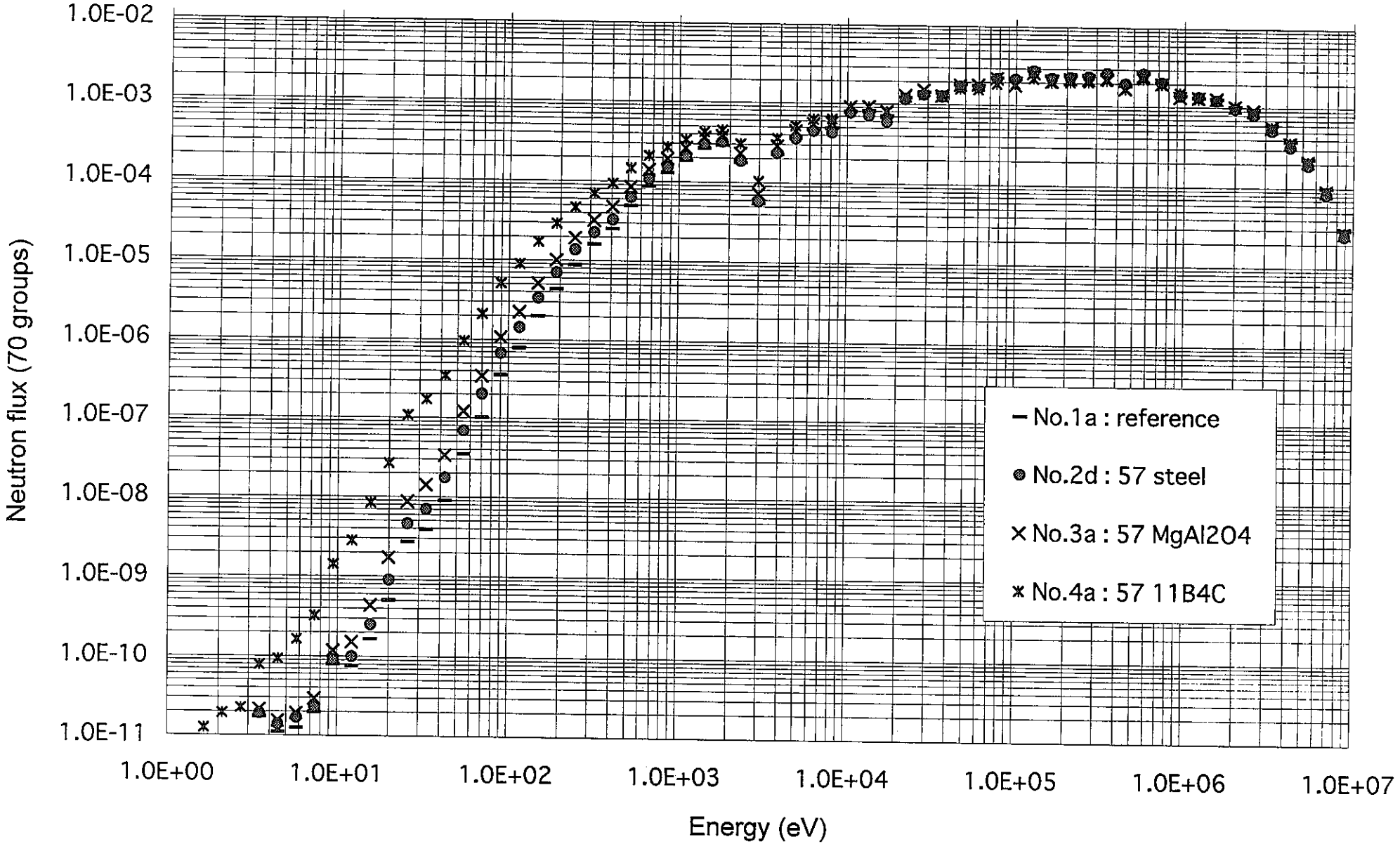

Figure 9 : Influence of steel, $MgAl_2O_4$ and $^{11}B_4C$ on the neutron spectrum

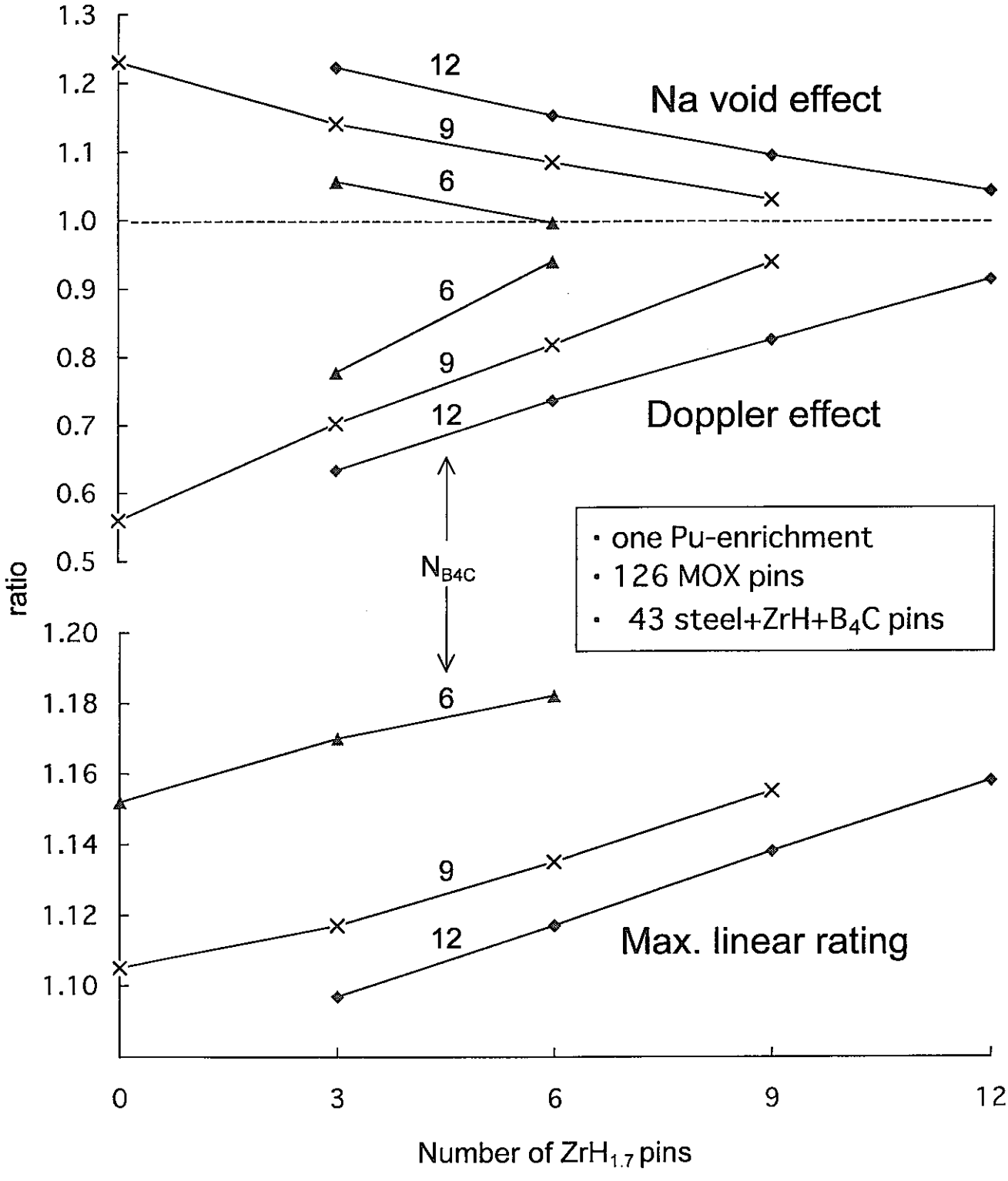

Figure 10: Na-void effect, Doppler effect and maximum linear rating of burner cores with different numbers of $ZrH_{1.7}$ and $^{nat}B_4C$ pins (relative to the reference core values)

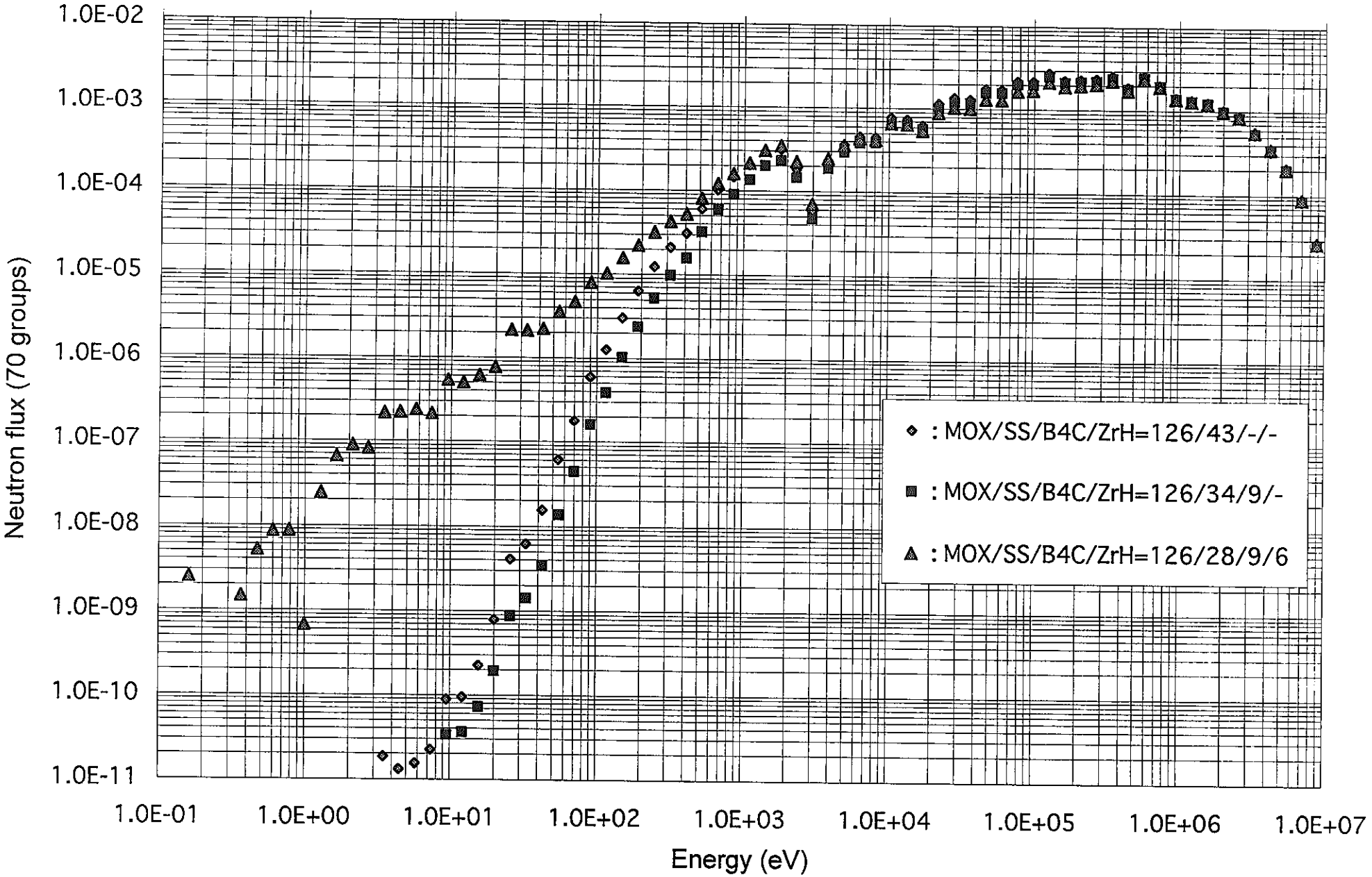

Figure 11 : Influence of $^{nat}B_4C$ and $ZrH_{1.7}$ on the neutron spectrum

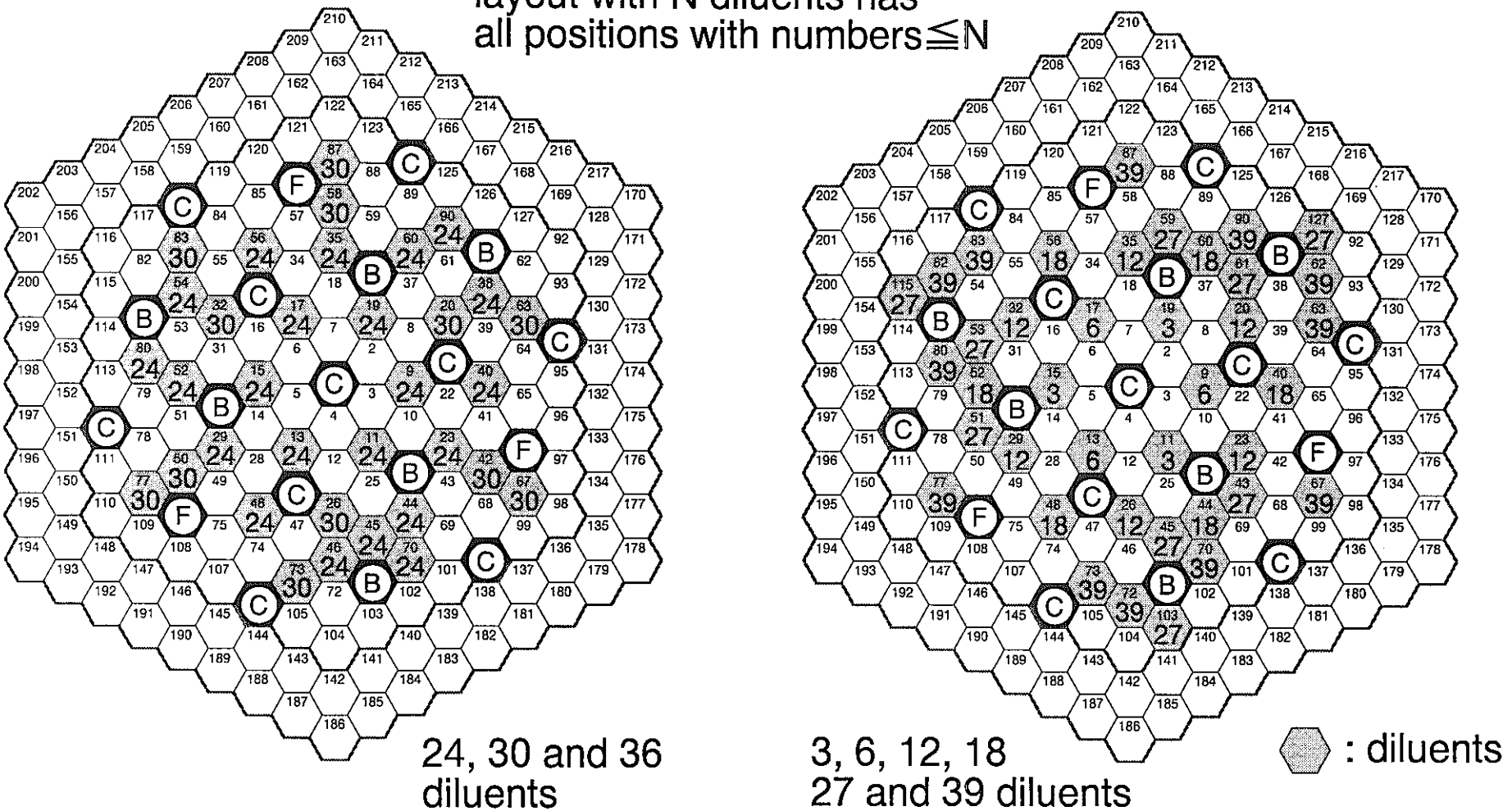

Figure 12: Core cross-sections with different numbers of steel diluents

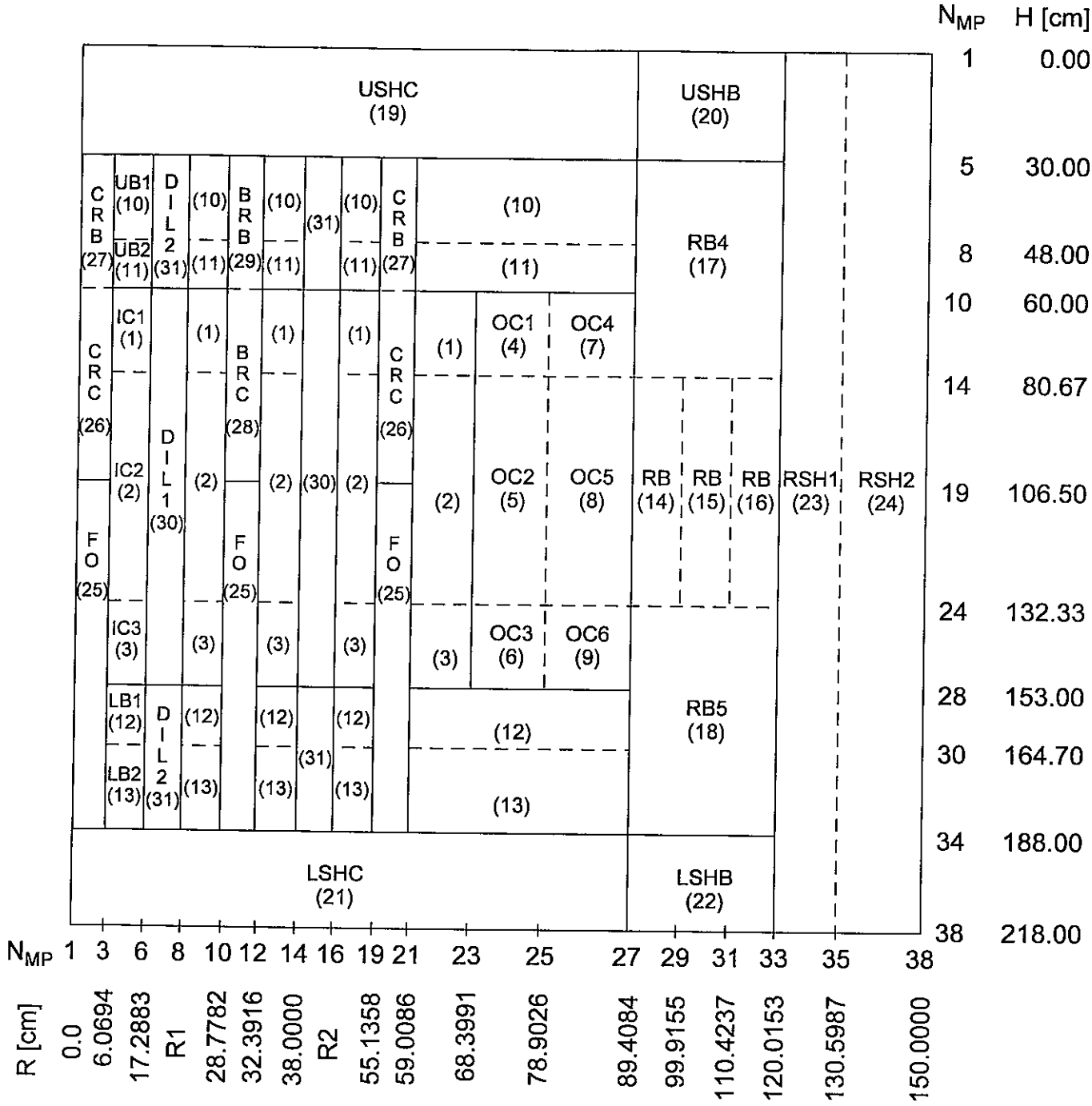

Figure 13 : RZ-Model for 70 groups CITATION calculations with diluents

(R1 / R2=22.8017 / 47.0913 cm for 27steel diluents
R1 / R2=20.2336 / 44.6829 cm for 18 B_4C diluents)

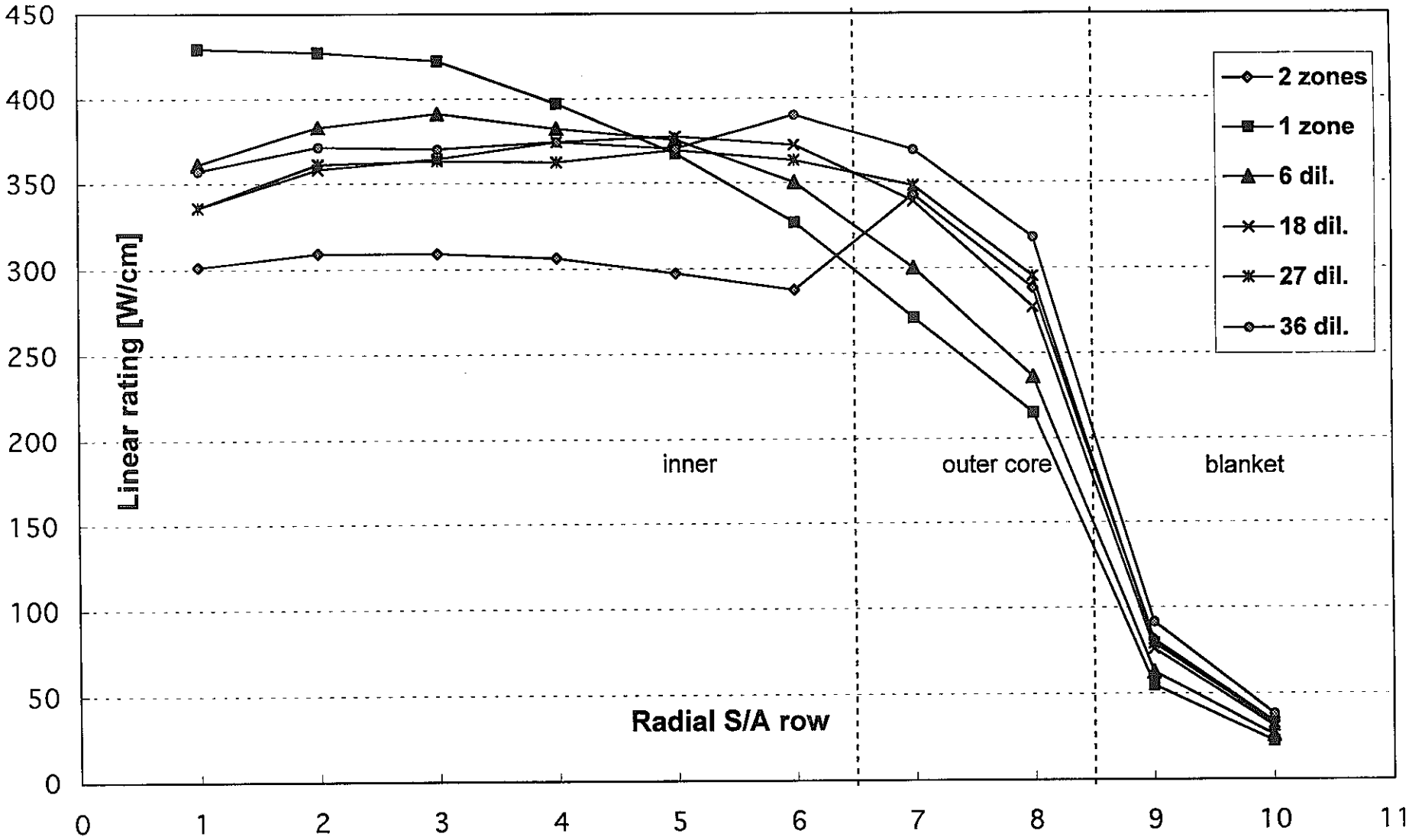

Figure 14: Radial linear power traverses for different steel diluent configurations

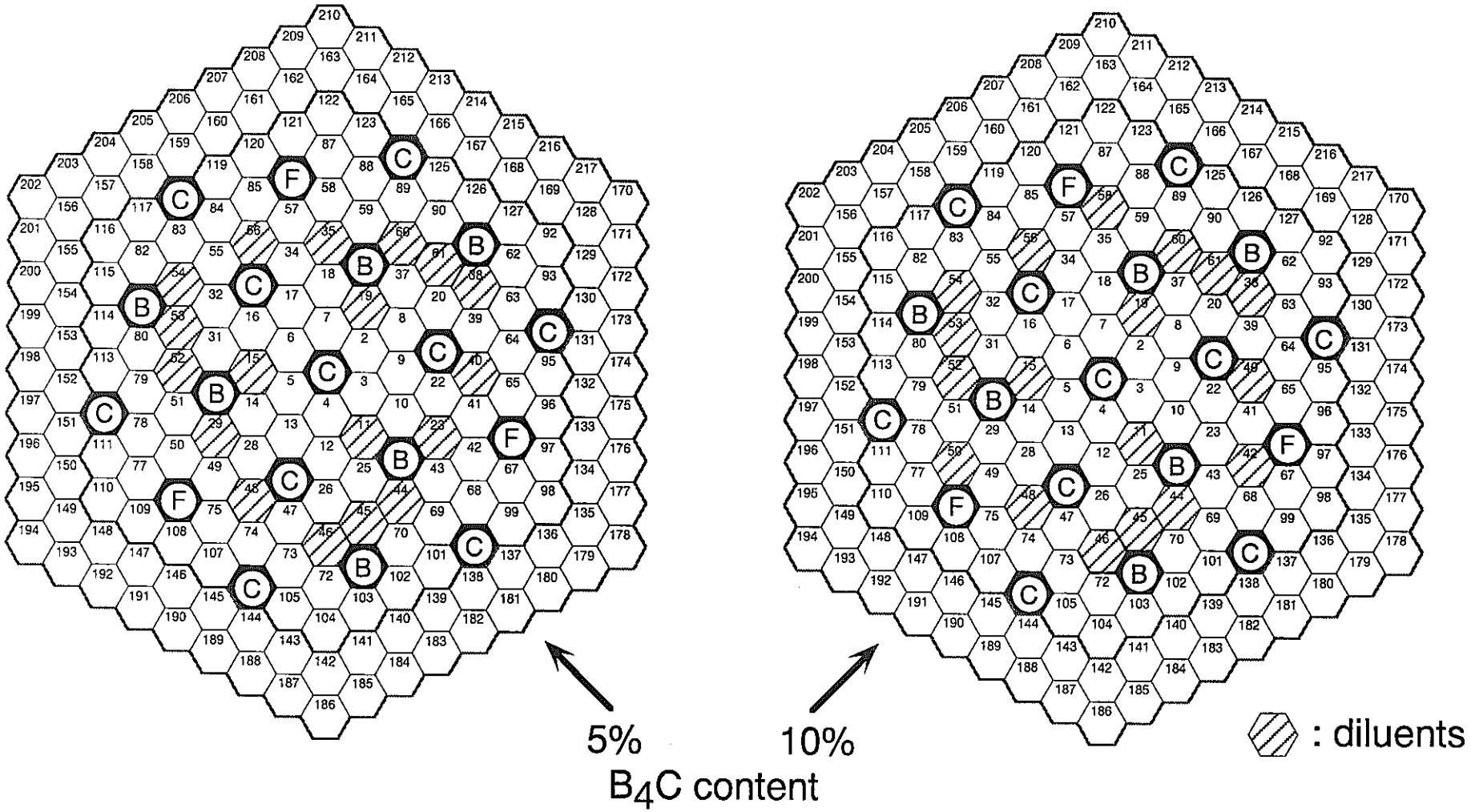

Figure 15: Core cross-sections with 18 B_4C diluents

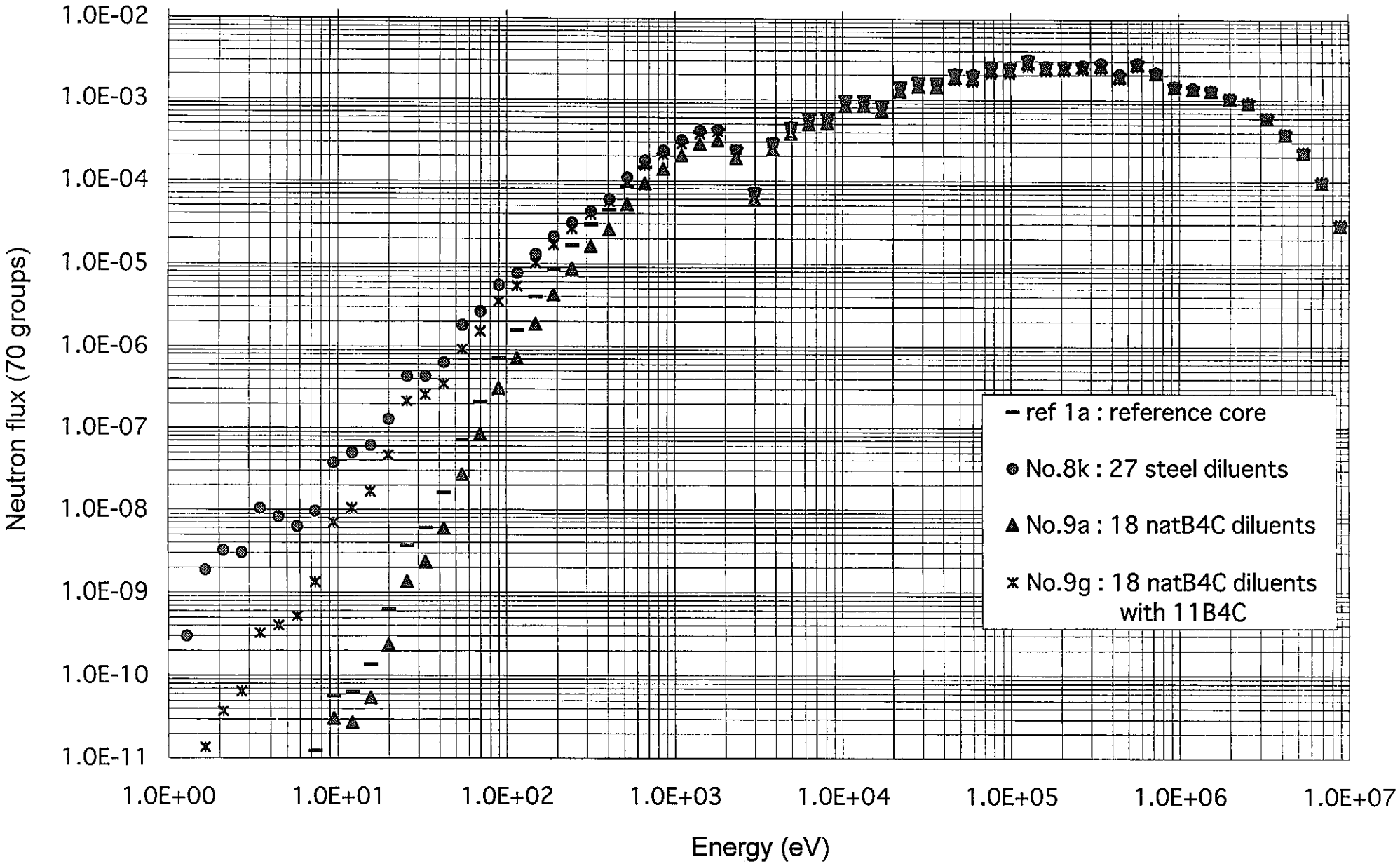

Figure 16 : Influence of diluents with steel, $^{nat}B_4C$ and $^{nat}B_4C+^{11}B_4C$ on the inner core neutron spectrum (at EOEC)

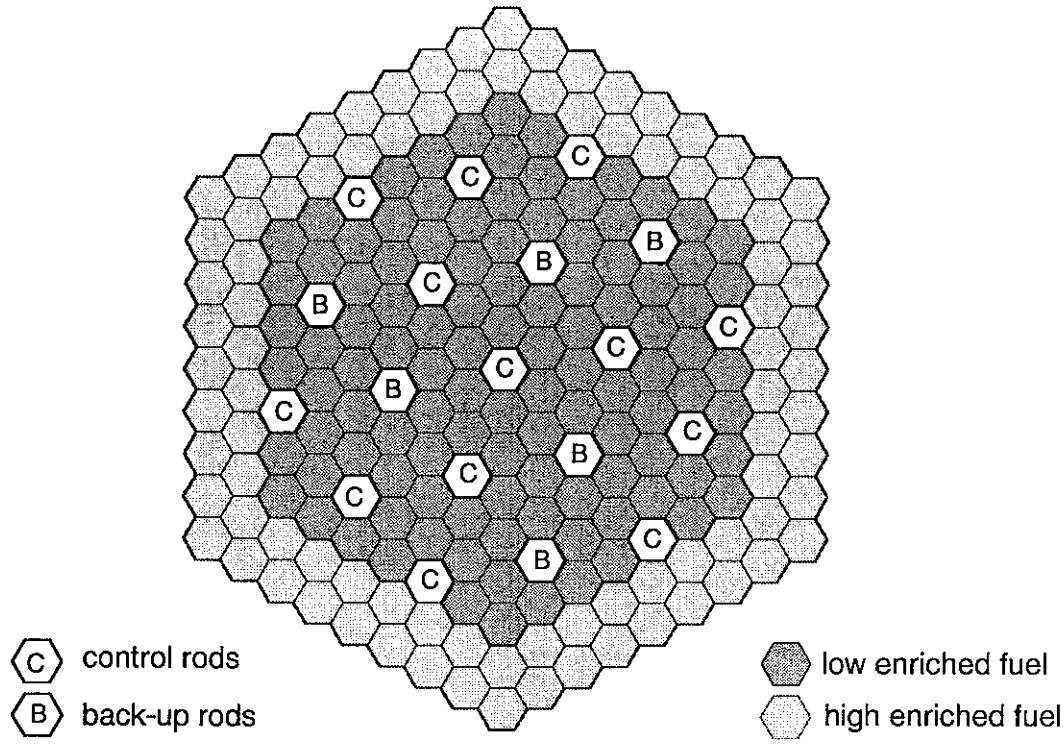

Reference core

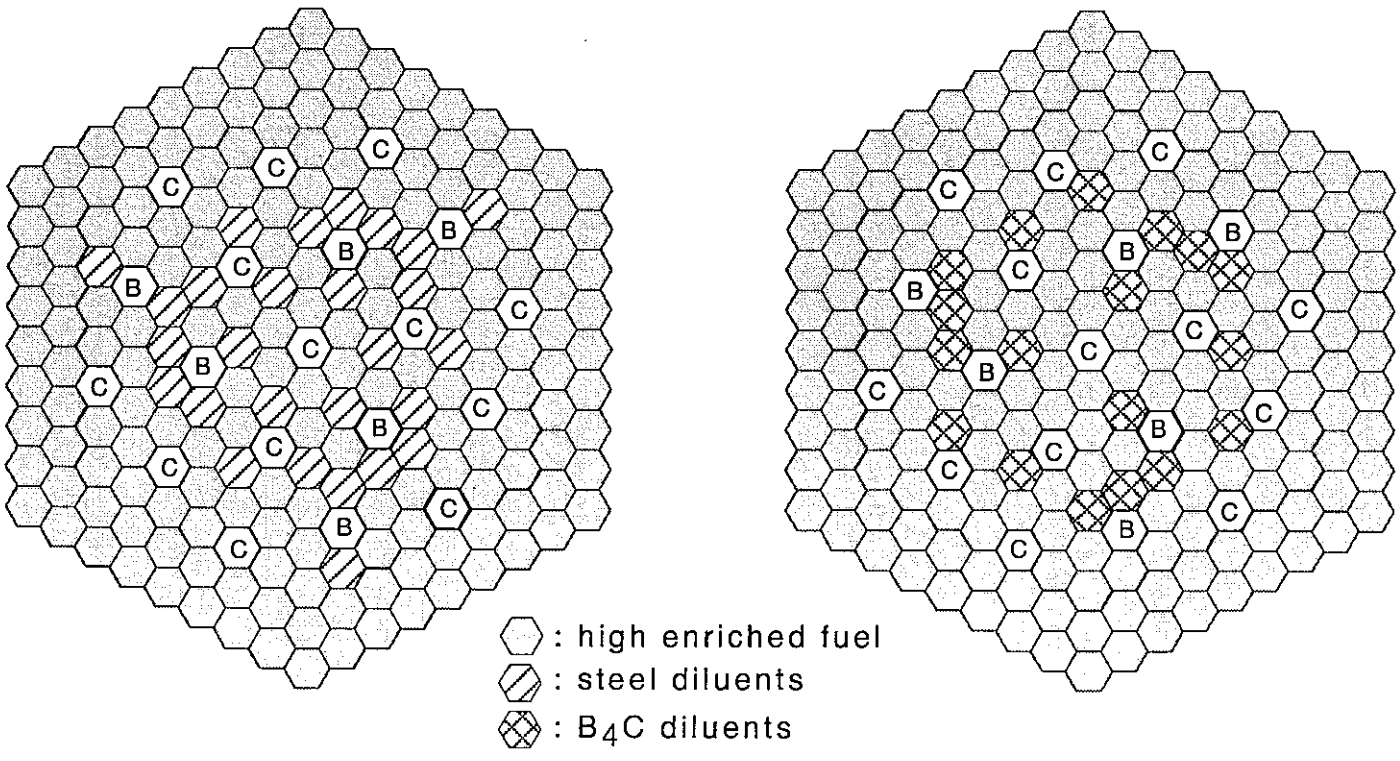

Core with 27 steel diluents

Core with 18 B_4C diluents
(10 volume % B_4C)

Figure 17: Cross-sections of the reference core and two burner cores

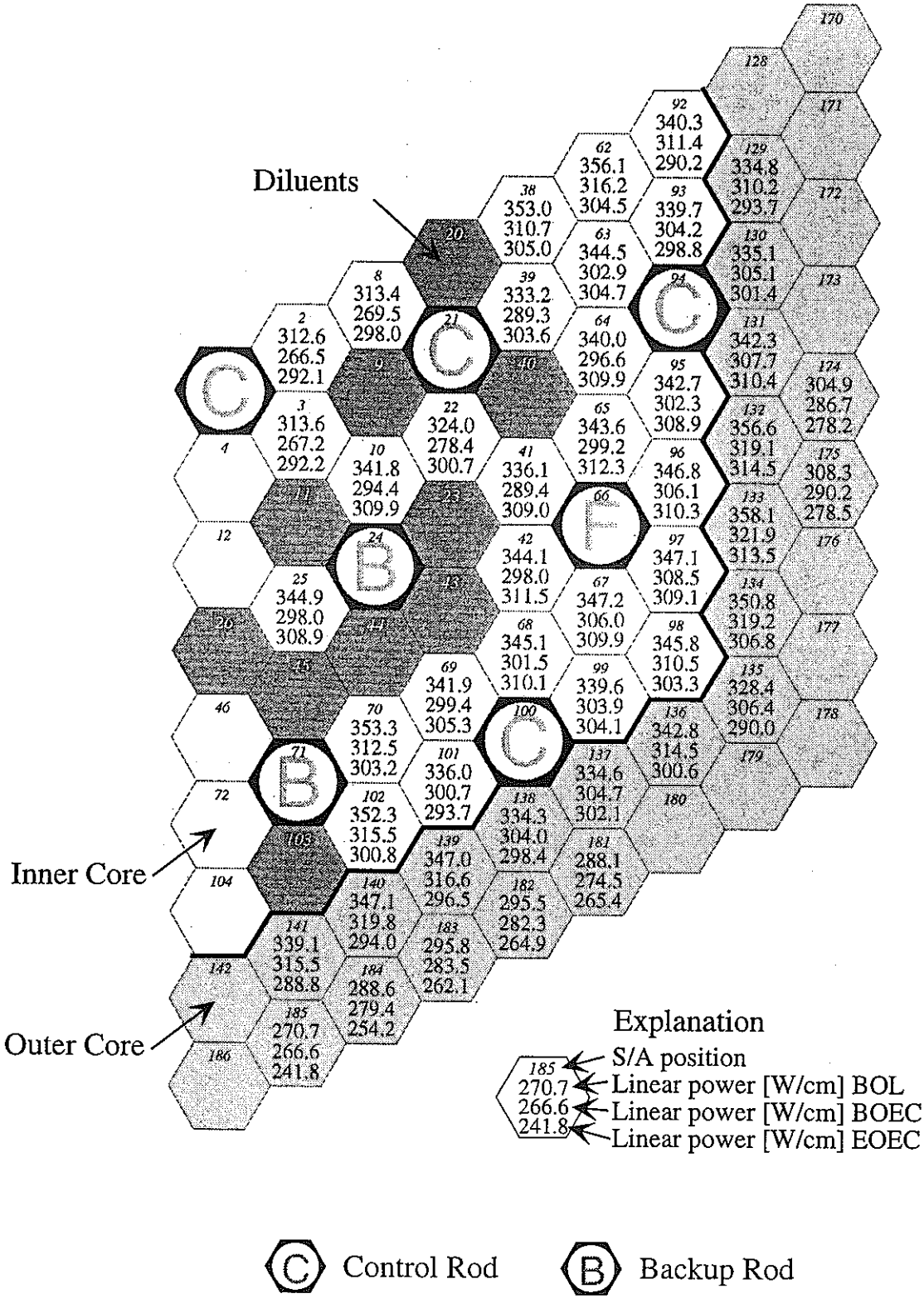

Figure 18 : Max. linear power per S/A of the burner core with 27 steel diluents (case 8k)

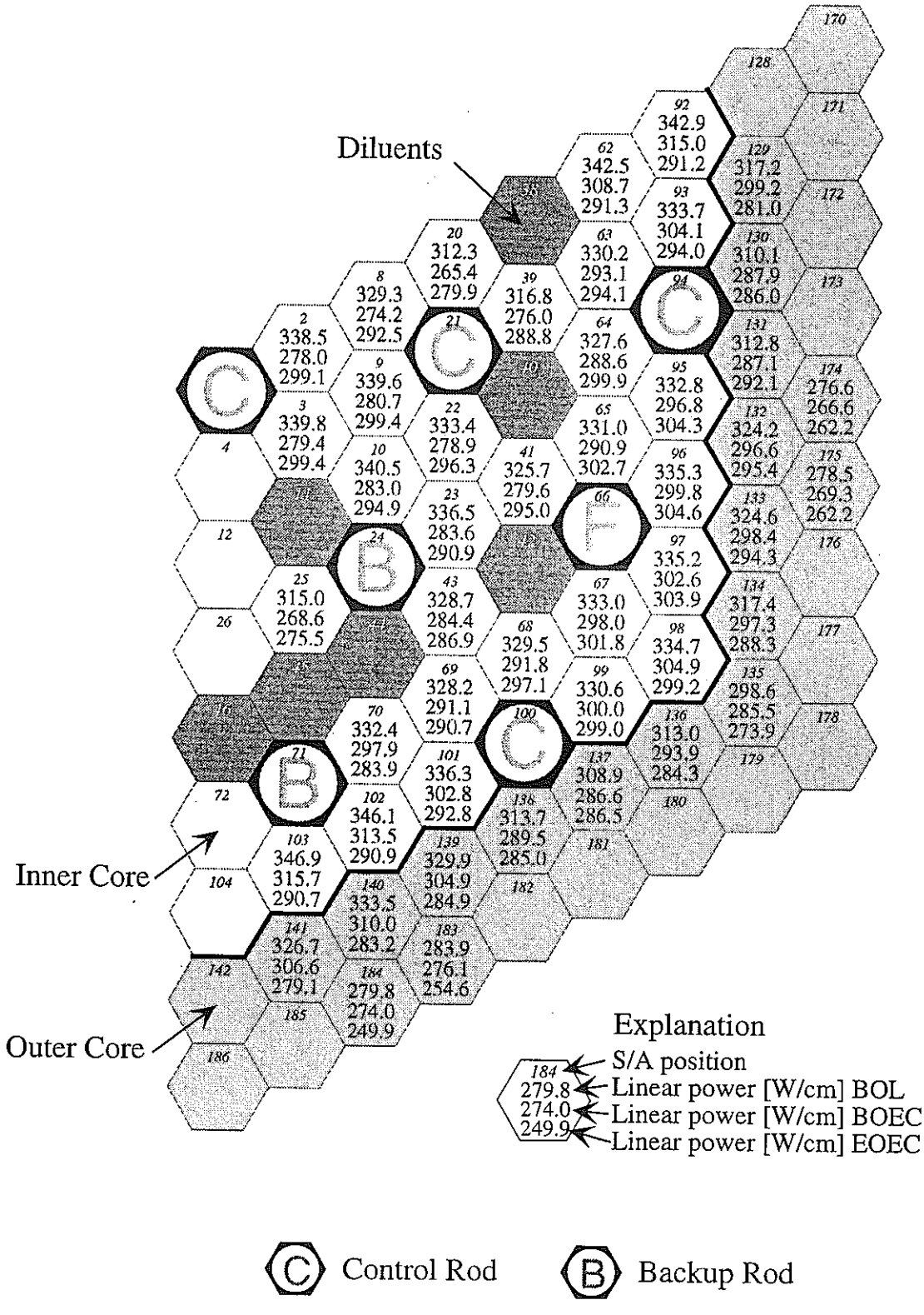

Figure 19 : Max. linear power per S/A of the burner core with 18 B_4C diluents (case 9a)

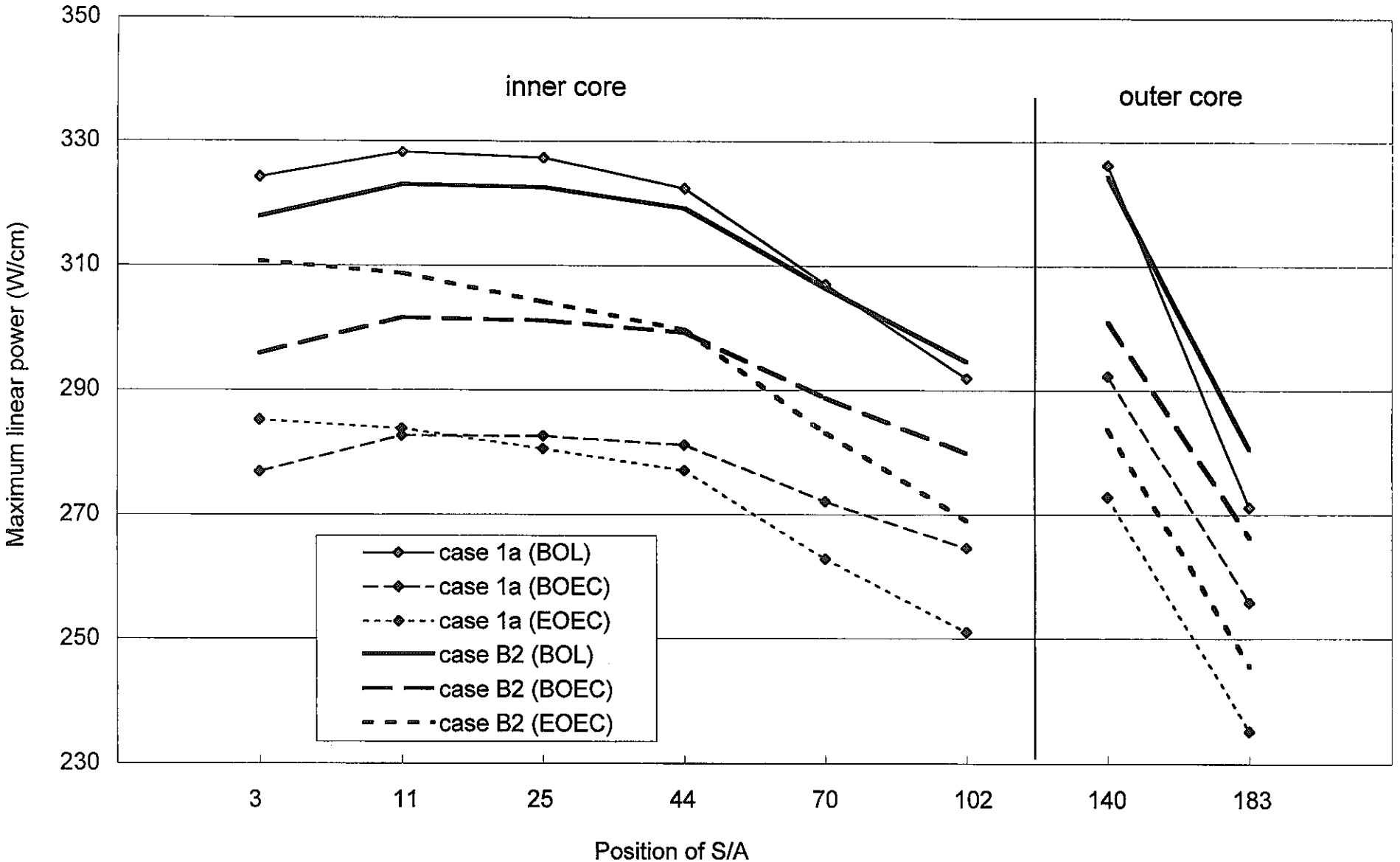

Figure 20: Radial maximum linear power traverses per S/A for the reference case 1a and case B2 without radial blanket

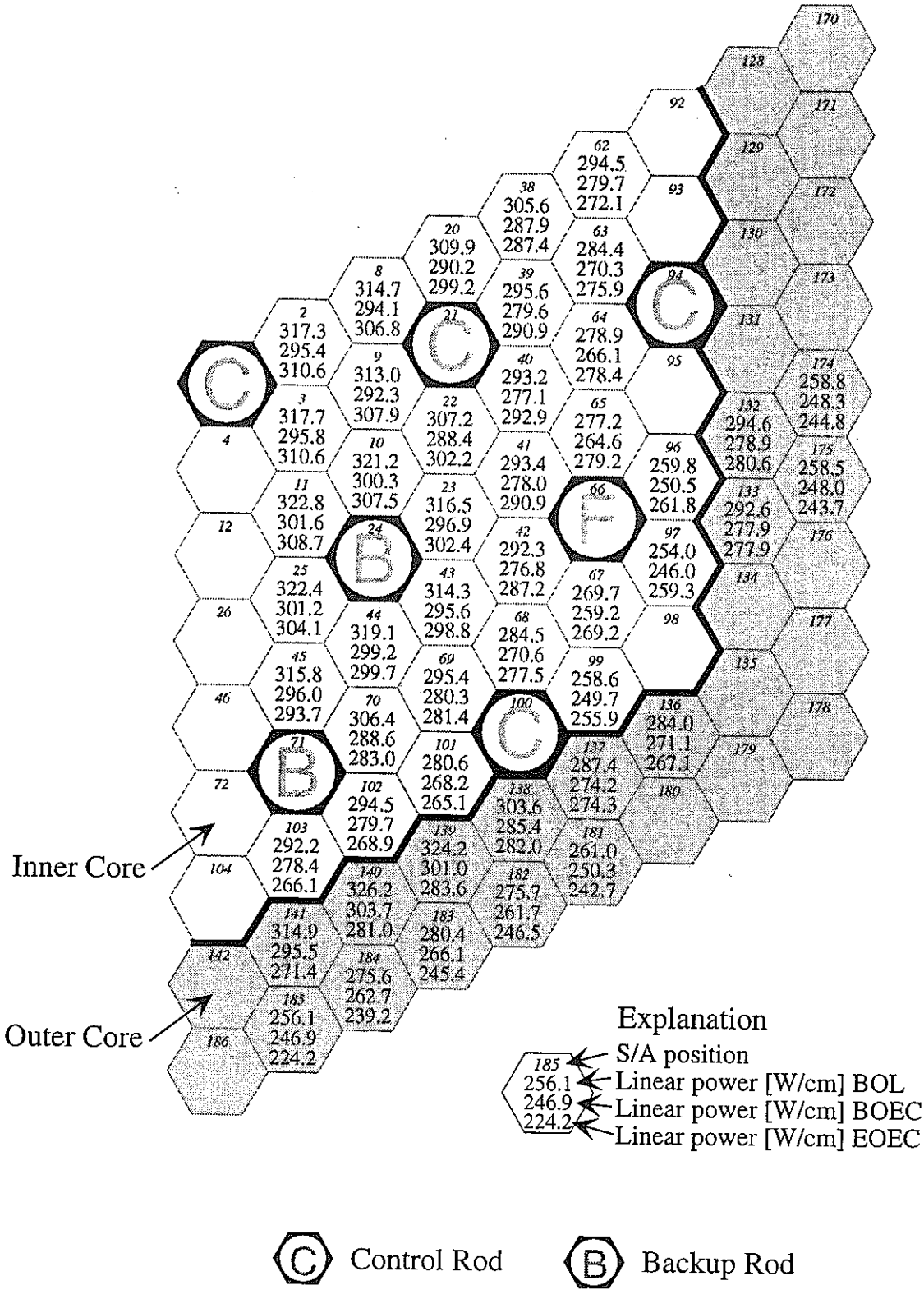

Figure 21 : Max. linear power per S/A in the core without radial blanket (core B2)

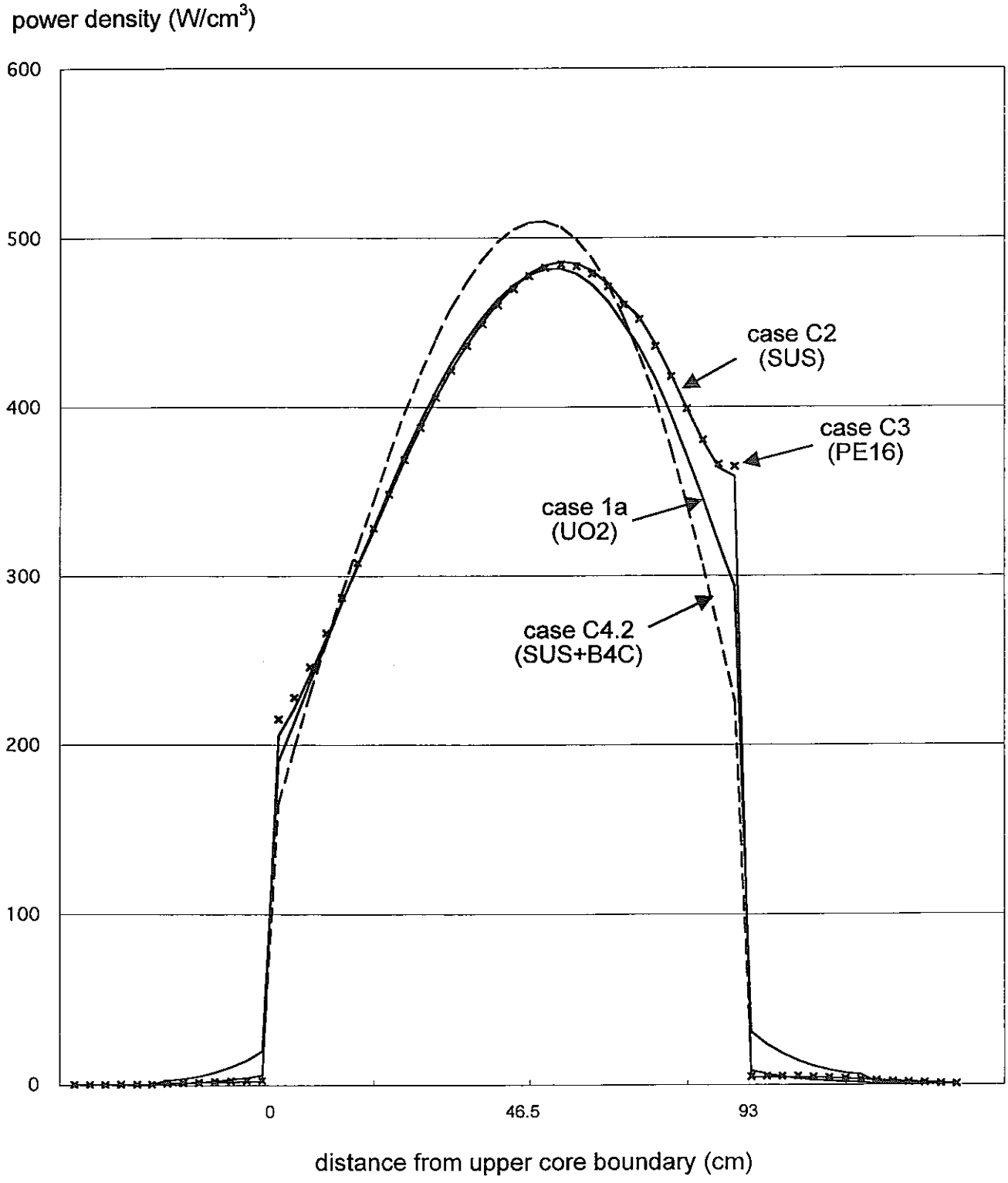

Figure 22: Influence of the axial blanket suppression on the axial power distribution at BOL in position 10

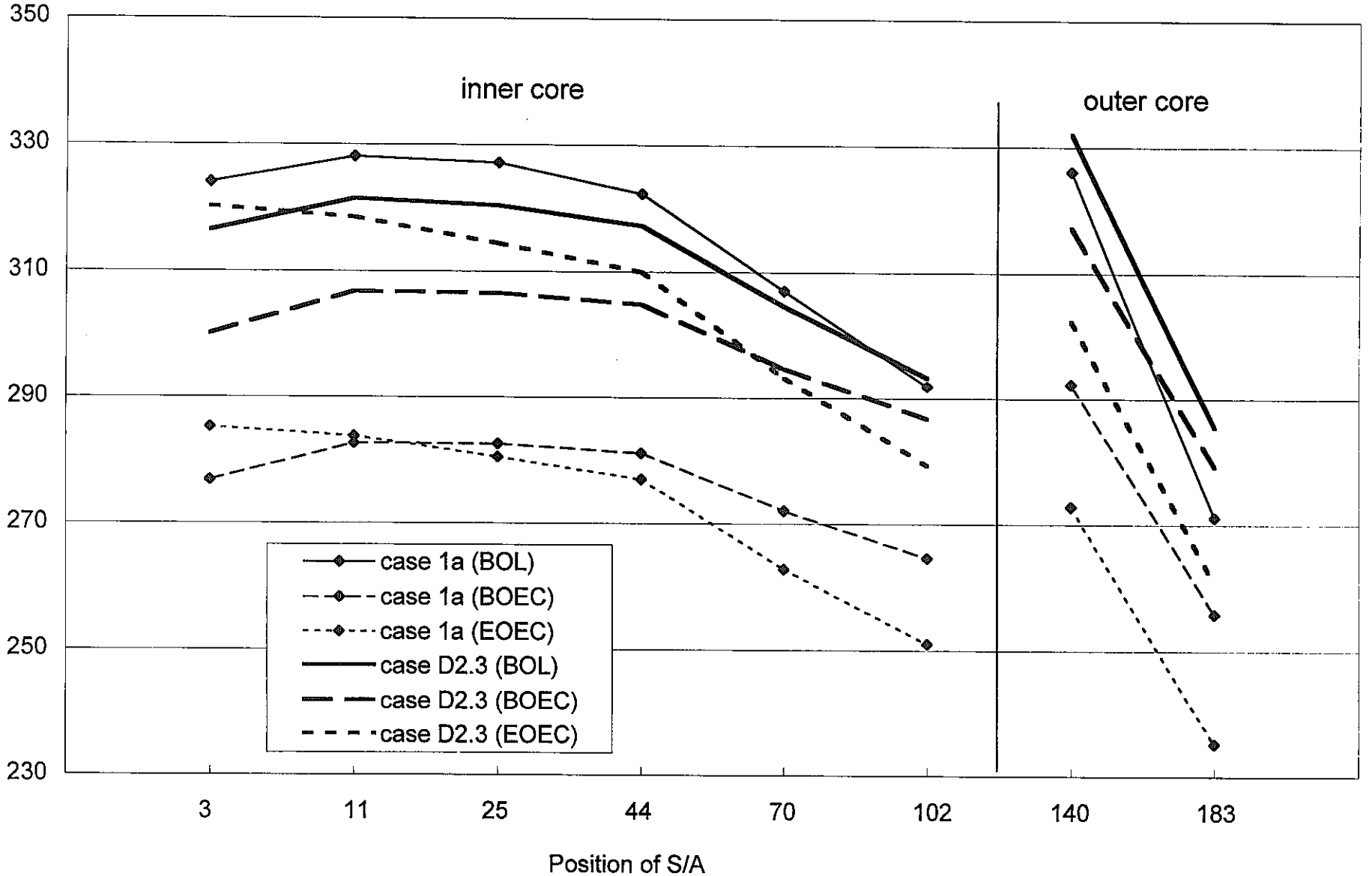

Figure 23: Radial maximum linear power traverses per S/A for the reference case 1a and case D2.3 without axial and radial blanket

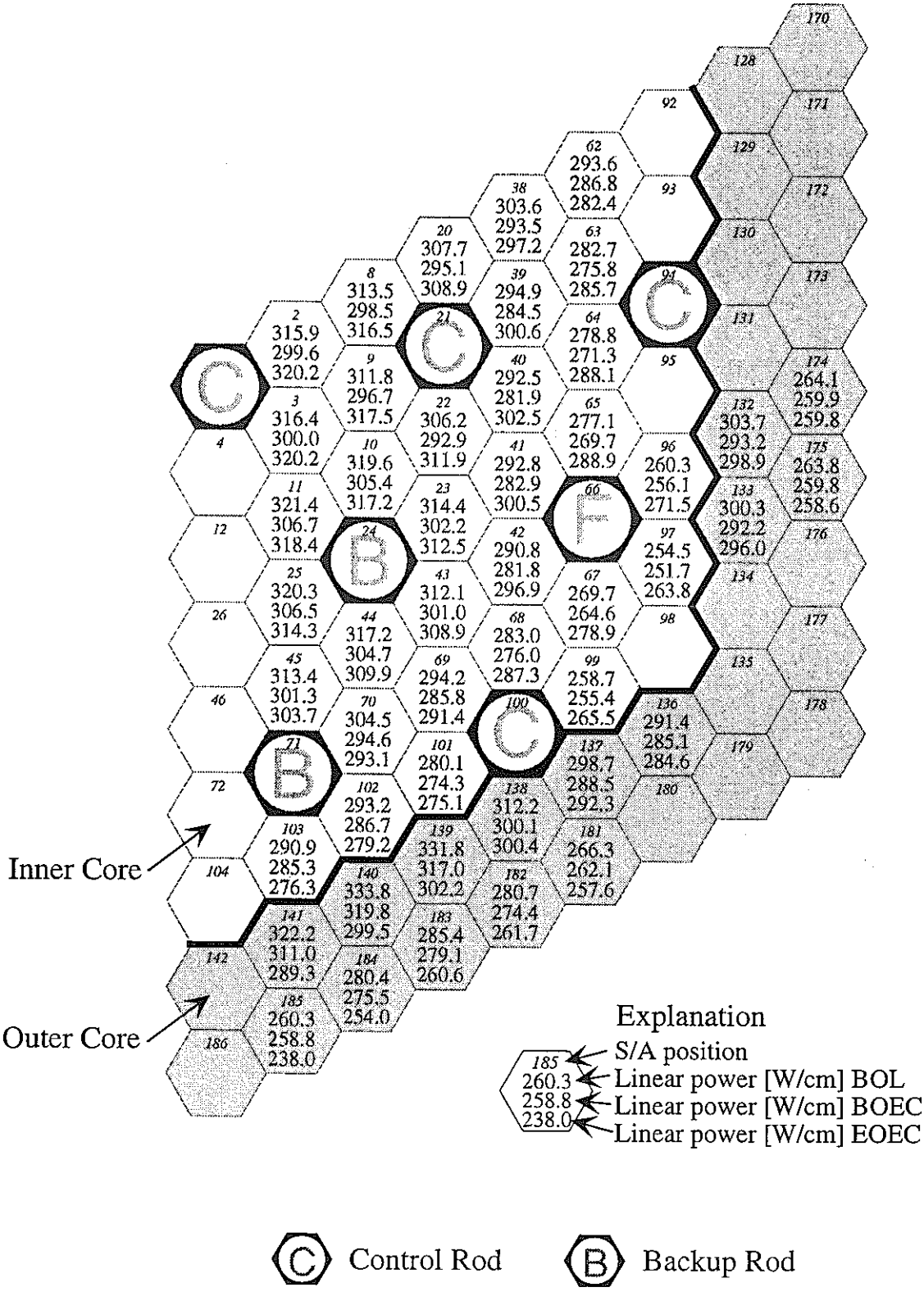

Figure 24 : Max. linear power per S/A in the core without radial and axial blanket (core D2.3)